P-06-288

# Oskarshamn site investigation

# Formation factor logging in situ by electrical methods in KLX07A, KLX08, KLX10 and KLX12A

Martin Löfgren, Kemakta Konsult AB

August 2007

**Svensk Kärnbränslehantering AB**
Swedish Nuclear Fuel
and Waste Management Co
Box 5864
SE-102 40 Stockholm Sweden
Tel 08-459 84 00
+46 8 459 84 00
Fax 08-661 57 19
+46 8 661 57 19

ISSN 1651-4416
SKB P-06-288

# Oskarshamn site investigation

# Formation factor logging in situ by electrical methods in KLX07A, KLX08, KLX10 and KLX12A

Martin Löfgren, Kemakta Konsult AB

August 2007

*Keywords:* AP PS 400-06-129, In situ, Formation factor, Rock resistivity, Electrical conductivity.

# Abstract

This report presents measurements and interpretations of the formation factor of the rock surrounding the boreholes KLX07A, KLX08, KLX10 and KLX12A in Laxemar, Sweden. The formation factor was logged in situ by electrical methods.

For KLX07A, the in situ rock matrix formation factors obtained range from $4.1 \cdot 10^{-5}$ to $2.1 \cdot 10^{-4}$. The in situ fractured rock formation factors obtained range from $2.1 \cdot 10^{-5}$ to $3.6 \cdot 10^{-3}$. The obtained rock matrix formation factor distribution deviates from the log-normal distribution. However, only a limited number of data points were obtained as the rock surrounding the borehole is extensively fractured. The fractured rock formation factor distribution corresponds fairly well to the log-normal distribution. The mean values and standard deviations of the obtained $\log_{10}$-normal distributions are –4.1 and 0.17, –3.8 and 0.33 for the in situ rock matrix and fractured rock formation factor, respectively.

For KLX08, the in situ rock matrix formation factors obtained range from $1.1 \cdot 10^{-5}$ to $2.3 \cdot 10^{-4}$. The in situ fractured rock formation factors obtained range from $1.0 \cdot 10^{-5}$ to $4.8 \cdot 10^{-3}$. The formation factor distributions are well described by the log-normal distribution. The mean values and standard deviations of the obtained $\log_{10}$-normal distributions are –4.5 and 0.24, –4.4 and 0.34 for the in situ rock matrix and fractured rock formation factor, respectively.

For KLX10, the in situ rock matrix formation factors obtained range from $7.8 \cdot 10^{-6}$ to $2.2 \cdot 10^{-4}$. The in situ fractured rock formation factors obtained range from $7.8 \cdot 10^{-6}$ to $3.9 \cdot 10^{-3}$. The distributions of the formation factors are fairly well described by the log-normal distribution. The mean values and standard deviations of the obtained $\log_{10}$-normal distributions are –4.5 and 0.32, –4.3 and 0.40 for the in situ rock matrix and fractured rock formation factor, respectively.

For KLX12A, the in situ rock matrix formation factors obtained range from $1.3 \cdot 10^{-5}$ to $1.0 \cdot 10^{-4}$. The in situ fractured rock formation factors obtained range from $1.3 \cdot 10^{-5}$ to $7.7 \cdot 10^{-4}$. The distributions of the formation factors are less well described by the log-normal distribution and feature double peaks. This may be due to the fact that the borehole penetrates through two different rock domains. The mean values and standard deviations of the obtained $\log_{10}$-normal distributions are –4.5 and 0.25, –4.3 and 0.32 for the in situ rock matrix and fractured rock formation factor, respectively.

When obtaining the electrical conductivity profiles of the groundwater in the boreholes, complementary data from other boreholes in the Laxemar area were used. In KLX08 also data from pore water characterisations were used. It is acknowledged that choosing the electrical conductivity profiles for a borehole is often a difficult and somewhat subjective task. As groundwater in the upper parts of the boreholes was not saline enough for the method, only in situ formation factors in the lower parts of the boreholes were logged.

In KLX10 and KLX12A the formation factor had previously been measured in the laboratory on drill core samples. However, too few samples had been measured to enable a statistical analysis.

# Sammanfattning

Denna rapport presenterar mätningar och tolkningar av bergets formationsfaktor runt borrhålen KLX07A, KLX08, KLX10 och KLX12A i Laxemar, Sverige. Formations-faktorn har loggats in situ med elektriska metoder.

För KLX07A varierar den erhållna in situ formationsfaktorn för bergmatrisen från $4{,}1 \cdot 10^{-5}$ till $2{,}1 \cdot 10^{-4}$. Den erhållna in situ formationsfaktorn för sprickigt berg varierar från $2{,}1 \cdot 10^{-5}$ till $3{,}6 \cdot 10^{-3}$. Den erhållna formationsfaktordistributionen för bergmatrisen avviker från log-normal fördelningen. Emellertid erhölls endast ett begränsat antal datapunkter eftersom det omgivande berget till en hög grad är uppsprucket. Den erhållna formationsfaktordistributionen för sprickigt berg beskrivs tämligen väl av log-normal fördelningen. Medelvärdena och standardavvikelserna för de erhållna $\log_{10}$-normalfördelningarna är –4,1 och 0,17, samt –3,8 och 0,33 för in situ formationsfaktorn för bergmatrisen respektive sprickigt berg.

För KLX08 varierar den erhållna in situ formationsfaktorn för bergmatrisen från $1{,}1 \cdot 10^{-5}$ till $2{,}3 \cdot 10^{-4}$. Den erhållna in situ formationsfaktorn för sprickigt berg varierar från $1{,}0 \cdot 10^{-5}$ till $4{,}8 \cdot 10^{-3}$. Formationsfaktorerna är väl log-normalfördelade. Medelvärdena och standardavvikelserna för de erhållna $\log_{10}$-normalfördelningarna är –4,5 och 0,24, samt –4,4 och 0,34 för in situ formationsfaktorn för bergmatrisen respektive sprickigt berg.

För KLX10 varierar den erhållna in situ formationsfaktorn för bergmatrisen från $7{,}8 \cdot 10^{-6}$ till $2{,}2 \cdot 10^{-4}$. Den erhållna in situ formationsfaktorn för sprickigt berg varierar från $7{,}8 \cdot 10^{-6}$ till $3{,}9 \cdot 10^{-3}$. Formationsfaktorerna är tämligen väl log-normalfördelade. Medelvärdena och standardavvikelserna för de erhållna $\log_{10}$-normalfördelningarna är –4,5 och 0,32, samt –4,3 och 0,40 för in situ formationsfaktorn för bergmatrisen respektive sprickigt berg.

För KLX12A varierar den erhållna in situ formationsfaktorn för bergmatrisen från $1{,}3 \cdot 10^{-5}$ till $1{,}0 \cdot 10^{-4}$. Den erhållna in situ formationsfaktorn för sprickigt berg varierar från $1{,}3 \cdot 10^{-5}$ till $7{,}7 \cdot 10^{-4}$. Formationsfaktordistibutionerna beskrivs mindre väl av log-normalfördelningen och uppvisar dubbeltoppar. Detta kan bero på att borrhålet löper genom två olika bergdomäner. Medelvärdena och standardavvikelserna för de erhållna $\log_{10}$-normalfördelningarna är –4,5 och 0,25, samt –4,3 och 0,32 för in situ formations-faktorn för bergmatrisen respektive sprickigt berg.

För att erhålla profiler över grundvattnets elektriska konduktivitet i borrhålen användes kompletterande data från andra borrhål i Laxemarområdet. För KLX08 användes vidare data från porvattenkarakteriseringar. Det medges att valet av profiler över grundvattnets elektriska konduktivitet i borrhålen ofta är svårt och i viss grad subjektivt. Eftersom grundvattnet i den övre delen av borrhålen inte är salint nog för metoden loggades endast in situ formationsfaktorn i den nedre delen av borrhålen.

I KLX10 and KLX12A har man sedan tidigare erhållit formationsfaktorer i laboratoriet på prov från borrkärnor. Emellertid har för få prov mäts på för att ge underlag till en statistisk analys.

# Contents


**1 Introduction** 7

**2 Objective and scope** 9

**3 Equipment** 11
3.1 Rock resistivity measurements 11
3.2 Groundwater electrical conductivity measurements 11
3.3 Difference flow loggings 12
3.4 Boremap loggings 12

**4 Execution** 13
4.1 Theory 13
4.1.1 The formation factor 13
4.1.2 Surface conductivity 13
4.1.3 Artefacts 14
4.1.4 Fractures in situ 14
4.1.5 Rock matrix and fractured rock formation factor 15
4.2 Rock resistivity measurements in situ 16
4.2.1 Rock resistivity log KLX07A 16
4.2.2 Rock matrix resistivity log KLX07A 16
4.2.3 Fractured rock resistivity log KLX07A 16
4.2.4 Rock resistivity KLX08 17
4.2.5 Rock matrix resistivity log KLX08 17
4.2.6 Fractured rock resistivity log KLX08 18
4.2.7 Rock resistivity KLX10 18
4.2.8 Rock matrix resistivity log KLX10 18
4.2.9 Fractured rock resistivity log KLX10 20
4.2.10 Rock resistivity KLX12A 20
4.2.11 Rock matrix resistivity log KLX12A 20
4.2.12 Fractured rock resistivity log KLX12A 21
4.3 Groundwater EC measurements in situ 22
4.3.1 General comments 22
4.3.2 Groundwater flow in KLX07A, KLX08, KLX10 and KLX12A 22
4.3.3 EC measurements in KLX07A 26
4.3.4 EC measurements in KLX08 27
4.3.5 EC measurements in KLX10 30
4.3.7 EC measurements in KLX12A 31
4.3.8 Groundwater EC in KLX03–KLX06 32
4.3.9 EC profiles in KLX07A, KLX08, KLX10 and KLX12A 32
4.3.10 Electrical conductivity of the pore water 35
4.4 Formation factor measurements in the laboratory 35
4.5 Nonconformities 36

**5 Results** 37
5.1 General 37
5.2 In situ formation factors KLX07A 37
5.3 In situ formation factors KLX08 37
5.4 In situ formation factors KLX10 40
5.5 In situ formation factors KLX12A 40
5.6 Comparison of formation factor distibutions 43

**6 Summary and discussions** 45

**References** 47

**Appendix A** 49
Appendix A1: In situ rock resistivities and fractures KLX07A 49
Appendix A2: In situ rock resistivities and fractures KLX08 53
Appendix A3: In situ rock resistivities and fractures KLX10 58
Appendix A4: In situ rock resistivities and fractures KLX12A 63

**Appendix B** 67
Appendix B1: In situ formation factors KLX07A 67
Appendix B2: In situ formation factors KLX08 69
Appendix B3: In situ and laboratory formation factors KLX10 71
Appendix B4: In situ and laboratory formation factors KLX12A 75

# 1 Introduction

This document reports the data gained from measurements of the formation factor of rock surrounding the boreholes KLX07A, KLX08, KLX10 and KLX12A, within the site investigation at Laxemar. Comparisons are made with a few formation factors obtained in the laboratory on samples from the drill cores of KLX10 and KLX12A. The work was carried out in accordance with Activity Plan AP PS 400-06-129. In Table 1-1, controlling documents for performing this activity are listed. Both Activity Plan and Method Descriptions are SKB's internal controlling documents.

The formation factor was logged by electrical methods. Other contractors performed the fieldwork and laboratory work, and that work is outside the framework of this activity. The interpretation of in situ data and compilation of formation factor logs were performed by Kemakta Konsult AB in Stockholm, Sweden.

Figure 1-1 shows the Laxemar subarea and the locations of different boreholes. Boreholes KLX07A, KLX08, KLX10 and KLX12A are pointed out by the red arrows.

**Table 1-1. Controlling documents for performance of the activity.**

| **Activity Plan** | **Number** | **Version** |
|---|---|---|
| Bestämning av formationsfaktorn från in situ resistivitetsmätningar i KLX07A, KLX08; KLX10 och KLX11A* | AP PS 400-06-129 | 1.0 |
| **Method Descriptions** | **Number** | **Version** |
| Bestämning av formationsfaktorn med elektriska metoder | SKB MD 530.007 | 1.0 |

*The AP was initially intended for work on KLX11A, which was in a later stage changed to KLX12A.

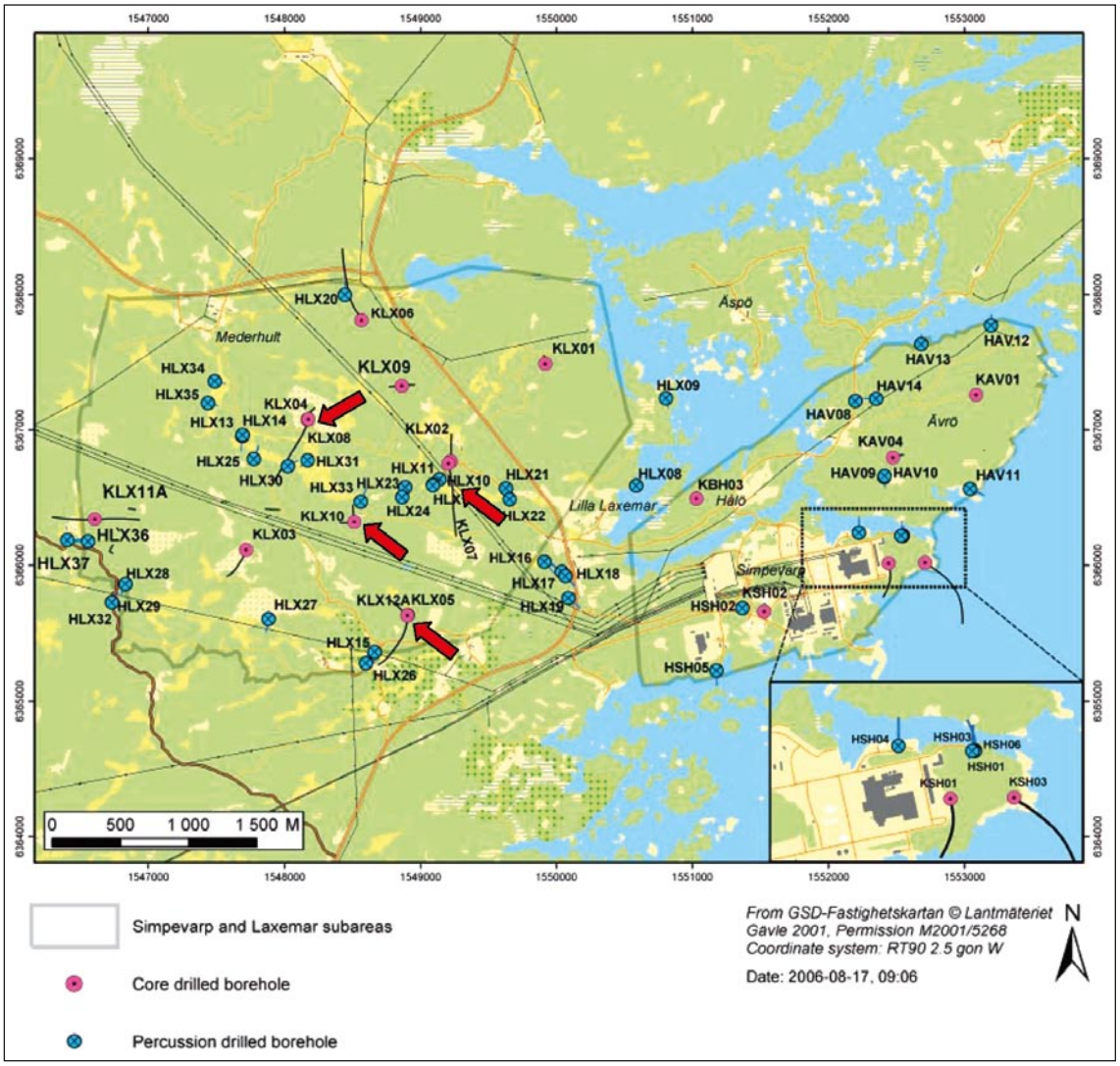


***Figure 1-1.*** *General overview over the Laxemar subarea.*

# 2 Objective and scope

The formation factor is an important parameter that may be used directly in safety assessment calculation of radionuclide transport in crystalline rock. The main objective of this work is to obtain the formation factor of the rock mass surrounding the boreholes KLX07A, KLX08, KLX10 and KLX12A. This has been achieved by performing formation factor loggings by electrical methods both in situ and in the laboratory. The in situ method gives a great number of formation factors obtained under more natural conditions than in the laboratory. To obtain the in situ formation factor, results from previous loggings were used. The laboratory formation factor was obtained by performing measurements on a few rock samples from the drill cores of KLX10 and KLX12A. Other contractors carried out the fieldwork and laboratory work.

# 3 Equipment

## 3.1 Rock resistivity measurements

The resistivity of the rock surrounding the boreholes KLX07A /1/, KLX08 /2/, KLX10 /3/ and KLX12A /4/ was logged using the focused rock resistivity tool Century 9072. The tool emits an alternating current perpendicular to the borehole axis from a main current electrode. The shape of the current field is controlled by electric fields emitted by guard electrodes. By using a focused tool, the disturbance from the borehole is minimised. The quantitative measurement range of the Century 9072 tool is 0–50,000 ohm.m according to the manufacturer. In the site investigations the rock resistivity may also be logged using the Century 9030 tool. However, this tool may not be suitable for quantitative logging in granitic rock and the results are not used in this report.

## 3.2 Groundwater electrical conductivity measurements

The EC (electrical conductivity) of the borehole fluid in KLX07A /5/, KLX08 /6/, KLX10 and KLX12A /7/ was logged using the POSIVA difference flow meter. The tool is shown in Figure 3-1.

When logging the EC of the borehole fluid, the lower rubber disks of the tool are not used. During the measurements, a drawdown can either be applied or not. Measurements were carried out before and after extensive pumping in the boreholes.

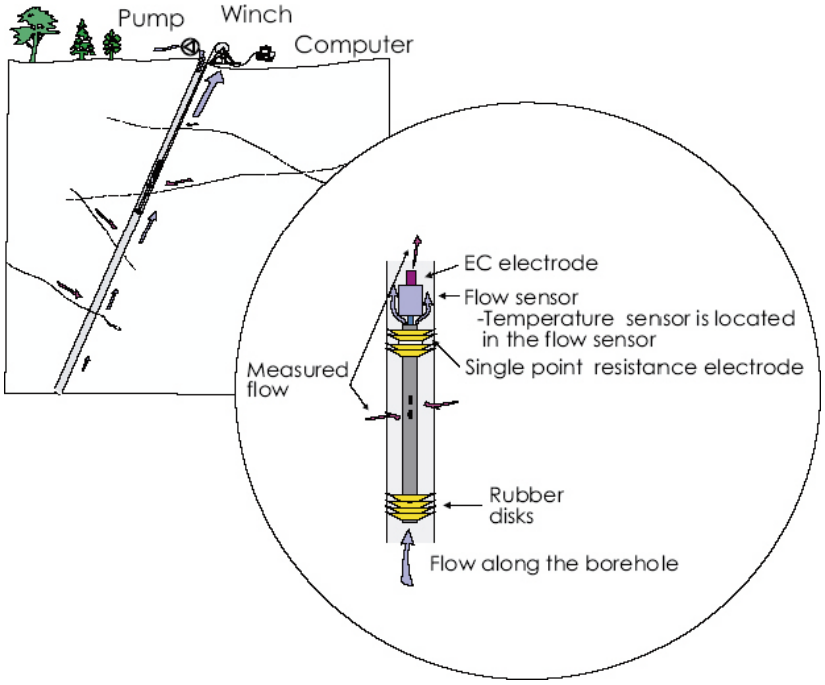


***Figure 3-1.*** *Schematics of the POSIVA difference flow meter (image taken from /5/).*

When using both the upper and the lower rubber disks, a section around a specific fracture can be packed off. By applying a drawdown at the surface, groundwater can thus be extracted from specific fractures. This is done in fracture specific EC measurements. By also measuring the groundwater flow out of the fracture, it is calculated how long time it will take to fill up the packed off borehole section three times. During this time the EC is measured and a transient EC curve is obtained. After this time it is assumed that the measured EC is representative for the groundwater flowing out of the fracture. The measurements may be disturbed by leakage of borehole fluid into the packed off section and development of gas from species dissolved in the groundwater. Interpretations of transient EC curves are discussed in /8/. The quantitative measurement range of the EC electrode of the POSIVA difference flow meter is 0.02–11 S/m.

In KLX08 samples were taken from the drill core for subsequent analysis of the chemical composition of the pore water (matrix fluid) /9/. In doing this, the samples were insulated by a protective wrapping to prevent evaporation directly upon drilling. The samples were then brought to the laboratory where the pore water was leached. The methodology is described in /e.g. 9/.

## 3.3 Difference flow loggings

By using the POSIVA difference flow meter, hydraulically conductive fractures can be located. The tool, shown in Figure 3-1, has a flow sensor and the flow from fractures in packed off sections can be measured. When performing these measurements, both the upper and the lower rubber disks are used. Measurements can be carried out both with and without applying a drawdown. The quantitative measurement range of the flow sensor is 0.1–5,000 ml/min.

Difference flow loggings were performed in different campaigns in KLX07A /5/, KLX08 /6/, KLX10 and KLX12A /7/.

## 3.4 Boremap loggings

The drill cores of KLX07A /10/, KLX08 /11/, KLX10 and KLX12A were logged together with a simultaneous study of video images of the borehole wall. This is called Boremap logging.

In the core log, fractures parting the core are recorded. Fractures parting the core that have not been induced during the drilling or core handling are called broken fractures. To decide if a fracture actually was open or sealed in the rock volume (i.e. in situ), SKB has developed a confidence classification expressed at three levels, “possible”, “probable” and “certain”, based on the weathering and fit of the fracture surfaces. However, there is a strong uncertainty associated with determining whether broken fractures were open or not before drilling /12/. For this reason, it was decided to treat all broken fractures as potentially open in situ in this present report.

In the Boremap logging, parts of the core that are crushed or lost are also recorded, as well as the spatial distribution of different rock types.

# 4 Execution

## 4.1 Theory

### 4.1.1 The formation factor

The theory applied for obtaining formation factors by electrical methods is described in /13/. The formation factor is the ratio between the diffusivity of the rock matrix to that of free pore water. If the species diffusing through the porous system is much smaller than the characteristic length of the pores and no interactions occur between the mineral surfaces and the species, the formation factor is only a geometrical factor that is defined by the transport porosity, the tortuosity and the constrictivity of the porous system:

$$F_f = \frac{D_e}{D_w} = \varepsilon_t \frac{\delta}{\tau^2} \qquad 4\text{-}1$$

where $F_f$ (–) is the formation factor, $D_e$ ($m^2/s$) is the effective diffusivity of the rock, $D_w$ ($m^2/s$) is the diffusivity in the free pore water, $\varepsilon_t$ (–) is the transport porosity, $\tau$ (–) is the tortuosity, and $\delta$ (–) is the constrictivity. When obtaining the formation factor with electrical methods, the Einstein relation between diffusivity and ionic mobility is used:

$$D = \frac{\mu RT}{zF} \qquad 4\text{-}2$$

where D ($m^2/s$) is the diffusivity, $\mu$ ($m^2/V{\cdot}s$) is the ionic mobility, z (–) the charge number and R (J/mol·K), T (K) and F (C/mol), are the gas constant, temperature, and Faraday constant, respectively. From the Einstein relation it is easy to show that the formation factor also is given by the ratio of the pore water resistivity to the resistivity of the saturated rock /14/:

$$F_f = \frac{\rho_w}{\rho_r} \qquad 4\text{-}3$$

where $\rho_w$ ($\Omega$m) is the pore water resistivity and $\rho_r$ ($\Omega$m) is the rock resistivity. The resistivity of the saturated rock can easily be obtained by standard geophysical methods.

At present it is not feasible to extract pore water from the rock matrix in situ. Therefore, it is assumed that the pore water is in equilibrium with the free water surrounding the rock, and measurements are performed on this free water. The validity of this assumption has to be discussed for every specific site.

In a new line of experiments, species in the pore water in drill core samples brought to the laboratory are leached. This has been done for a number of boreholes and was also done in KLX08 /9/. From the measured chloride content the EC of the pore water can be assessed. The assessed pore water EC was used as an integrated part when assessing the electrical conductivity profiles of the groundwater in KLX08 in this present report.

The resistivity is the reciprocal to electrical conductivity. Traditionally the EC (electrical conductivity) is used when measuring on water and resistivity is used when measuring on rock.

### 4.1.2 Surface conductivity

In intrusive igneous rock the mineral surfaces are normally negatively charged. As the negative charge often is greater than what can be balanced by cations specifically adsorbed on the mineral surfaces, an electrical double layer with an excess of mobile cations will form at the pore wall. If a potential gradient is placed over the rock, the excess cations in the electrical

double layer will move. This process is called surface conduction and this additional conduction may have to be accounted for when obtaining the formation factor of rock saturated with a pore water of low ionic strength. If the EC of the pore water is around 0.5 S/m or above, errors associated with surface conduction are deemed to be acceptable. This criterion is based on laboratory work by /15/ and /16/. The effect of the surface conduction on rock with formation factors below $1 \cdot 10^{-5}$ was not investigated in these works. In this report, surface conduction has not been accounted for, as in general only the groundwater in the upper 100 or 200 m of the boreholes has a low ionic strength and as more knowledge is needed on surface conduction before performing corrections.

### 4.1.3 Artefacts

Comparative studies have been performed on a large number of 1–2 cm long samples from Äspö /15/. Formation factors obtained with an electrical resistivity method using alternating current were compared to those obtained by a traditional through diffusion method, using Uranine as the tracer. The results show that formation factors obtained by the electrical resistivity measurements are a factor of about 2 times larger that those obtained by through diffusion measurements. A similar effect was found on granitic samples up to 12 cm long from Laxemar, using iodide in tracer experiments /17/. The deviation of a factor 2 between the methods may be explained by anion exclusion of the anionic tracers. Previously performed work suggests that the Nernst-Einstein equation between the diffusivity and electrical conductivity is generally applicable in granitic rock and that no artefacts give rise to major errors. It is uncertain, however, to what extent anion exclusion is related to the degree of compression of the porous system in situ due to the overburden.

### 4.1.4 Fractures in situ

In situ rock resistivity measurements are highly disturbed by free water in open fractures. The current sent out from the downhole tool in front of an open fracture will be propagated both in the porous system of the rock matrix and in the free water in the open fracture. Due to the low formation factor of the rock matrix, current may be preferentially propagated in a fracture intersecting the borehole if its aperture is on the order of $10^{-5}$ m or more.

There could be some confusion concerning the terminology of fractures. In order to avoid confusion, an organization sketch of different types of fractures is shown in Figure 4-1. The subgroups of fractures that interfere with the rock resistivity measurements are marked with grey.

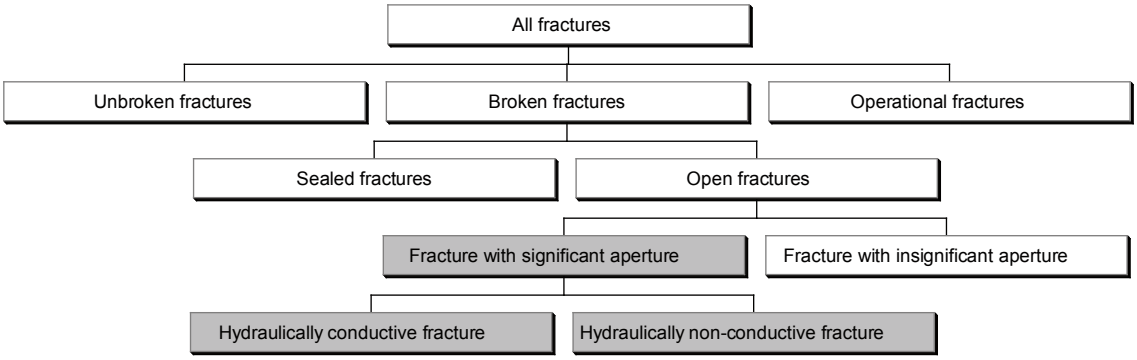


***Figure 4-1.*** *Organization sketch of different types of fractures in situ.*

The information concerning different types of fractures in situ is obtained from the interpretation of the Boremap logging and in the hydraulic flow logging. A fracture intersecting the borehole is most likely to part the drill core. In the core log, fractures that part the core are either broken or operational (drill-induced). Unbroken fractures, which do not part the core, are sealed or only partly open. Laboratory results suggest that sealed fractures generally have no major interference on rock resistivity measurements. The water-filled void in partly open fractures can be included in the porosity of the rock matrix.

Broken fractures are either interpreted as open or sealed. Open fractures may have a significant or insignificant aperture. With insignificant aperture means an aperture so small that the amount of water held by the fracture is comparable with that held in the adjacent porous system. In this case the "adjacent porous system" is the porous system of the rock matrix the first few centimetres from the fracture.

If the fracture has a significant aperture, it holds enough water to interfere with the rock resistivity measurements. Fractures with a significant aperture may be hydraulically conductive or non-conductive, depending on how they are connected to the fracture network.

Due to uncertainties in the interpretation of the core logging, all broken fractures are assumed to potentially have a significant aperture in this present report.

### 4.1.5 Rock matrix and fractured rock formation factor

In this report the rock resistivity is used to obtain formation factors of the rock surrounding the borehole. The obtained formation factors may later be used in models for radionuclide transport in fractured crystalline rock. Different conceptual approaches may be used in the models. Therefore this report aims to deliver formation factors that are defined in two different ways. The first is the "rock matrix formation factor", denoted by $F_f^{rm}$ (–). This formation factor is representative for the solid rock matrix, as the traditional formation factor. The other one is the "fractured rock formation factor", denoted by $F_f^{fr}$ (–), which represents the diffusive properties of a larger rock mass, where fractures and voids holding stagnant water is included in the porous system of the rock matrix. Further information on the definition of the two formation factors could be found in /8/.

The rock matrix formation factor is obtained from rock matrix resistivity data. When obtaining the rock matrix resistivity log from the in situ measurements, all resistivity data that may have been affected by open fractures have to be sorted out. With present methods one cannot with certainty separate open fractures with a significant aperture from open fractures with an insignificant aperture in the interpretation of the core logging. It should be mentioned that there is an attempt to assess the fracture aperture in the interpretation of the core logging. However, this is done on a millimetre scale. Fractures may be significant even if they only have apertures some tens of micrometers.

By investigating the rock resistivity log at a fracture, one could draw conclusions concerning the fracture aperture. However, for formation factor logging by electrical methods this is not an independent method and cannot be used. Therefore, all broken fractures have to be considered as potentially open and all resistivities obtained close to a broken fracture detected in the core logging are sorted out. By examining the resistivity logs obtained by the Century 9072 tool, it has been found that resistivity values obtained within 0.5 m from a broken fracture generally should be sorted out. This distance includes a safety margin of 0.1–0.2 m.

The fractured rock formation factor is obtained from fractured rock resistivity data. When obtaining the fractured rock resistivity log from the in situ measurements, all resistivity data that may have been affected by free water in hydraulically conductive fractures, detected in the in situ flow logging, have to be sorted out. By examining the resistivity logs obtained by the Century 9072 tool, it has been found that resistivity values obtained within 0.5 m from a hydraulically conductive fracture generally should be sorted out. This distance includes a safety margin of 0.1–0.2 m.

## 4.2 Rock resistivity measurements in situ

### 4.2.1 Rock resistivity log KLX07A

The rock resistivity of KLX07A was logged on the date 2005-07-05 (SICADA activity id 13078634) /1/. The in situ rock resistivity was obtained using the focused rock resistivity tool Century 9072. In situ rock resistivities, used in this present report, were obtained between the borehole lengths 103.0–834.0 m. According to /1/ an accurate depth calibration was obtained.

### 4.2.2 Rock matrix resistivity log KLX07A

All resistivity data obtained within 0.5 m from a broken fracture, detected in the core log, were sorted out from the in situ rock resistivity log. In the core log (SICADA activity id 13078634), a total of 3,152 broken fractures are recorded between 102.0–835.7 m. 44 zones where the core has been crushed lost are recorded. A total of 20.5 m of the core has been crushed or lost. Broken fractures can potentially intersect the borehole in zones where the core is crushed or lost. Therefore, a broken fracture was assumed every decimetre in these zones. The locations of broken fractures in KLX07A are shown in Appendix A1. A total of 713 rock matrix resistivities were obtained between 103.0–834.0 m. 99.6% of the rock matrix resistivities were within the quantitative measurement range of the Century 9072 tool. The rock matrix resistivity log between 103.0–834.0 m is shown in Appendix A1.

Figure 4-2 shows the distribution of the rock matrix resistivities obtained between 103.0–834.0 m in KLX07A. The histogram ranges from 0–100,000 Ωm and is divided into sections of 5,000 Ωm.

### 4.2.3 Fractured rock resistivity log KLX07A

All resistivity data obtained within 0.5 m from a hydraulically conductive fracture, detected in the difference flow logging /5/, were sorted out from the in situ rock resistivity log. For the difference flow log, no correction in the reported borehole length was needed. A total of 240 hydraulically conductive fractures were detected in KLX07A between 100.1–829.6 m.

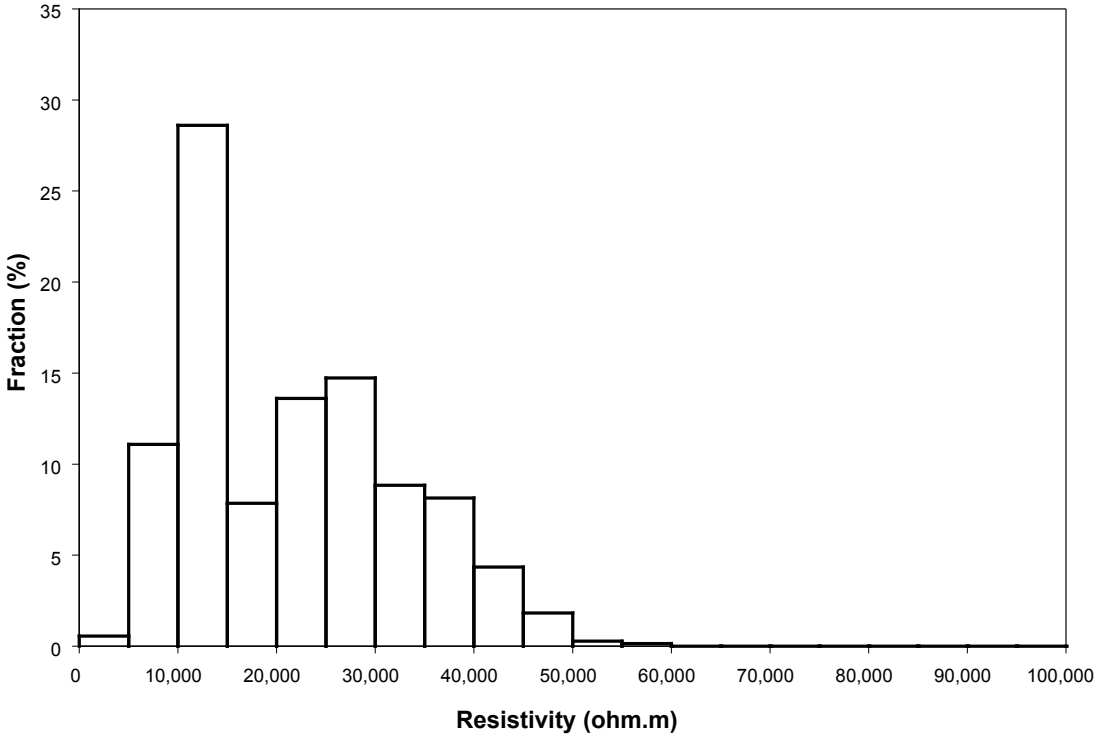


***Figure 4-2.*** *Distribution of rock matrix resistivities in KLX07A.*

The locations of hydraulically conductive fractures in KLX07A are shown in Appendix A1. A total of 4,979 fractured rock resistivities were obtained between 103–829 m. 99.1% of the fractured rock resistivities were within the quantitative measurement range of the Century 9072 tool. The fractured rock resistivity log between 103–829 m is shown in Appendix A1.

Figure 4-3 shows a histogram of the fractured rock resistivities obtained between 103–829 m in KLX07A. The histogram ranges from 0–100,000 Ωm and is divided into sections of 5,000 Ωm.

### 4.2.4 Rock resistivity KLX08

The rock resistivity of KLX08 was logged on the date 2005-10-25 (SICADA activity id 13089212) /2/. The in situ rock resistivity was obtained using the focused Century 9072 tool. In situ rock resistivities, used in this present report, were obtained between the borehole lengths 102.1–988.8 m. According to /2/ an accurate depth calibration was obtained.

### 4.2.5 Rock matrix resistivity log KLX08

All resistivity data obtained within 0.5 m from a broken fracture, detected in the core log, were sorted out from the in situ rock resistivity log. In the core log (SICADA activity id 13083977), a total of 2,219 broken fractures are recorded between 101.0–993.4 m. In addition 35 zones where the core is crushed or lost are recorded. A total of 9.8 m of the core is crushed or lost. Broken fractures can potentially intersect the borehole in zones where the core is crushed or lost. Therefore, a broken fracture was assumed every decimetre in these zones. The locations of broken fractures in KLX08 are shown in Appendix A2. A total of 1,980 rock matrix resistivities were obtained between 102.1–988.8 m. 82% of the rock matrix resistivities were within the quantitative measurement range of the Century 9072 tool. The rock matrix resistivity log between 102.1–988.8 m is shown in Appendix A2.

Figure 4-4 shows a histogram of the rock matrix resistivities obtained between 102.1–988.8 m in KLX08. The histogram ranges from 0–100,000 Ωm and is divided into sections of 5,000 Ωm.

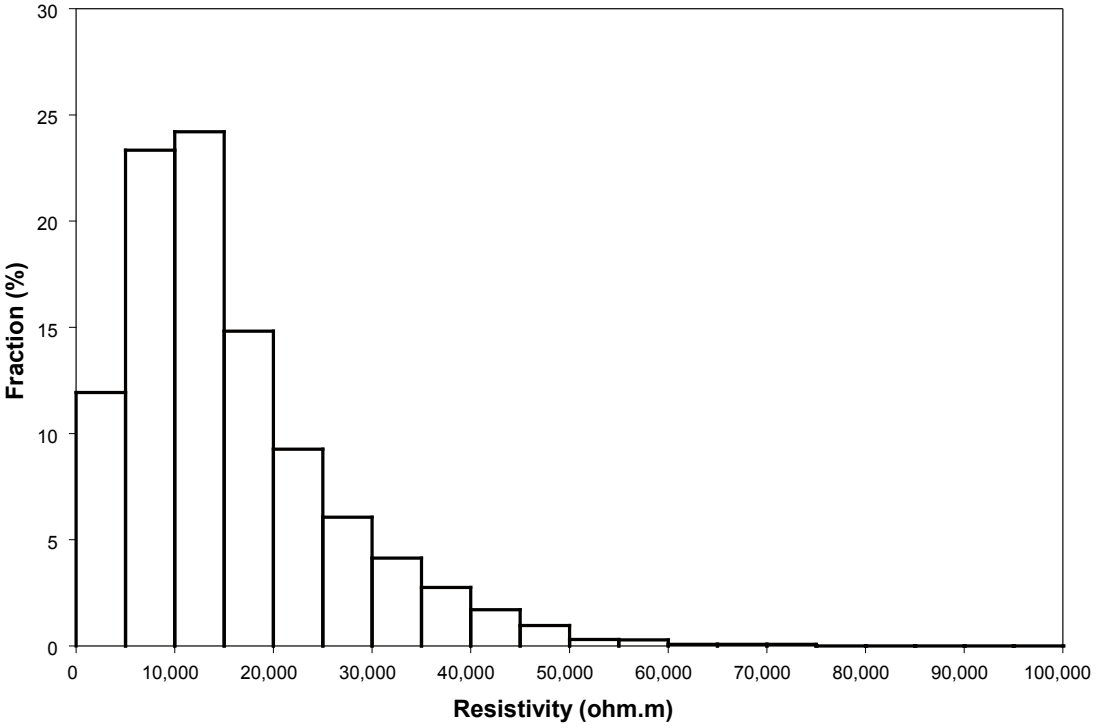


***Figure 4-3.*** *Histogram of fractured rock resistivities in KLX07A.*

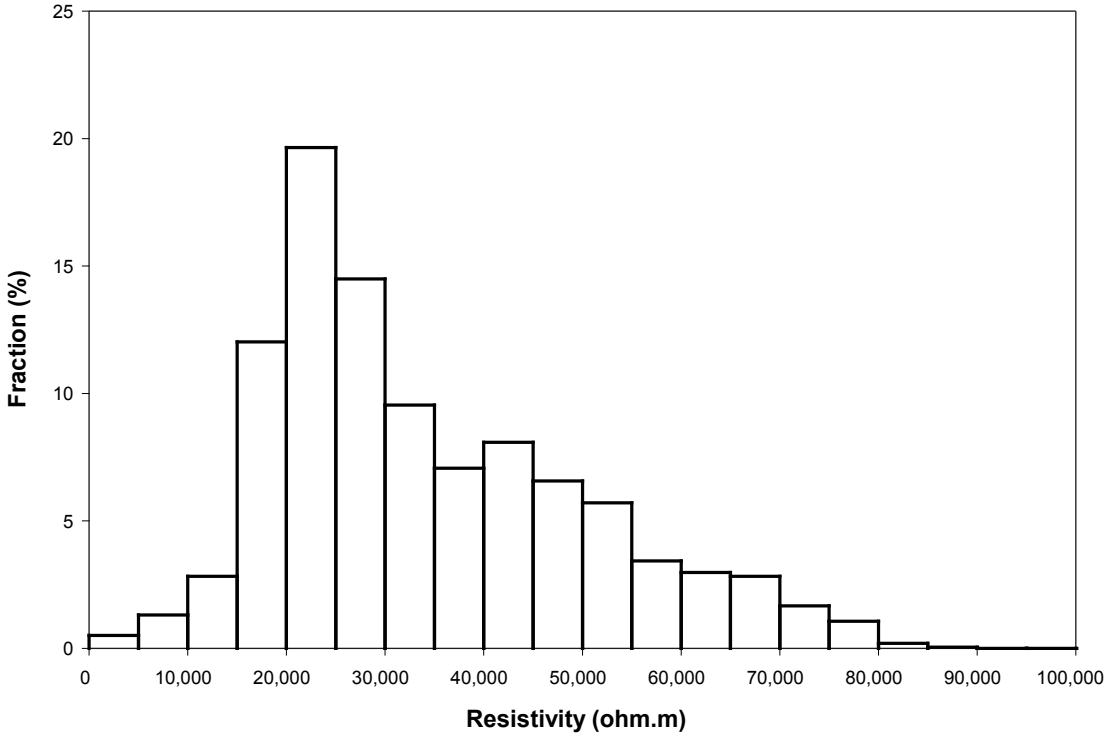


***Figure 4-4.*** *Histogram of rock matrix resistivities in KLX08.*

### 4.2.6 Fractured rock resistivity log KLX08

All resistivity data obtained within 0.5 m from a hydraulically conductive fracture, detected in the difference flow logging /6/, were sorted out from the in situ rock resistivity log. For the difference flow log, no correction in the reported borehole length was needed. A total of 138 hydraulically conductive fractures were detected in KLX08 between 100–982 m. The locations of hydraulically conductive fractures in KLX08 are shown in Appendix A2. A total of 7,518 fractured rock resistivities were obtained between 102.1–982 m. 90% of the fractured rock resistivities were within the quantitative measurement range of the Century 9072 tool. The fractured rock resistivity log between 102.1–982 m is shown in Appendix A2.

Figure 4-5 shows a histogram of the fractured rock resistivities obtained between 102.1–982 m in KLX08. The histogram ranges from 0–100,000 Ωm and is divided into sections of 5,000 Ωm.

### 4.2.7 Rock resistivity KLX10

The rock resistivity of KLX10 was logged on the date 2005-11-17 (SICADA activity id 13094107) /3/. The in situ rock resistivity was obtained using the focused Century 9072 tool. In situ rock resistivities, used in this present report, were obtained between the borehole lengths 101.7–999.5 m. According to /3/ an accurate depth calibration was obtained.

### 4.2.8 Rock matrix resistivity log KLX10

All resistivity data obtained within 0.5 m from a broken fracture, detected in the core log, were sorted out from the in situ rock resistivity log. In the core log (SICADA activity id 13132089), a total of 2,576 broken fractures are recorded between 101.9–996.5 m. In addition 29 zones where the core is crushed or lost are recorded. A total of 11.1 m of the core is crushed or lost. Broken fractures can potentially intersect the borehole in zones where the core is crushed or lost. Therefore, a broken fracture was assumed every decimetre in these zones. The locations of broken fractures in KLX10 are shown in Appendix A3. A total of 2,412 rock matrix resistivities

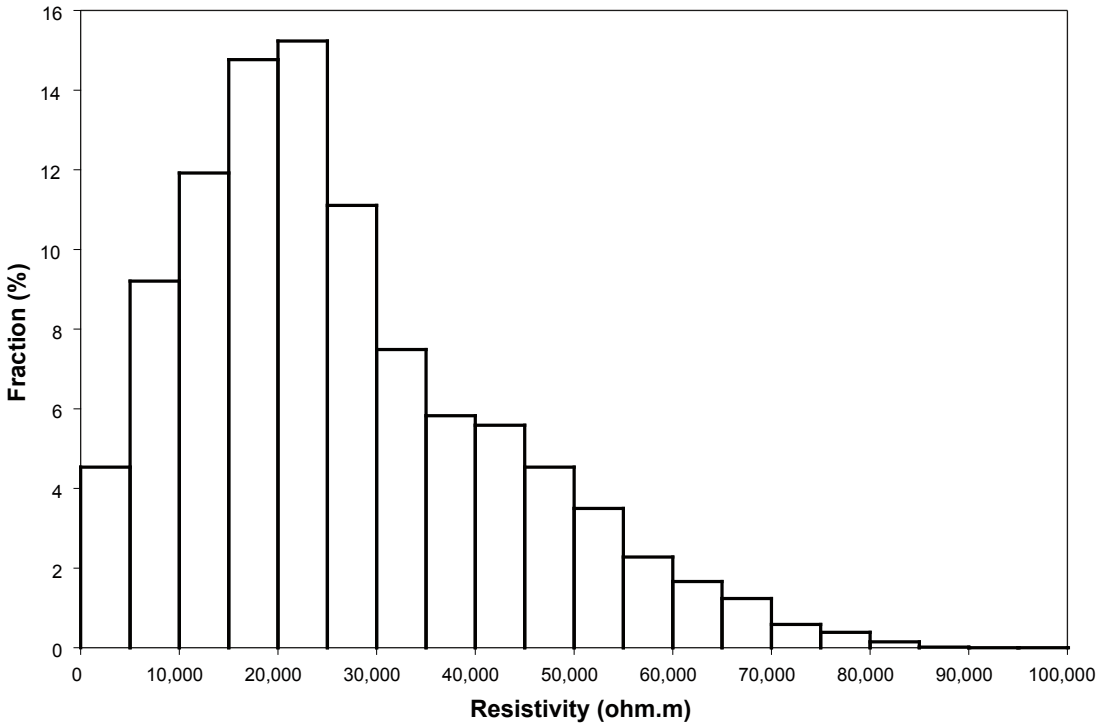


***Figure 4-5.*** *Histogram of fractured rock resistivities in KLX08.*

were obtained between 101.9–996.5 m. 85% of the rock matrix resistivities were within the quantitative measurement range of the Century 9072 tool. The rock matrix resistivity log between 101.9–996.5 m is shown in Appendix A3.

Figure 4-6 shows a histogram of the rock matrix resistivities obtained between 101.9–996.5 m in KLX10. The histogram ranges from 0–100,000 Ωm and is divided into sections of 5,000 Ωm.

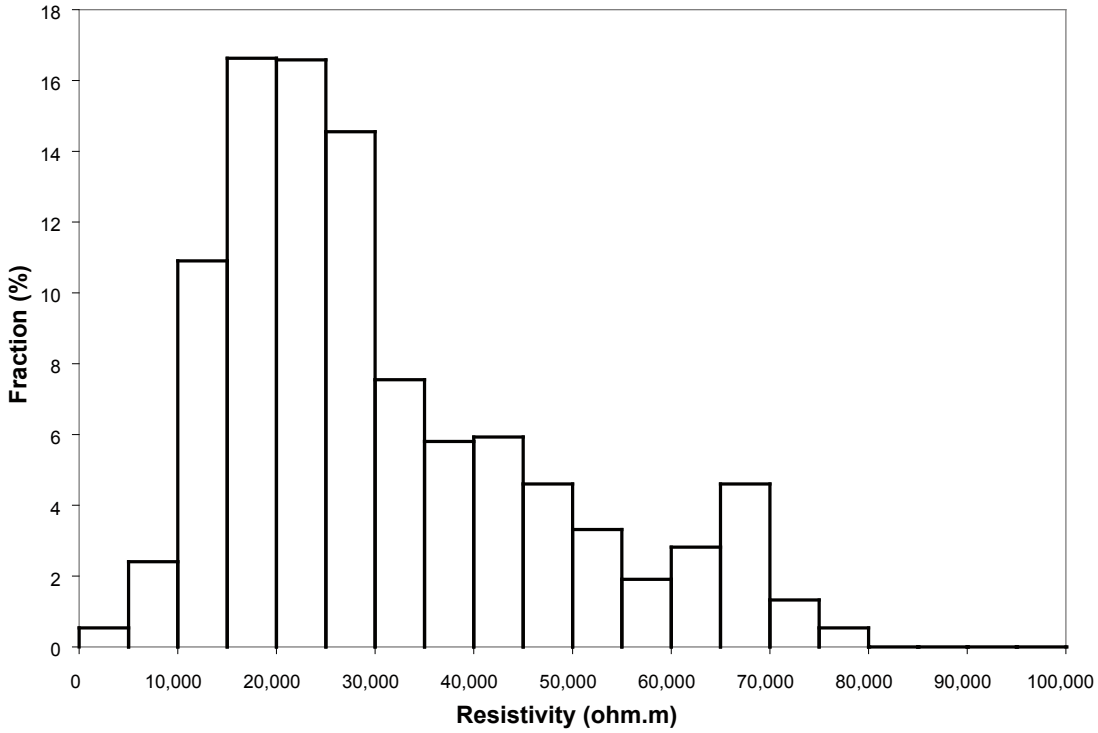


***Figure 4-6.*** *Histogram of rock matrix resistivities in KLX10.*

### 4.2.9 Fractured rock resistivity log KLX10

All resistivity data obtained within 0.5 m from a hydraulically conductive fracture, detected in the difference flow logging, were sorted out from the in situ rock resistivity log. For the difference flow log, no correction in the reported borehole length was needed. A total of 191 hydraulically conductive fractures were detected in KLX10 between 92.2–996.2 m (SICADA activity id 13098945). The locations of hydraulically conductive fractures in KLX10 are shown in Appendix A3. A total of 7,265 fractured rock resistivities were obtained between 101.7–996.2 m. 92% of the fractured rock resistivities were within the quantitative measurement range of the Century 9072 tool. The fractured rock resistivity log between 101.7–996.2 m is shown in Appendix A3.

Figure 4-7 shows a histogram of the fractured rock resistivities obtained between 101.7–996.2 m in KLX10. The histogram ranges from 0–100,000 Ωm and is divided into sections of 5,000 Ωm.

### 4.2.10 Rock resistivity KLX12A

The rock resistivity of KLX12A was logged on the date 2006-03-22 (SICADA activity id 13107192) /4/. The in situ rock resistivity was obtained using the focused Century 9072 tool. In situ rock resistivities, used in this present report, were obtained between the borehole lengths 103.7–598.8 m. However, there is a larger gap in the data between 138.8–171.6 m. According to /2/ an accurate depth calibration was obtained.

### 4.2.11 Rock matrix resistivity log KLX12A

All resistivity data obtained within 0.5 m from a broken fracture, detected in the core log, were sorted out from the in situ rock resistivity log. In the core log (SICADA activity id 13134837), a total of 1,225 broken fractures are recorded between 102.0–601.0 m. In addition 58 zones

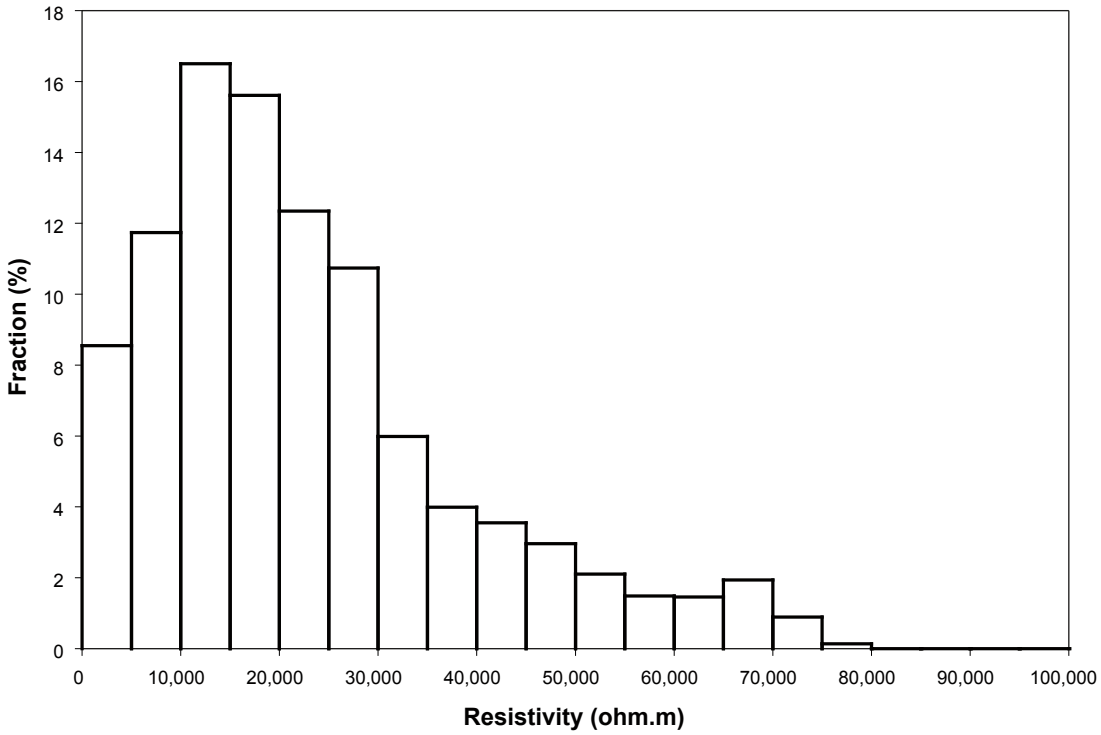


***Figure 4-7.*** *Histogram of fractured rock resistivities in KLX10.*

where the core is crushed or lost are recorded. A total of 5.5 m of the core is crushed or lost. Broken fractures can potentially intersect the borehole in zones where the core is crushed or lost. Therefore, a broken fracture was assumed every decimetre in these zones. The locations of broken fractures in KLX12A are shown in Appendix A4. A total of 448 rock matrix resistivities were obtained between 103.7–598.8 m. Only 66% of the rock matrix resistivities were within the quantitative measurement range of the Century 9072 tool. The rock matrix resistivity log between 103.7–598.8 m is shown in Appendix A4.

Figure 4-8 shows a histogram of the rock matrix resistivities obtained between 103.7–598.8 m in KLX12A. The histogram ranges from 0–100,000 Ωm and is divided into sections of 5,000 Ωm.

### 4.2.12 Fractured rock resistivity log KLX12A

All resistivity data obtained within 0.5 m from a hydraulically conductive fracture, detected in the difference flow logging /7/, were sorted out from the in situ rock resistivity log. For the difference flow log, no correction in the reported borehole length was needed. A total of 76 hydraulically conductive fractures were detected in KLX12A between 97–596.2 m. The locations of hydraulically conductive fractures in KLX12A are shown in Appendix A4. A total of 4,088 fractured rock resistivities were obtained between 103.7–596.2 m. 84% of the fractured rock resistivities were within the quantitative measurement range of the Century 9072 tool. The fractured rock resistivity log between 103.7–596.2 m is shown in Appendix A4.

Figure 4-9 shows a histogram of the fractured rock resistivities obtained between 103.7–596.2 m in KLX12A. The histogram ranges from 0–100,000 Ωm and is divided into sections of 5,000 Ωm.

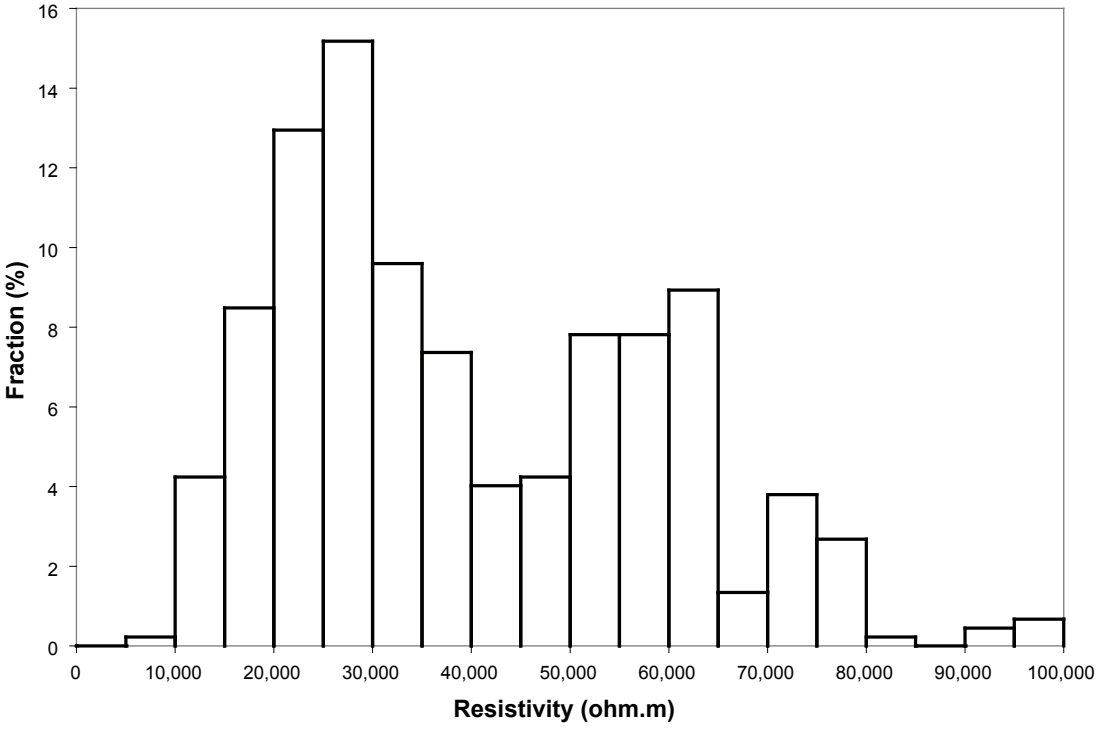


***Figure 4-8.*** *Histogram of rock matrix resistivities in KLX12A.*

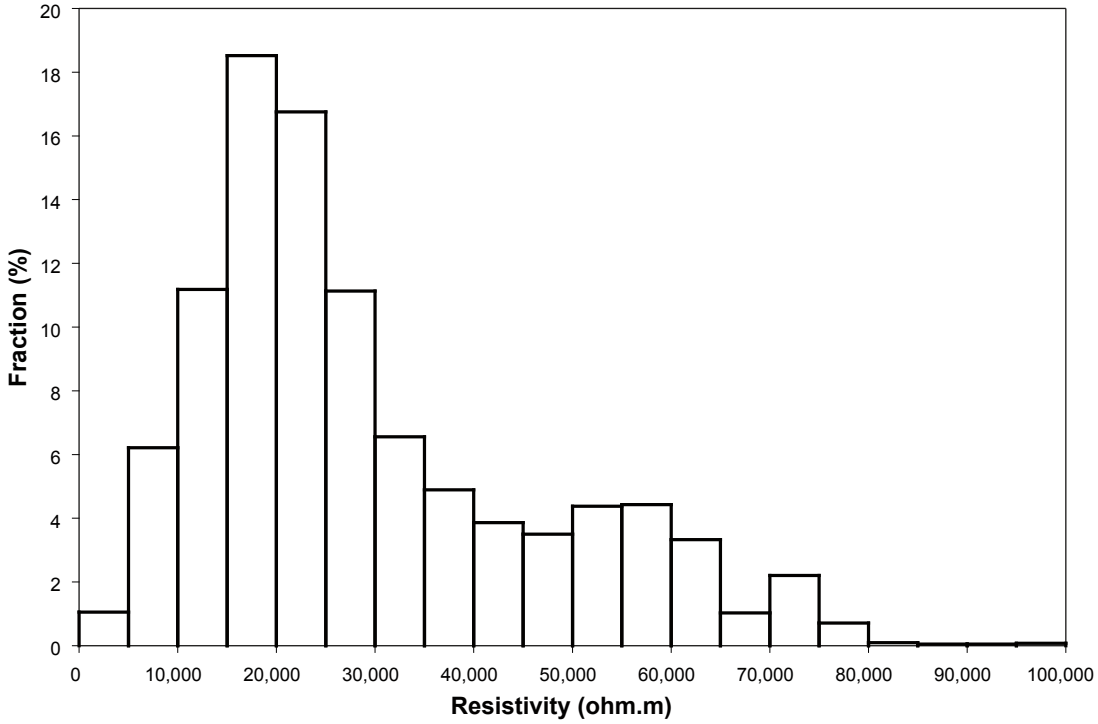


***Figure 4-9.*** *Histogram of fractured rock resistivities in KLX12A.*

## 4.3 Groundwater EC measurements in situ

### 4.3.1 General comments

In background reports concerning the EC of the groundwater, some data have been corrected for temperature, so that they correspond to data at 25°C. Other EC data are uncorrected. Data that correspond to the temperature in situ should be used in in situ evaluations. Even though these corrections are small in comparison to the natural variation of the formation factor, measures have been taken to use data that correspond to the in situ temperature. Such data can be found in SICADA /18/.

Concerning borehole coordinates, unless specifically stated when the elevation is discussed, the borehole length is used.

### 4.3.2 Groundwater flow in KLX07A, KLX08, KLX10 and KLX12A

When performing chemical characterisations of the groundwater at depth at the Laxemar subarea, the representativeness of the data should be considered, due to the hydraulic situation of the site. When a borehole is drilled it functions as a hydraulic conductor, short-circuiting different hydraulic systems that the borehole intersects. At Laxemar, the hydraulic gradients in the open boreholes are large and this results in large flows of groundwater in the boreholes. The fact that groundwater quickly flows from one depth to another in a borehole may affects the representativeness of the groundwater data obtained at a specific depth.

When measuring a fracture specific EC, by using the POSIVA difference flow meter or in the hydrochemical characterisations, a small section of the borehole is packed off. Water is then withdrawn from the fracture/fractures in the packed off borehole section and its EC is measured. However, if a large quantity of groundwater, representative for another depth, has flown along the short-circuiting borehole and into the fractures for weeks before the measurement, one can question the representativeness of the data obtained of that specific depth. It should be clarified that the measurements themselves may be accurate and still non-representative.

In measurements in KLX07A /5/, KLX08 /6/, KLX10 and KLX12A /7/, 5-metre sections have been packed off and the flow in or out of the boreholes in these sections has been measured by the POSIVA difference flow meter. This has been done when applying no drawdown. The entire boreholes, except for the upper 100 metres or so, have been logged in this way by moving the tool stepwise. Based on these flow data, the flow along the boreholes when performing no pumping can be assessed. When doing this, a few assumptions are made.

1) If the flow in a section is below the measurement limit of the tool, no flow is accounted for.
2) It is assumed that there is no flow in or out of the lower end of the borehole.
3) The flow in and out of the borehole should be equal. In many cases no flow measurements are performed in the upper 100 m. This may be due to a casing or to other reasons. This is handled by lumping the in- and outflows, distributed over the section, into one in- or outflow term at ground surface.

Figure 4-10 shows the flow situation in borehole KLX07A. The red diamonds show the flow, where one could be found, into or out from the borehole in the packed off sections. A positive value represents a flow into the borehole and a negative value represents a flow out from the borehole. The grey line shows the flow along the borehole required to feed the in- and outflows. A positive value represents a flow down the borehole and a negative value represents a flow up the borehole.

As can be seen in Figure 4-10 there is a major flow down the borehole. The borehole diameter is 76 mm, which is the diameter of all the boreholes of interest for this report. A flow of $4.5 \cdot 10^3$ ml/h along the borehole axis corresponds to a plug flow velocity of the borehole fluid of about 1 m/h. In KLX07A, the plug flow velocity at the borehole length 100 m should be about 80 m/h. Groundwater from the upper 100 m should reach down to the major outflow point at 762 m within a 24-hour period and down to 823 m within a week. The groundwater flow down the borehole was measured in situ at the borehole length 102 m to $2.0 \cdot 10^5$ ml/h when performing no pumping /5/. Based on a mass balance approach, the flow down the borehole was assessed to $3.7 \cdot 10^5$ ml/h in this report. The deviation may be partly due to experimental errors and partly to fractures with a flow below the measurement limit of the tool. Such fractures were detected when using a drawdown. In addition it is likely that the position of the tool somewhat affects the flow in the borehole. When measuring the flow in or out of a fracture, the small fracture aperture poses the largest resistance to the flow. When measuring the flow down the borehole, the tool blocks a part of the borehole cross section (see Figure 3-1), which should reduce the flow. Other artefacts are also possible but the measurement confirms a large flow down the borehole.

Figure 4-11 shows the flow situation in KLX08. The legends are the same as in Figure 4-10.

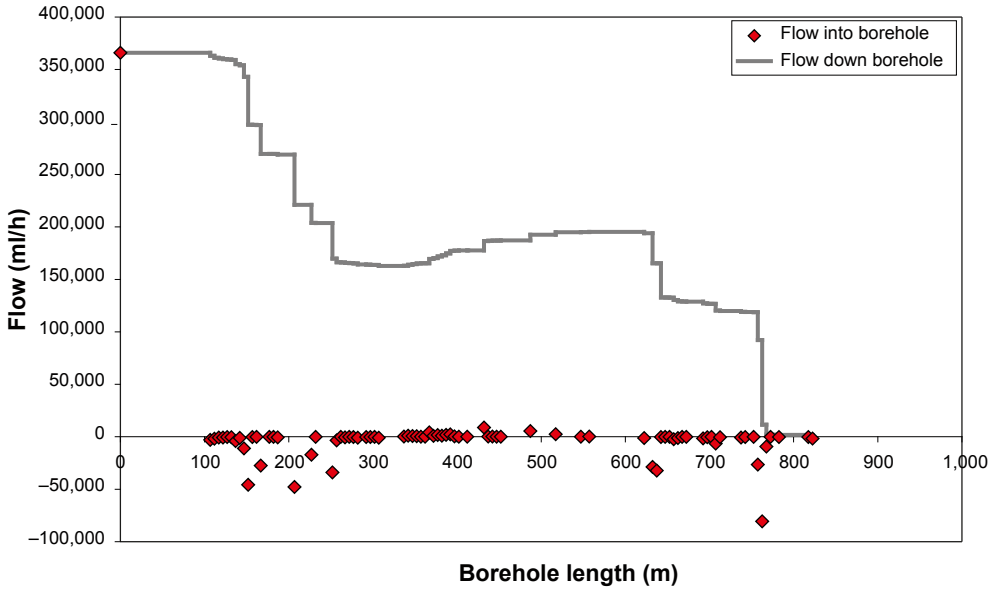


***Figure 4-10.*** *Flow into/out from and down/up borehole KLX07A.*

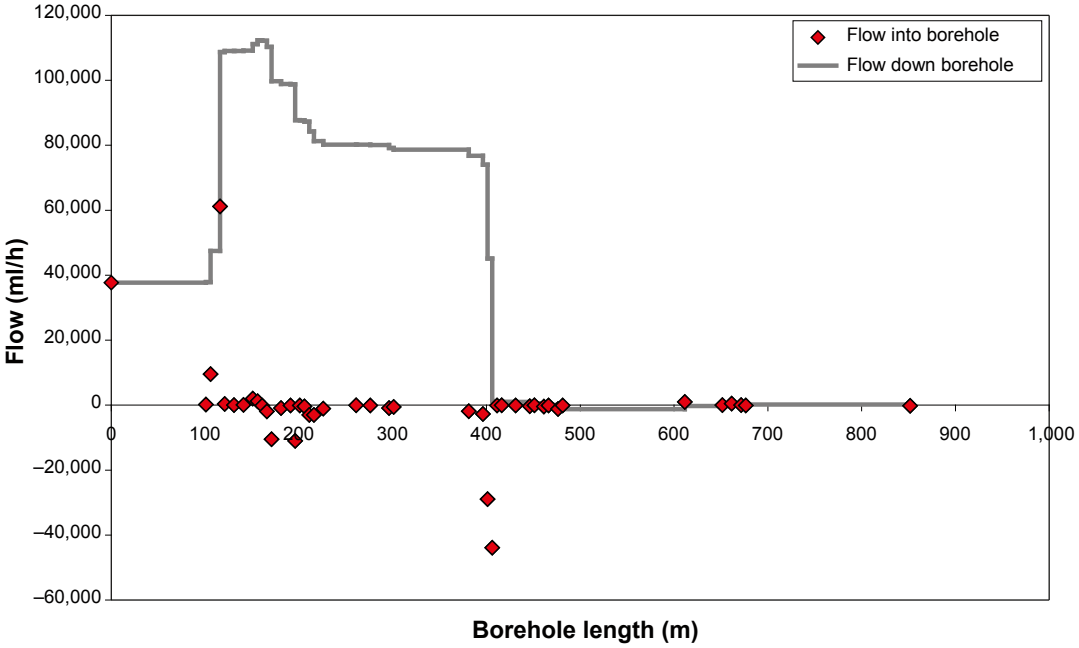


***Figure 4-11.*** *Flow into/out from and down/up borehole KLX08.*

As one can see by the grey line in Figure 4-11, there is a substantial flow down the borehole down to about 406 m. The groundwater flow down the borehole was measured in situ at the borehole length 101 m to about $6.6 \cdot 10^4$ ml/h when performing no pumping /6/. Based on the mass balance approach, the flow down the borehole was assessed to $3.8 \cdot 10^4$ ml/h in this report. Water from the upper 100 m of the borehole should penetrate down to 406 m within a 24-hour period. According to the mass balance there is a slight flow up the borehole below 406 m originating from the inflow at 611 m. Determining the direction of such a small flow based on so many measuring points is somewhat speculative but the flow direction is supported by interpretations of the borehole fluid EC log, discussed in association with Figure 4-15.

Figure 4-12 shows the flow situation in KLX10 based on the sequential PFL flow logging (SICADA activity id 13098957). The legends are the same as in Figure 4-10.

As one can see by the grey line in Figure 4-12, there is a significant, but not major, flow down the borehole down to about 317 m, with a plug flow velocity of between 2–3 m/h. According to the mass balance there is a flow up the borehole between 317 and 427 m, while below 427 m there is a downward flow to 698 m. It can be expected that at repository depth and below, there is little interference of groundwater flowing from near surface rock. However, at the end of the borehole where no fractures could be found when not pumping, there is a risk that drilling fluid still remains. When performing pumping, an additional hydraulically conductive section in the lower part of the borehole was found at around 840 m.

Figure 4-13 shows the flow situation in KLX12A based on the sequential PFL flow logging (SICADA activity id 13117651). The legends are the same as in Figure 4-10.

As one can see by the grey line in Figure 4-13, there is a small flow down the borehole down to about 393 m with a plug flow velocity of less than 0.4 m/h. The exception is for just above 200 m where there, according to the mass balance, is an upward flow for a short distance. The borehole is only 601 m long and when pumping, the lowest hydraulically conductive section was found at about 545 m.

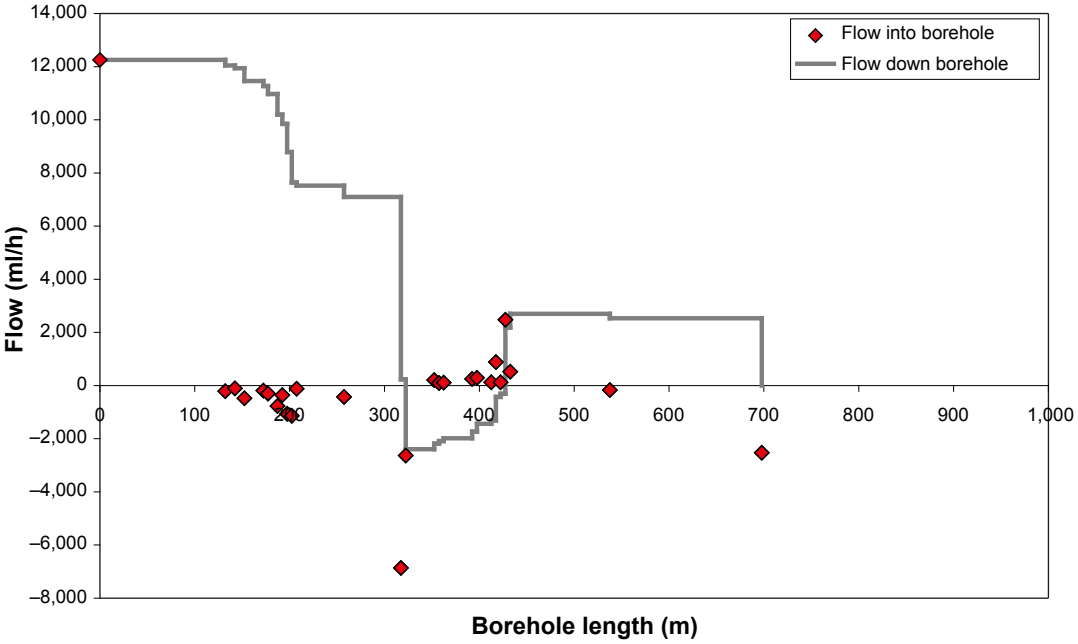


***Figure 4-12.*** *Flow into/out from and down/up borehole KLX10.*

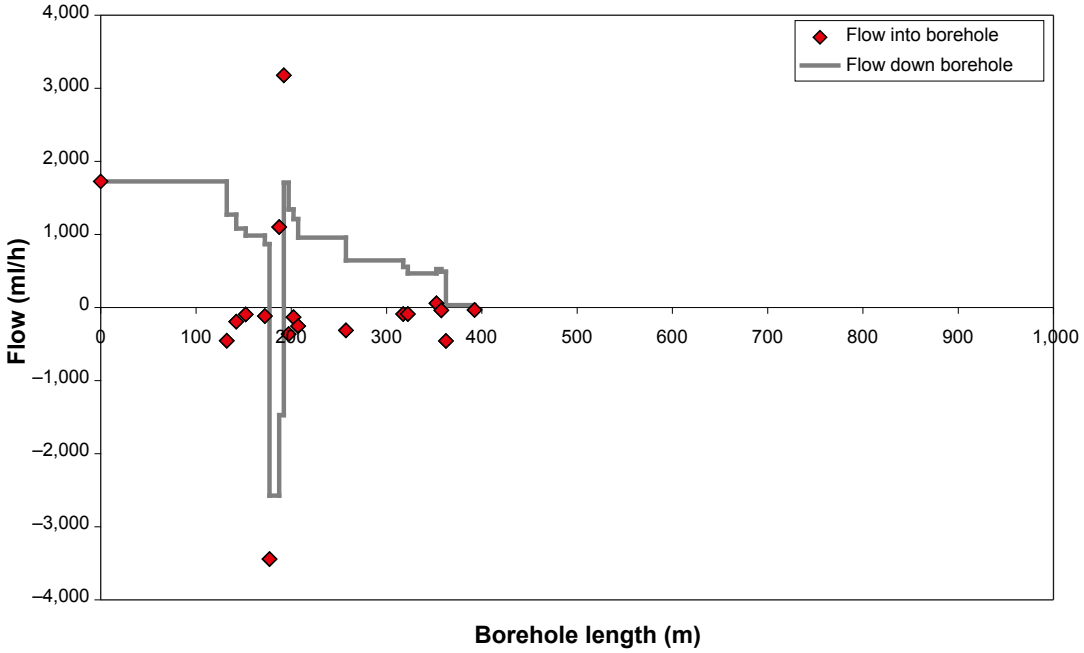


***Figure 4-13.*** *Flow into/out from and down/up borehole KLX12A.*

### 4.3.3 EC measurements in KLX07A

The EC of the borehole fluid in KLX07A was measured before and after performing extensive pumping on the dates 2005-06-12 and 2005-06-22, respectively /5/. The lines in Figure 4-14 represent the borehole fluid EC logs obtained before (blue) and after (green) performing extensive pumping. The EC of the borehole fluid was measured both when lowering the tool down and when winching the tool up the borehole, hence the four borehole fluid EC logs. The fracture specific EC was measure on five locations on the date 2005-06-22 and the obtained fracture specific ECs are shown in Figure 4-14 as black crosses. The purple dots represent transient (time series) fracture specific ECs.

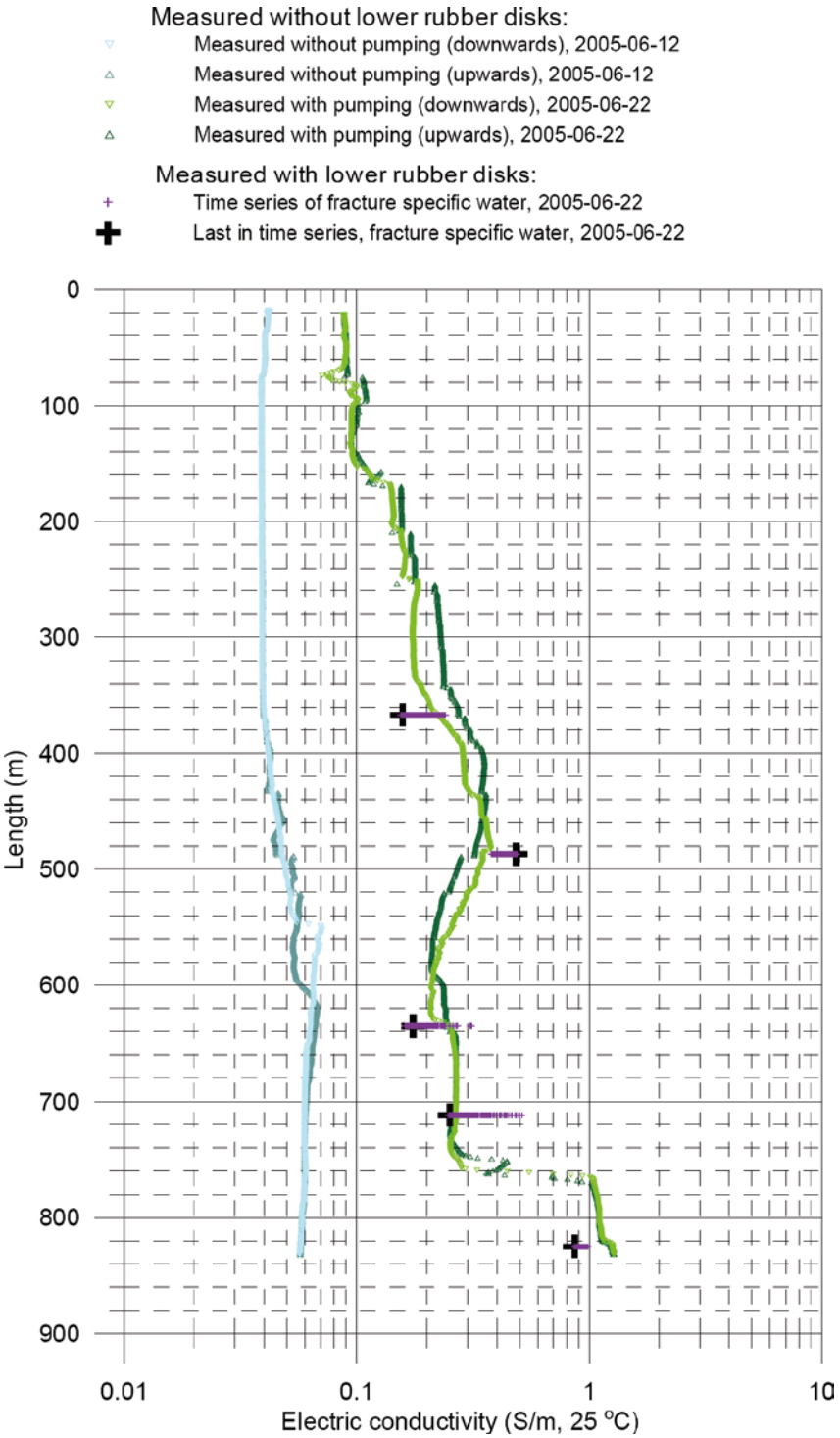


***Figure 4-14.*** *EC logs in KLX07A. Image taken from /5/.*

Prior to the campaign, and the pumping, it appears that non-saline water from shallow depth had penetrated down the full length of the borehole. As a result of the pumping, groundwater in hydraulically conductive fractures in the rock mass surrounding the borehole was withdrawn into and up the borehole, hence increasing the salinity and EC of the borehole fluid. From the borehole fluid EC logs one can draw the conclusion that in the lowest part of the borehole, the fracture specific EC is at least 1 S/m at 25°C.

From Figure 4-10 one can see that when no pumping is performed, large quantities of groundwater flowing from shallow rock (and potentially overburden) penetrates the borehole down to around 825 m. If groundwater originating from shallower depth has flown down the borehole and into a fracture system for a long period of time, one may question the representativeness of the groundwater EC obtained at depth, even if reversing the hydraulic gradient for a few days or weeks.

In KLX07A, five fracture specific ECs were obtained by using the POSIVA difference flow meter /15/ on the date 2005-06-22. Data are shown in Table 4-1. By inspecting the transient fracture specific EC curves /15/, all measurements seem to have been carried out without any problems.

In Table 4-1, the elevation is calculated from borehole length using a designated tool in SICADA /18/. In the sequential flow logging performed without applying a drawdown, it was identified that at 367.4 m and 487.4 m, groundwater flows into the borehole. Therefore, the fracture specific ECs obtained here were judged as representative for those borehole lengths. At the other fractures in Table 4-1, groundwater flows into the fracture system from the borehole when not pumping and considering the large groundwater flows down the borehole, the fracture specific ECs obtained here were judged as dubious. These values are put in parentheses in Table 4-1.

From the borehole fluid EC logs shown in Figure 4-10 (green curves), there is evidence that in the lower part of the borehole, groundwater with an EC of 1.04 S/m (at in situ temperature) or potentially higher can be withdrawn. The "fracture specific" EC at the lower end of the borehole (at 835.7 m) was assigned this value. It is recognised that this value may be affected by shallower water and also drilling fluid but it is still judged as acceptable.

### 4.3.4 EC measurements in KLX08

The EC of the borehole fluid in KLX08 was measured before and after extensive pumping in a difference flow logging campaign on the dates 2005-10-08 and 2005-10-16, respectively /6/. The lines in Figure 4-15 represent the borehole fluid EC logs obtained before (turquoise) and after (green) performing the pumping. The fracture specific EC was measure on five locations on the date 2005-10-15 and the obtained fracture specific ECs are shown in Figure 4-15 as black crosses. The purple dots represent transient fracture specific ECs.

**Table 4-1. Fracture specific ECs, KLX07A.**

| Measurment | Borehole section (m) | Location of fracture Borehole length (m) | Location of fracture Elevation (m.a.s.l.) | EC in situ (S/m) | EC 25°C (S/m)[1] |
|---|---|---|---|---|---|
| Frac. Spec. EC | 366.66–367.66 | 367.4 | –265.18 | 0.11[2] | 0.16 |
| Frac. Spec. EC | 486.99–487.99 | 487.4 | –350.11 | 0.36[2] | 0.48 |
| Frac. Spec. EC | 635.21–636.21 | 635.7 | –465.76 | (0.14)[2] | (0.17) |
| Frac. Spec. EC | 712.00–713.00 | 712.4 | –525.73 | (0.20)[2] | (0.25) |
| Frac. Spec. EC | 825.17–826.17 | 825.5 | –613.48 | (0.71)[2] | (0.86) |
| Borehole fluid | End of borehole | 844.7 | –628.31 | 1.04[3] | |

[1] Data from /5/.
[2] Data from /SICADA activity id 13078282/.
[3] Data from /SICADA activity id 13092035/.

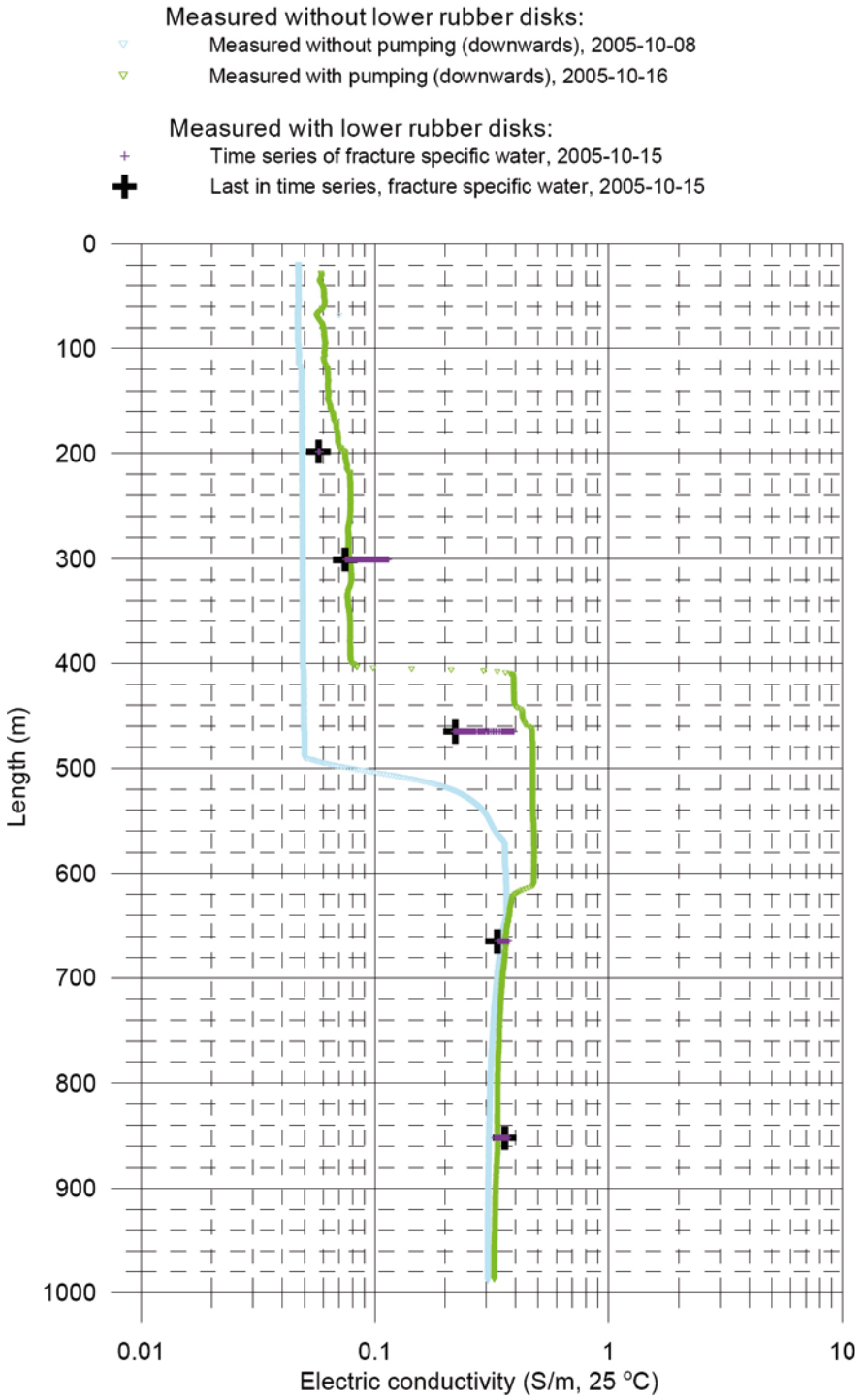


***Figure 4-15.*** *EC logs in KLX08. Image taken from /6/.*

The borehole fluid EC logs, showing unusually low ECs in the lower part of the borehole, suggest that groundwater from shallow depths has penetrated down the entire borehole. Even after pumping, no major increase in the borehole fluid EC was achieved, which indicates that saline water could not be withdrawn from fractures at depth with the applied hydraulic gradients over the time period of the pumping (although not necessarily that no saline water exists at depth).

By inspecting the transient fracture specific EC curves /6/, all measurements, except for that at 852 m, seem to have been carried out without any problems. At 852 m there appear to have been some initial problems in the measurement. In the sequential flow logging performed without applying a drawdown, it was identified that at 664.8 m groundwater flows into the borehole. Therefore, the fracture specific EC obtained here was judged as representative. At the other

fractures in Table 4-2, groundwater flows into the fracture system and based on the reasoning above, the fracture specific ECs obtained were judged as dubious and put in parentheses in Table 4-2.

In Table 4-2, the elevation is calculated from borehole length using a designated tool in SICADA /18/.

In addition to measuring the fracture specific EC at certain depths, an attempt was made to obtain the chloride concentration of the matrix fluid (pore water) of samples taken from the drill core /9/. Table 4-3 shows the obtained chloride concentrations. In order to convert chloride concentrations to EC data (at 25°C), an equation taken from /19/ was used:

$$EC\ (S/m) = 0.37 + 0.22 \cdot Cl^{-}\ (g/kg\ H_2O) \qquad 4\text{-}4$$

Even though this equation was intended for the Forsmark site, the relation between the chloride concentration and EC should not deviate much from site to site in the range of interest for formation factor measurements. To correct the obtained EC data at 25°C to EC data at in situ temperatures, the same temperature correction as used in /6/ was used at corresponding depth (based on SICADA activity id 13089178). The result is shown in Table 4-3.

It should be carefully noted that Equation 4-4 may poorly represent the groundwater of Oskarshamn below the EC range of interest for formation factor measurements (EC < 0.5 S/m). EC data in the upper 700 m of the borehole shown in Table 4-3 may thus be dubious.

**Table 4-2. Fracture specific ECs, KLX08.**

| Measurment | Borehole section (m) | Location of fracture Borehole length (m) | Location of fracture Elevation (m.a.s.l.) | EC in situ (S/m)[1] | EC 25°C (S/m)[2] |
|---|---|---|---|---|---|
| Frac. Spec. EC | 198.31–198.81 | 198.5 | –147.75 | (0.040) | (0.060) |
| Frac. Spec. EC | 300.97–301.47 | 301.2 | –236.69 | (0.054) | (0.070) |
| Frac. Spec. EC | 464.99–465.49 | 465.2 | –377.74 | (0.17) | (0.22) |
| Frac. Spec. EC | 664.70–665.20 | 664.8 | –548.36 | 0.27 | 0.34 |
| Frac. Spec. EC | 852.10–852.60 | 852.4 | –707.67 | (0.31) | (0.36) |

[1] Data from /SICADA activity id 13089175/.
[2] Data from /6/.

**Table 4-3. Matrix fluid ECs in KLX08.**

| SICADA Activity id | Borehole length (m) | Elevation (m.a.s.l.) | Chloride concentration (mg $Cl^-$/kg) | EC at 25°C (S/m) | EC at in situ temperature (S/m) |
|---|---|---|---|---|---|
| 13134285 | 150.00 | –105.64 | 99 | 0.39 | 0.27 |
| 13134286 | 199.30 | –148.45 | 139 | 0.40 | 0.28 |
| 13134287 | 200.07 | –149.11 | 164 | 0.41 | 0.29 |
| 13134288 | 250.07 | –192.49 | 117 | 0.40 | 0.28 |
| 13134289 | 302.17 | –237.52 | 705 | 0.53 | 0.38 |
| 13134290 | 346.92 | –276.06 | 773 | 0.54 | 0.40 |
| 13134291 | 395.49 | –317.86 | 365 | 0.45 | 0.33 |
| 13134293 | 499.66 | –407.26 | 614 | 0.51 | 0.39 |
| 13134294 | 550.10 | –450.42 | 998 | 0.59 | 0.46 |
| 13134295 | 601.54 | –494.37 | 240 | 0.42 | 0.33 |
| 13134296 | 659.90 | –544.18 | 388 | 0.46 | 0.37 |
| 13134297 | 701.86 | –579.94 | 687 | 0.52 | 0.42 |
| 13134298 | 750.64 | –621.44 | 1,534 | 0.71 | 0.59 |
| 13134299 | 802.06 | –665.10 | 2,722 | 0.97 | 0.82 |
| 13134300 | 857.82 | –712.24 | 2,764 | 0.98 | 0.84 |
| 13134301 | 903.10 | –750.28 | 6,059 | 1.70 | 1.49 |
| 13134302 | 945.69 | –785.91 | 3,041 | 1.04 | 0.92 |
| 13134303 | 983.00 | –817.00 | 8,228 | 2.18 | 1.96 |

### 4.3.5 EC measurements in KLX10

The EC of the borehole fluid in KLX10 was measured before and after extensive pumping in a difference flow logging campaign on the dates 2005-12-10 and 2005-12-20, respectively. The blue curves in Figure 4-16 represent the borehole fluid EC logged downwards (SICADA activity id 13098854) and upwards (SICADA activity id 13100557) before performing the pumping. The green curves in Figure 4-16 represent the borehole fluid EC logged downwards (SICADA activity id 13098947) and upwards (SICADA activity id 13100558) after performing the pumping. The fracture specific EC (SICADA activity id 13098946) was measured on five locations on the dates 2005-12-19 and 2005-12-20 and the obtained fracture specific ECs are shown in Figure 4-16 as black crosses. The purple dots represent transient fracture specific ECs.

If examining the assumed flow situation in the borehole (Figure 4-12), there will be a flow down the borehole to the borehole length about 320 m. Below this depth, groundwater from around 430 m will flow both up the borehole and down the borehole down to about 700 m. Below 700 m the water should be fairly stagnant and potentially the drilling fluid remains. This assumed flow situation nicely explains the EC profile of the borehole fluid obtained before performing pumping (blue curves). As a result, the borehole fluid EC obtained before pumping at around 430 m should correspond to the fracture specific EC at that borehole length.

By inspecting the transient fracture specific EC curves, all measurements seem to have been carried out without any problems. In the sequential flow logging performed without applying a drawdown, it was identified that at 353.9 m groundwater flows into the borehole. At 538.9 m only a very minute flow from the borehole into the fractures was measured and at 119.7 m and 842.7 m, no flow was detected. Therefore the fracture specific ECs obtained at these borehole lengths are judged as representative. At 669.9 m, groundwater flows from the borehole into the fracture system at a significant rate and therefore the fracture specific EC obtained is judged as dubious and put in parentheses in Table 4-4.

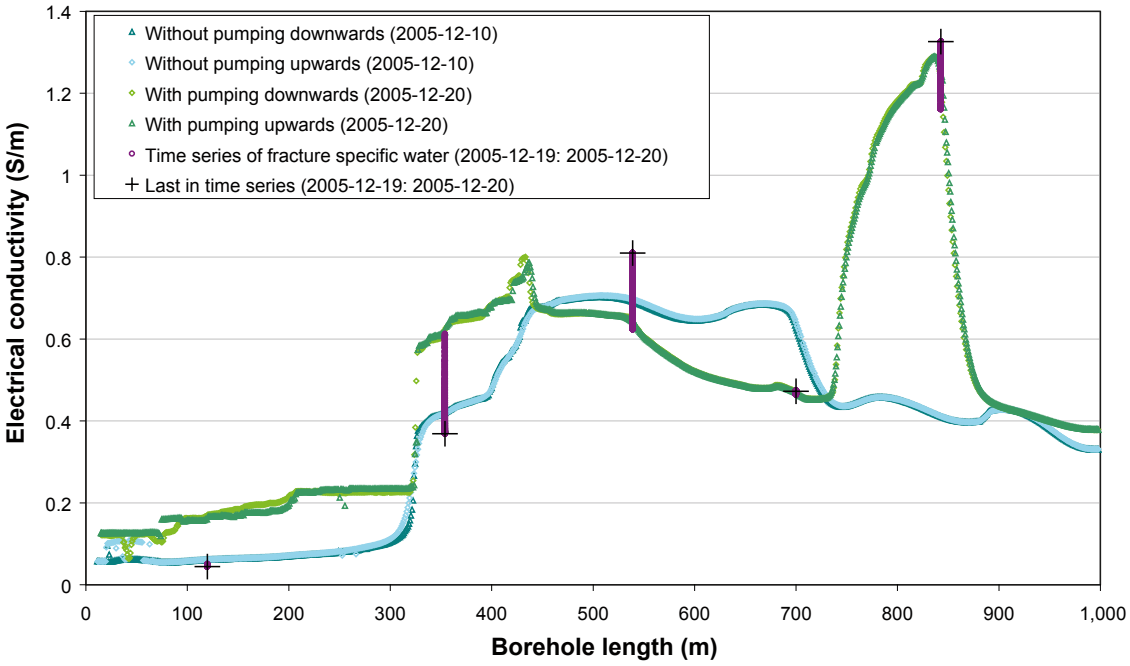


***Figure 4-16.*** *In situ temperature EC logs in KLX10. Data taken from /18/.*

**Table 4-4. Fracture specific ECs, KLX10.**

| Measurment | Borehole length (m) | Elevation (m.a.s.l.) | EC at in situ temperature (S/m) |
|---|---|---|---|
| Frac. Spec. EC | 119.7 | –100.64 | 0.045 |
| Frac. Spec. EC | 353.9 | –333.42 | 0.37 |
| Borehole fluid EC | 430 | –409.15 | 0.62 |
| Frac. Spec. EC | 538.9 | –517.50 | 0.81 |
| Frac. Spec. EC | 699.9 | –677.66 | (0.47) |
| Frac. Spec. EC | 842.7 | –819.62 | 1.33 |

### 4.3.7 EC measurements in KLX12A

The EC of the borehole fluid in KLX12A was measured before and after extensive pumping in a difference flow logging campaign on the dates 2006-06-09 and 2006-06-15, respectively. The blue curves in Figure 4-17 represent the borehole fluid EC logged downwards (SICADA activity id 13117652) and upwards (SICADA activity id 13117653) before performing the pumping. The green curves in Figure 4-17 represent the borehole fluid EC logged downwards (SICADA activity id 13117655) and upwards (SICADA activity id 13117656) after performing the pumping. The fracture specific EC (SICADA activity id 13118190) was measured on five locations on the dates 2006-06-14 and 2006-06-15 and the obtained fracture specific ECs are shown in Figure 4-17 as black crosses. The purple dots represent transient fracture specific ECs.

By inspecting the transient fracture specific EC curves /7/, all measurements except for at 139.3 m seem to have been carried out without any problems. At 139.3 m there may have been leakage of borehole fluid past the packers and into the tool and the obtained EC is put in parenthesis in Table 4-5. As the flow along the borehole is small (Figure 4-13) all other fracture specific ECs were judged as representative.

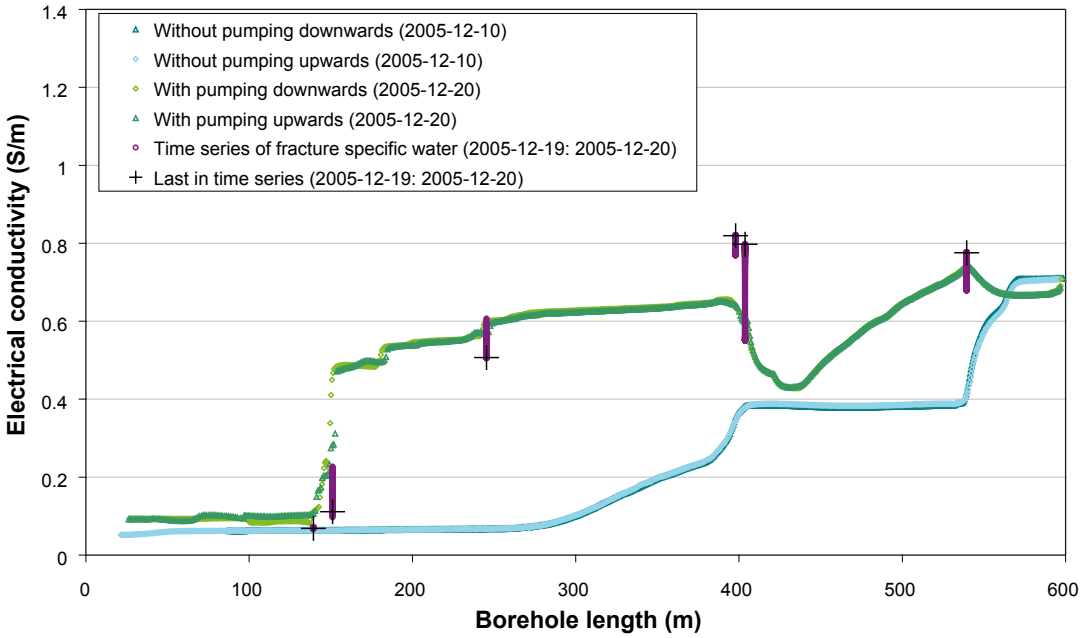


*Figure 4-17. In situ temperature EC logs in KLX12A. Data taken from /18/.*

**Table 4-5. Fracture specific ECs, KLX12A.**

| Measurement | Borehole length (m) | Elevation (m.a.s.l.) | EC in situ (S/m) |
|---|---|---|---|
| Frac. Spec. EC | 139.3 | –116.58 | (0.069) |
| Frac. Spec. EC | 151.1 | –127.92 | 0.11 |
| Frac. Spec. EC | 245.4 | –218.63 | 0.51 |
| Frac. Spec. EC | 397.9 | –364.49 | 0.82 |
| Frac. Spec. EC | 403.7 | –369.99 | 0.80 |
| Frac. Spec. EC | 539.4 | –498.50 | 0.78 |

### 4.3.8 Groundwater EC in KLX03–KLX06

In /20/ a similar evaluation as made above was made for the groundwater EC data obtained in KLX03, KLX04, KLX05 and KLX06. In this present report these tabulated data (taken from Appendix C in /20/) are used as supporting data. The conversion from borehole length to elevation in Table 4-6 was made by a designated tool in SICADA /18/.

### 4.3.9 EC profiles in KLX07A, KLX08, KLX10 and KLX12A

In this subsection EC data taken from Tables 4-1 to 4-6 are plotted versus elevation and borehole length. In Figure 4-18 the groundwater EC at in situ temperature of the boreholes KLX03, KLX04, KLX05, KLX06, KLX07A, KLX10 and KLX12A is plotted versus elevation.

As can be seen, the EC in these boreholes seems to follow the same general trend and the data occur within a relatively small range. It should be noted that borehole KLX08 is not included in Figure 4-18. As the data display such shattering, it is difficult to motivate using a more complex way of fitting the data than by a linear fitting, at least within the EC range of interest for formation factor measurements.

Figure 4-19 shows the EC data for boreholes KLX07A, KLX10 and KLX12A versus borehole length. As can be seen, the data sets are fitted by different linear fittings.

**Table 4-6. ECs in KLX03–KLX06.**

| Borehole | Borehole length (m) | Elevation (m.a.s.l.) | EC at 25°C (S/m) | EC at in situ temperature (S/m) | Method |
|---|---|---|---|---|---|
| KLX03 | 195.3 | –170.10 | 0.14 | 0.098 | Difference flow meter |
| KLX03 | 196.8 | –171.55 | | 0.14 | Hydrochemical characterisation |
| KLX03 | 266.8 | –239.14 | 0.30 | 0.21 | Difference flow meter |
| KLX03 | 619.4 | –579.62 | 1.36 | 1.13 | Difference flow meter |
| KLX03 | 970.3 | –918.45 | | 2.6 | Hydrochemical characterisation |
| KLX03 | 970.1 | –922.58 | 2.87 | 2.7 | Difference flow meter |
| KLX04 | 973.1 | –943.78 | 1.72 | 1.6 | Difference flow meter |
| KLX05 | 303.8 | –254.91 | 0.56 | 0.4 | Difference flow meter |
| KLX05 | 628.6 | –547.90 | 1.56 | 1.3 | Difference flow meter |
| KLX05 | 791.1 | –693.31 | 1.31 | 1.1 | Difference flow meter |
| KLX06 | 196.0 | –159.98 | 0.05 | 0.034 | Difference flow meter |
| KLX06 | 377.0 | –324.04 | 0.084 | 0.11 | Difference flow meter |

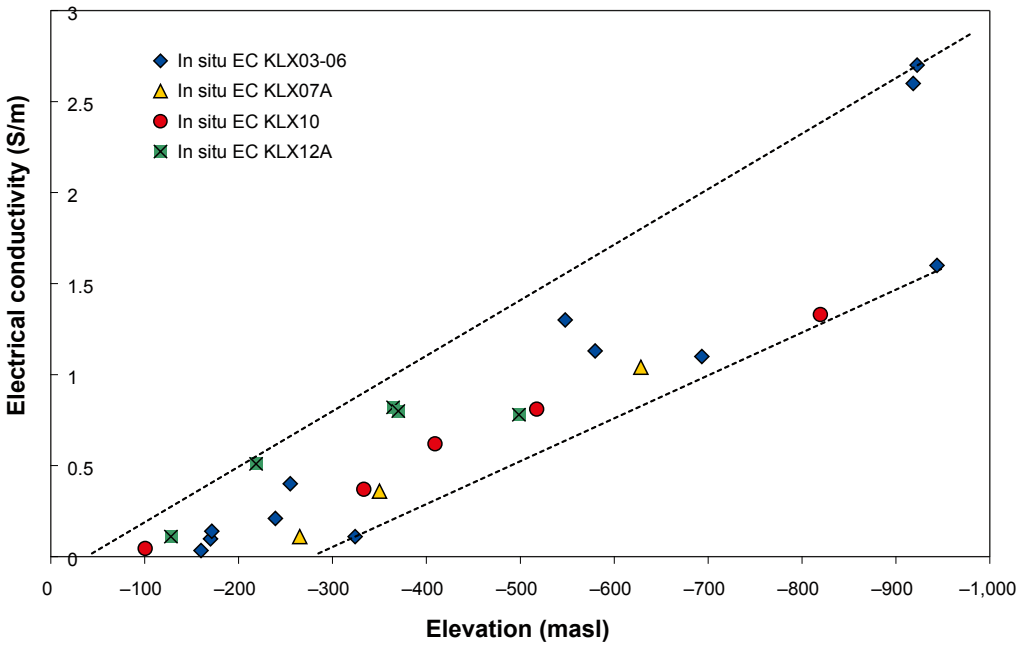


***Figure 4-18.*** *In situ EC data in Laxemar vs. elevation.*

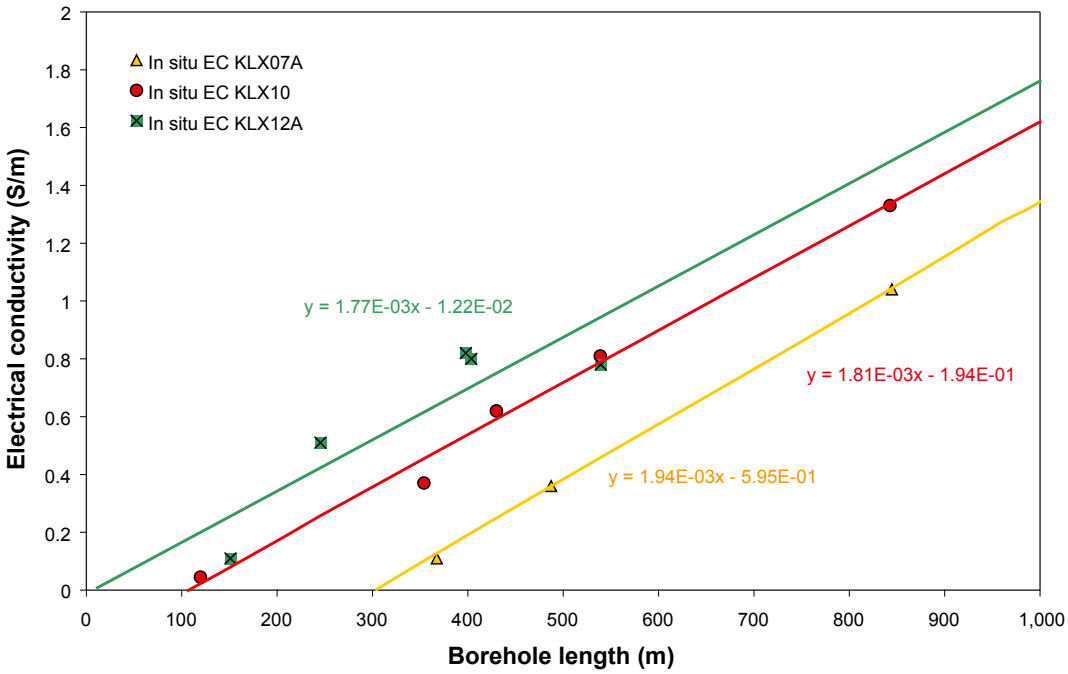


***Figure 4-19.*** *In situ EC data in KLX07A, KLX10, and KLX12A vs. borehole length.*

The equations for the EC-profiles shown in Figure 4-19 are the following:

**KLX07A**: borehole length 367–845 m,

$$EC\ (S/m) = 1.94 \cdot 10^{-3} \times \text{borehole length (m)} - 5.95 \cdot 10^{-1} \quad 4\text{-}5$$

**KLX10**: borehole length 120–1,001 m,

$$EC\ (S/m) = 1.81 \cdot 10^{-3} \times \text{borehole length (m)} - 1.94 \cdot 10^{-1} \quad 4\text{-}6$$

**KLX12A**: borehole length 151–600 m,

$$EC\ (S/m) = 1.77 \cdot 10^{-3} \times \text{borehole length (m)} - 1.22 \cdot 10^{-2} \quad 4\text{-}7$$

It is recommended not to extrapolate the data outside the given ranges. Due to the criterion discussed in subsection 4.1.2 (EC ≥ 0.5 S/m) formation factors should not be obtained at shallower depth than the borehole length 564.8 m for KLX07A, 382.8 m for KLX10 and 288.9 m for KLX12A.

The EC in borehole KLX08 deviated from the general trend shown in Figure 4-18. A good indication of this is shown in Figure 4-15 where the EC of the borehole fluid could not be significantly raised by performing extensive pumping, which is atypical for the site. Figure 4-20 shows the EC data from Tables 4-2 and 4-3 and the assessed linear fittings.

The EC values in Figure 4-20 are predominantly based upon pore water measurements (diamonds) while only one EC value was obtained on freely flowing groundwater (triangle). As can be seen in Figure 4-20, the EC range of the fitting for the shallower part of the borehole is below 0.5 S/m and therefore this fitting is not relevant for formation factor loggings by electrical methods. The fitting for the deeper part is:

**KLX08**: borehole length 751–992 m,

$$EC\ (S/m) = 5.71 \cdot 10^{-3} \times \text{borehole length (m)} - 3.90 \quad 4\text{-}8$$

It is recommended not to extrapolate the data outside the given ranges. Due to the criterion discussed in subsection 4.1.2 (EC ≥ 0.5 S/m) formation factors should not be obtained at shallower depth than the borehole length 770.9 m.

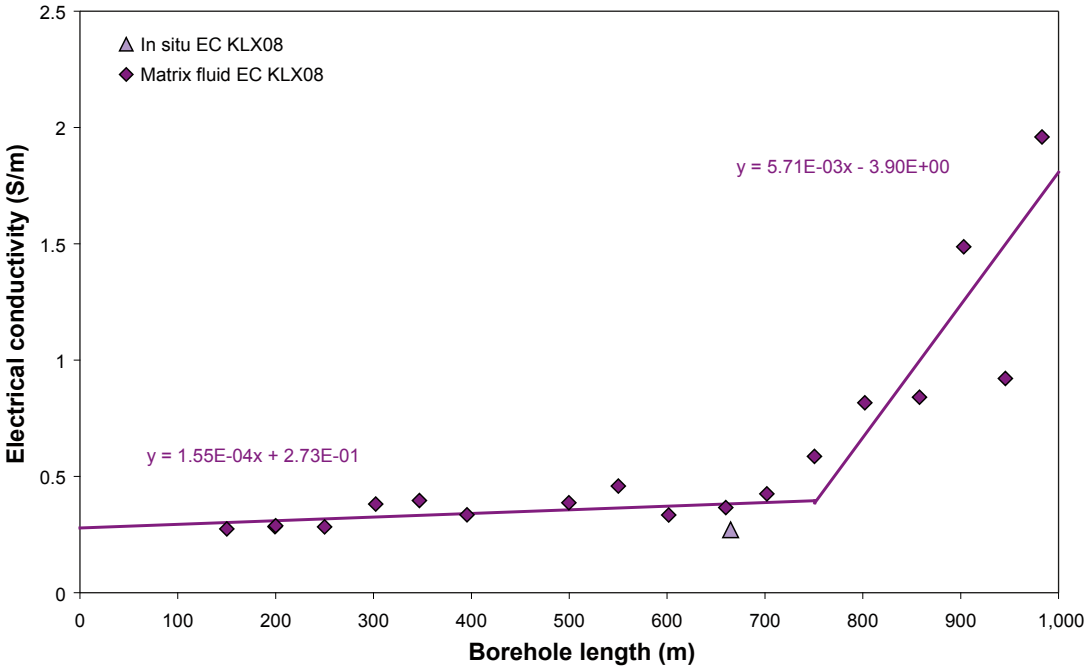


***Figure 4-20.*** *In-situ EC data in KLX08 vs. borehole length.*

It is acknowledged that there is a degree of subjectivity in assessing the EC profiles described by Equations 4-5 to 4-8, especially in boreholes where only few data points are available. However, even though different ways in performing the fitting greatly would affect the assessed in EC in very shallow rock (on a logarithmic scale), the effect on the results should be much smaller at depths of interest for formation factor loggings by electrical methods.

### 4.3.10 Electrical conductivity of the pore water

In KLX07A, on average 2.5 broken fractures per metre part the drill core. From the rock resistivity log one can see that in the entire borehole, a substantial number of the broken fractures are open with a significant aperture. By visual inspection of the rock resistivity logs, shown in Appendix A1, one can see that the typical block of solid rock between open fractures with significant apertures is a few metres wide or less. According to measurements with the difference flow meter /5/, hydraulically conductive fractures are frequent in the entire borehole. Based on this, it is reasonable to suggest that the matrix pore water is fairly well equilibrated with freely flowing groundwater at a corresponding depth. Therefore, the assessed EC profile is judged as representative for the pore water.

As the EC profile for KLX08 predominantly is based upon pore water characterisations, the assessed EC profile is judged as representative for the pore water.

In KLX10, on average 2.9 broken fractures per metre part the drill core. From the rock resistivity log one can see that in the entire borehole, a substantial number of the broken fractures are open with a significant aperture. By visual inspection of the rock resistivity logs, shown in Appendix A2, one can see that the typical block of solid rock between open fractures with significant apertures is a few metres wide or less. According to measurements with the difference flow meter /6/, hydraulically conductive fractures are frequent in the upper half of the borehole but scarcer in the lower half. Even so, due to the high degree of fracturing it is reasonable to suggest that the matrix pore water is fairly well equilibrated with freely flowing groundwater at a corresponding depth. Therefore, the assessed EC profile is judged as representative for the pore water.

In KLX12A, on average 2.5 broken fractures per metre part the drill core. From the rock resistivity log one can see that in the entire borehole, a substantial number of the broken fractures are open with a significant aperture. By visual inspection of the rock resistivity logs, shown in Appendix A4, one can see that the typical block of solid rock between open fractures with significant apertures is a few metres wide or less. According to measurements with the difference flow meter, hydraulically conductive fractures occur in clusters separated by larger sections of hydraulically non-conductive rock. Even so, due to the high degree of fracturing it is reasonable to suggest that the matrix pore water is fairly well equilibrated with freely flowing groundwater at a corresponding depth. Therefore, the assessed EC profile is judged as representative for the pore water.

## 4.4 Formation factor measurements in the laboratory

The formation factor was measured in the laboratory on two drill core samples from KLX10 and three drill core samples from KLX12A /21/. The method for doing this is described in /21/. The locations of the samples and obtained (rock matrix) formation factors are shown in Table 4-7.

The grounds for choosing the samples may not necessarily be such that comparisons should be made between averaged laboratory and in situ data.

**Table 4-7. Laboratory formation factors.**

| Borehole | Borehole length (m) | Formation factor (–) |
|---|---|---|
| KLX10 | 159.15–159.18 | $8.56 \cdot 10^{-3}$ |
| KLX10 | 768.03–768.06 | $1.03 \cdot 10^{-5}$ |
| KLX12A | 240.24–240.27 | $3.10 \cdot 10^{-5}$ |
| KLX12A | 240.69–240.72 | $4.03 \cdot 10^{-5}$ |
| KXL12A | 430.50–430.53 | $2.12 \cdot 10^{-6}$ |

## 4.5 Nonconformities

The work was carried out in accordance with the Activity Plan and the Method Description without nonconformities. However, the limited quantitative measurement range of the in situ rock resistivity tool may give rise to overestimations of formation factors in the lower formation factor range, especially for KLX08, KLX10 and KLX12A.

# 5 Results

## 5.1 General

Original data from the reported activity are stored in the primary database Sicada, where they are traceable by the Activity Plan number (AP PF 400-016-129). Only data in SKB's databases are accepted for further interpretation and modelling. The data presented in this report are regarded as copies of the original data. Data in the databases may be revised, if needed. Such revisions will not necessarily result in a revision of the P-report, although the normal procedure is that major data revisions entail a revision of the P-report. Minor data revisions are normally presented as supplements, available at www.skb.se.

## 5.2 In situ formation factors KLX07A

The in situ rock matrix and fractured rock formation factors obtained in KLX07A were treated statistically. By using the normal-score method, as described in /22/, to determine the likelihood that a set of data is normally distributed, the mean value and standard deviation of the logarithm ($\log_{10}$) of the formation factors could be determined. Figure 5-1 (upper) shows the distribution of the rock matrix formation factors obtained in situ between 564.8–829.0 m. Figure 5-1 (lower) shows the fractured rock formation factor distribution obtained in situ between 564.8–834.0 m.

The distribution of the obtained rock matrix formation factors of KLX07A deviates from the log-normal distribution. However, in KLX07A only 74 rock matrix formation factors were obtained, partly due to the relatively short section measured on and partly due to the great fracturing of the surrounding rock mass. For the fractured rock formation factor, 2,166 data points were obtained and the appearance of the histogram shown in Figure 5-1 (lower) is typical for the Laxemar site. One notice the deviation from the log-normal distribution in the upper formation factor range, due to the multitude of water-bearing but hydraulically non-conductive fractures. This indicates that the rock matrix formation factors of the surrounding rock are also fairly well log-normally distributed.

Table 5-1 presents mean values and standard deviations of the log-normal distributions shown in Figure 5-1. In addition, the number of data points obtained and the arithmetic mean values for the different formation factors are shown.

The in situ formation factor logs of KLX07A are shown in Appendix B1.

## 5.3 In situ formation factors KLX08

The in situ rock matrix and fractured rock formation factors obtained in KLX08 were treated statistically in the same way as the data for KLX07A. Figure 5-2 (upper) shows the distribution of the rock matrix formation factors obtained in situ between 770.9–988.8 m. Figure 5-1 (lower) shows the fractured rock formation factor distribution obtained in situ between 770.9–982.0 m.

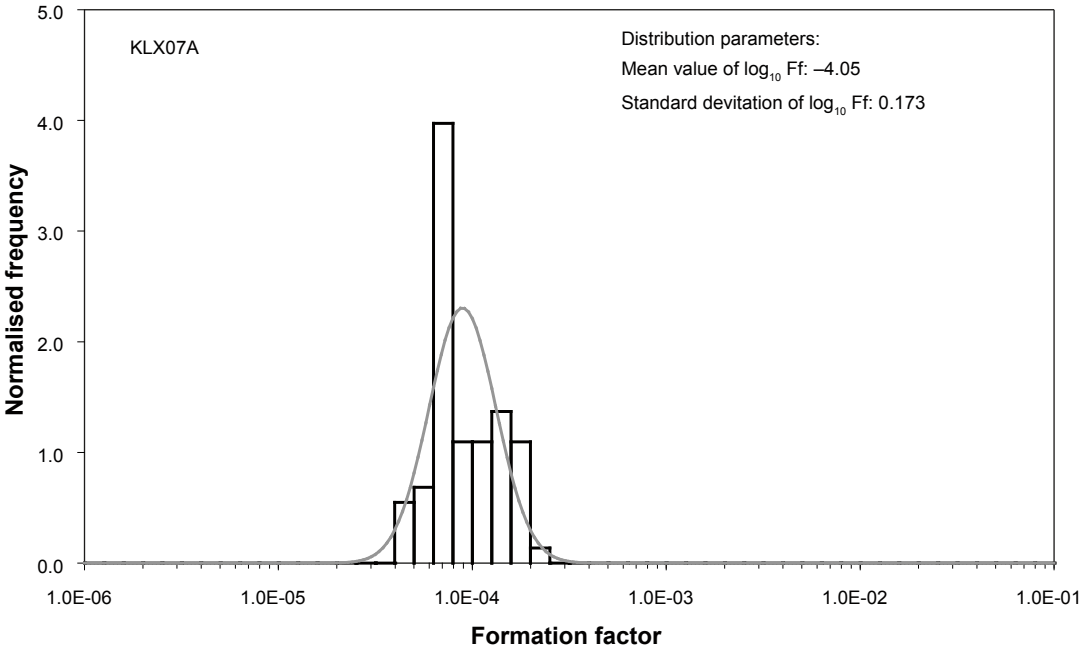


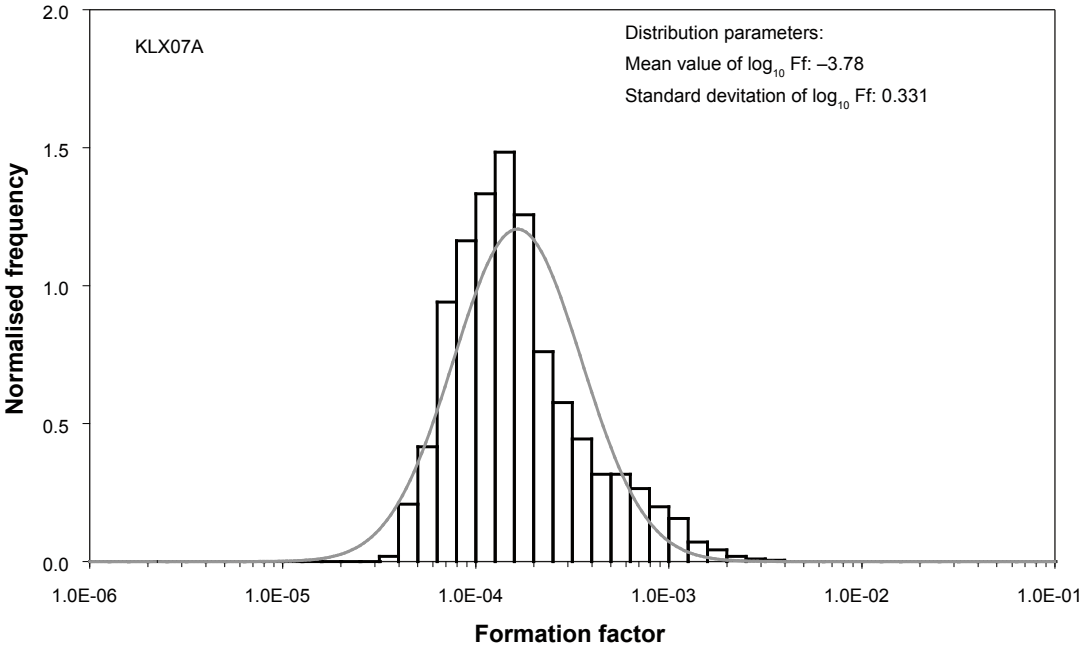


***Figure 5-1.*** *Distributions of in situ rock matrix (upper image) and fractured rock (lower image) formation factors in KLX07A.*

**Table 5-1. Distribution parameters and arithmetic mean value of the formation factor, KLX07A.**

| Formation factor | Number of data points | Mean $\log_{10}(F_f)$ | Standard deviation $\log_{10}(F_f)$ | Arithmetic mean $F_f$ |
|---|---|---|---|---|
| In situ rock matrix $F_f$ | 74 | –4.05 | 0.173 | $9.63 \cdot 10^{-5}$ |
| In situ fractured rock $F_f$ | 2,166 | –3.78 | 0.331 | $2.37 \cdot 10^{-4}$ |

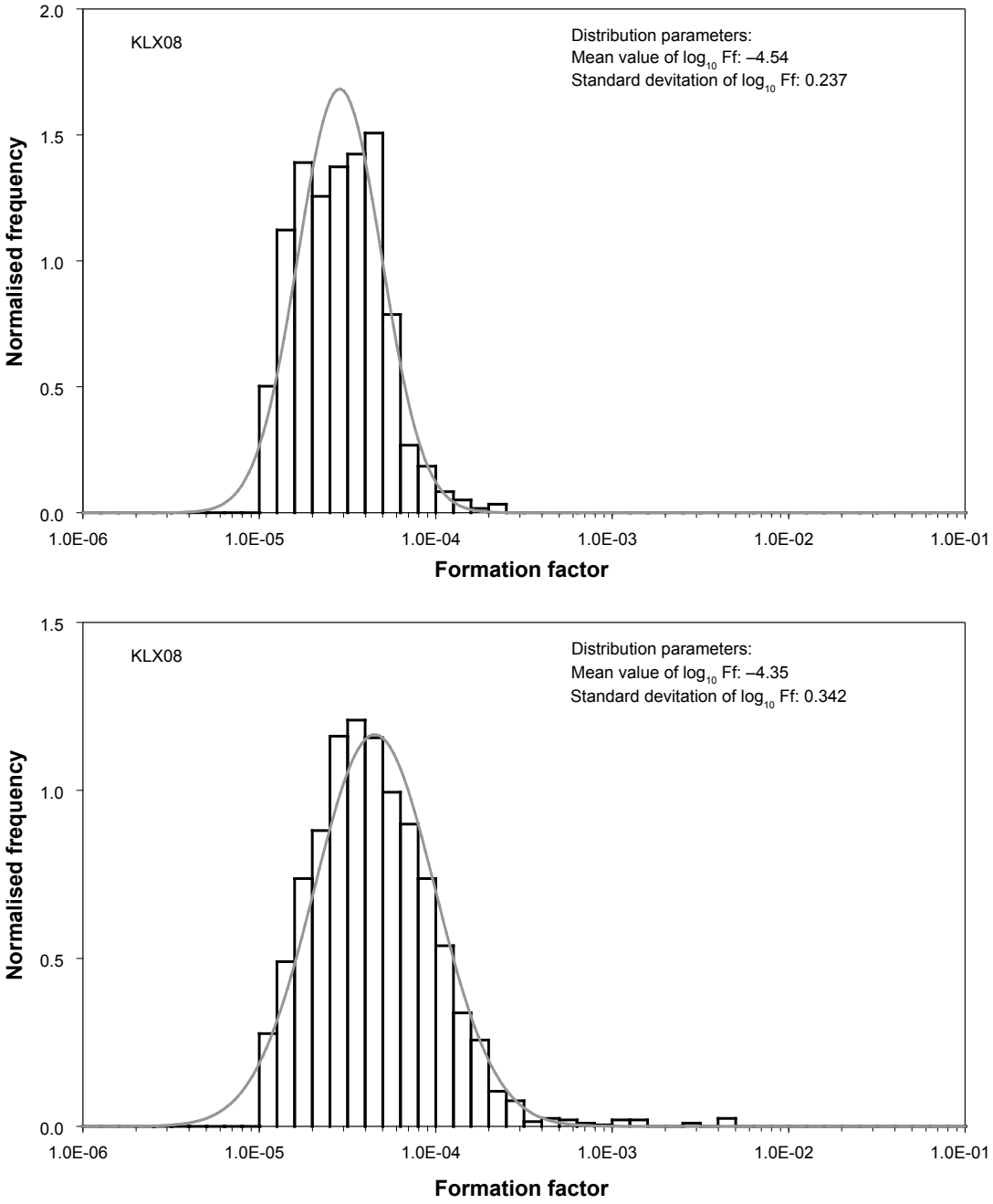


***Figure 5-2.*** *Distributions of in situ rock matrix (upper image) and fractured rock (lower image) formation factors in KLX08.*

As can be seen in Figure 5-2, both the rock matrix and fractured rock formation factor distributions are well described by the log-normal distribution. As can be seen in Figures 4-4 and 4-5, a significant fraction of the rock resistivities obtained have resistivities exceeding the upper quantitative measurement limit of the logging tool. Due to this there is a deviation in the histograms, from the log-normal distribution, in the lower formation factor range. If comparing the fractured rock formation factor distribution with that of KLX07A, a smaller deviation in the upper formation factor range is seen. In Appendices A1 and A2 one can also see that the rock surrounding KLX08 is not as extensively fractured as that surrounding KLX07A.

Table 5-2 presents mean values and standard deviations of the log-normal distributions shown in Figure 5-2. In addition, the number of data points obtained and the arithmetic mean values for the different formation factors are shown.

The in situ formation factor logs of KLX08 are shown in Appendix B2.

**Table 5-2. Distribution parameters and arithmetic mean value of the formation factor, KLX08.**

| Formation factor | Number of data points | Mean $\log_{10}(F_f)$ | Standard deviation $\log_{10}(F_f)$ | Arithmetic mean $F_f$ |
|---|---|---|---|---|
| In situ rock matrix $F_f$ | 597 | –4.54 | 0.237 | $3.37 \cdot 10^{-5}$ |
| In situ fractured rock $F_f$ | 2,101 | –4.35 | 0.342 | $7.74 \cdot 10^{-5}$ |

## 5.4 In situ formation factors KLX10

The in situ rock matrix and fractured rock formation factors obtained in KLX10 were treated statistically in the same way as the data for KLX07A. Figure 5-3 (upper) shows the distribution of the rock matrix formation factors obtained in situ between 382.8–996.5 m. Figure 5-3 (lower) shows the fractured rock formation factor distribution obtained in situ between 382.8–996.2 m.

As can be seen in Figure 5-3, both the rock matrix and fractured rock formation factor are fairly well log-normally distributed. As can be seen in Figures 4-6 and 4-7, a significant fraction of the rock resistivities obtained had resistivities exceeding the upper quantitative measurement limit of the logging tool. Due to this there is a deviation in the histogram, from the log-normal distribution, in the lower formation factor range. For the fractured rock formation factor distribution the typical deviation in the upper formation factor range can be seen.

Table 5-3 presents mean values and standard deviations of the log-normal distributions shown in Figure 5-2.

The in situ formation factor logs of KLX10 are shown in Appendix B3. In addition, the laboratory formation factors shown in Table 4-7 are included for comparison in Appendix B3. As only two laboratory formation factors were obtained, no statistical analysis was made. The basis for choosing the laboratory samples was not necessarily that they should be representative for the larger rock mass and therefore, caution should be taken when comparing the in situ and laboratory data sets. With this in mind, in Appendix B3 at 768 m one can se that the obtained laboratory formation factor is similar (less than a factor of two lower) than the in situ formation factors at the corresponding depth.

## 5.5 In situ formation factors KLX12A

The in situ rock matrix and fractured rock formation factors obtained in KLX12A were treated statistically in the same way as the data for KLX07A. Figure 5-4 (upper) shows the distribution of the rock matrix formation factors obtained in situ between 288.9–598.8 m. Figure 5-4 (lower) shows the fractured rock formation factor distribution obtained in situ between 288.9–596.2 m.

As can be seen in Figure 5-4, both the rock matrix and fractured rock formation factor distributions features dual peaks. This behaviour is also seen in Figure 4-8 and to a lesser extent in Figure 4-9. An explanation for this behaviour is perhaps that borehole KLX12A is drilled to intersect the interface between two rock domains. Therefore, the upper and lower parts of the borehole are found in different domains. It is beyond the scope of this report, however, to analyse formation factor distributions in different rock domains.

Table 5-4 presents mean values and standard deviations of the log-normal distributions shown in Figure 5-4.

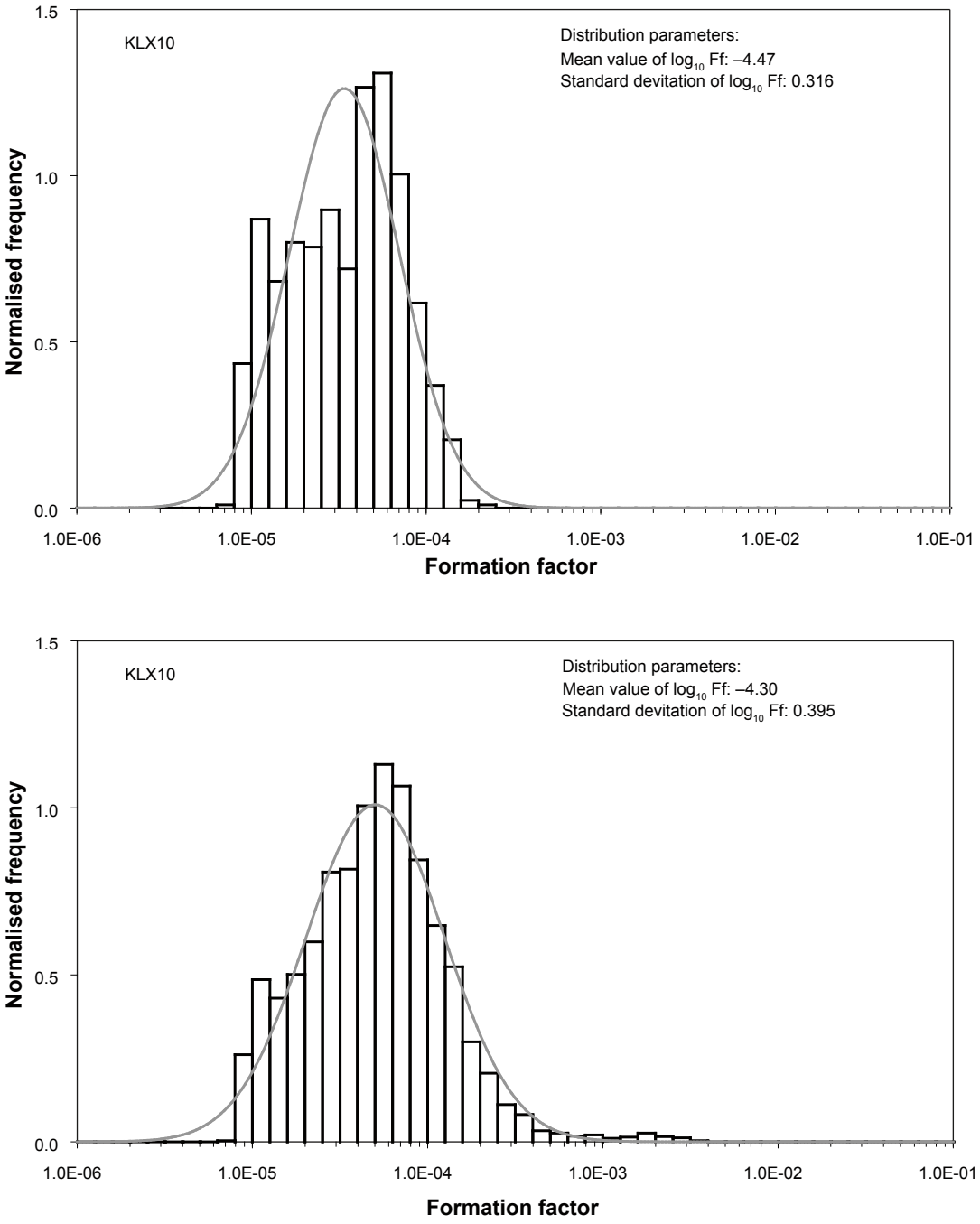


*Figure 5-3. Distributions of in situ rock matrix (upper image) and fractured rock (lower image) formation factors in KLX10.*

**Table 5-3. Distribution parameters and arithmetic mean value of the formation factor, KLX10.**

| Formation factor | Number of data points | Mean $\log_{10}(F_f)$ | Standard deviation $\log_{10}(F_f)$ | Arithmetic mean $F_f$ |
|---|---|---|---|---|
| In situ rock matrix $F_f$ | 2,140 | –4.47 | 0.316 | $4.38 \cdot 10^{-5}$ |
| In situ fractured rock $F_f$ | 5,744 | –4.30 | 0.395 | $8.72 \cdot 10^{-5}$ |

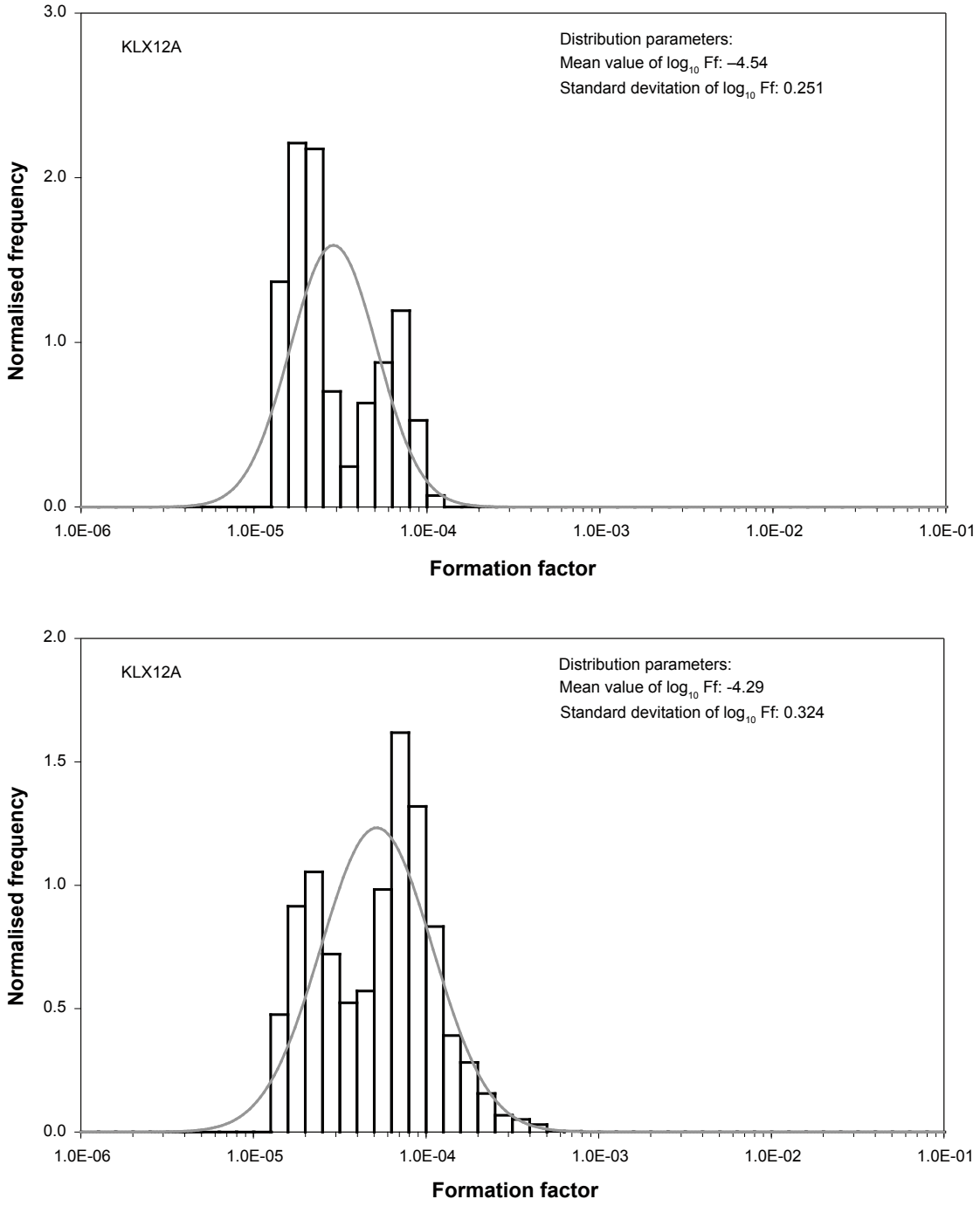


***Figure 5-4.*** *Distributions of in situ rock matrix (upper image) and fractured rock (lower image) formation factors in KLX12A.*

**Table 5-4. Distribution parameters and arithmetic mean value of the formation factor, KLX12A.**

| Formation factor | Number of data points | Mean $\log_{10}(F_f)$ | Standard deviation $\log_{10}(F_f)$ | Arithmetic mean $F_f$ |
|---|---|---|---|---|
| In situ rock matrix $F_f$ | 285 | –4.54 | 0.251 | $3.49 \cdot 10^{-5}$ |
| In situ fractured rock $F_f$ | 2,941 | –4.29 | 0.324 | $6.85 \cdot 10^{-5}$ |

The in situ formation factor logs of KLX12A are shown in Appendix B4. In addition, the laboratory formation factors shown in Table 4-7 are included for comparison in Appendix B4. As only three laboratory formation factors were obtained, no statistical analysis was made. The basis for choosing the laboratory samples was not necessarily that they should be representative for the larger rock mass and therefore, caution should be taken when comparing the in situ and laboratory data sets. With this in mind, in Appendix B4 at 430 m one can se that the obtained laboratory formation factor is substantially (about one order of magnitude) lower than the in situ formation factors at the corresponding depth.

## 5.6 Comparison of formation factor distibutions

Figure 5-5 shows the mean $\log_{10}$ and standard deviation $\log_{10}$ of all formation factor distributions presented in Section 5-1 to 5-4. As can be seen all fractured rock formation factor distributions have larger mean value and standard deviation, compared to the rock matrix formation factor distribution of the same borehole.

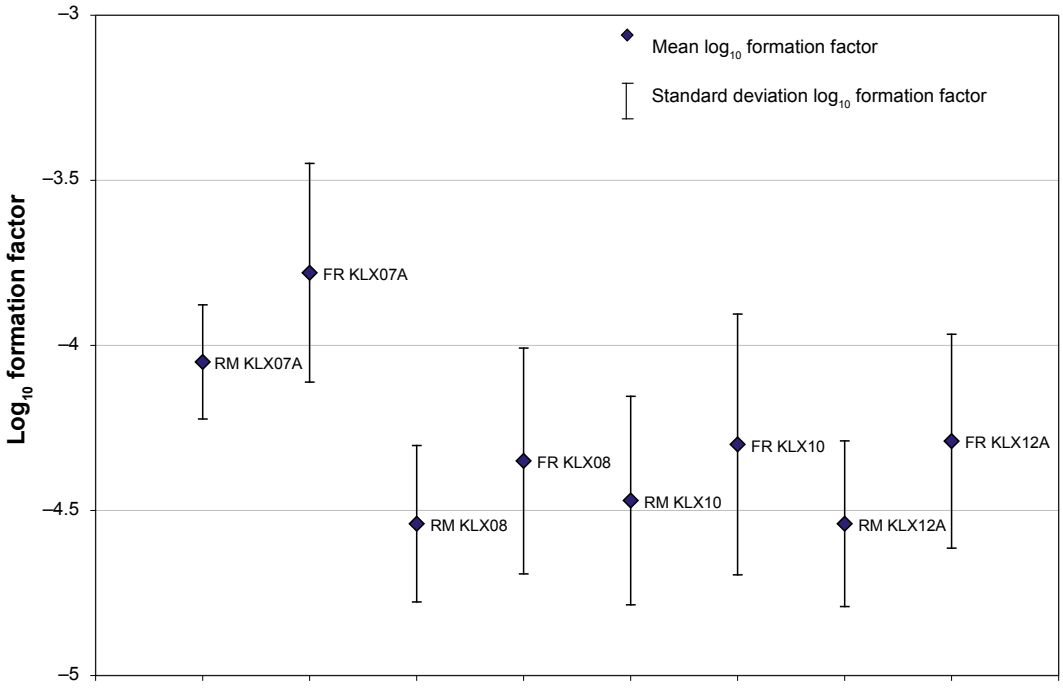


***Figure 5-5.*** *Distributions of in situ rock matrix (RM) and fractured rock (FR) formation factors in KLX07A, KLX08, KLX10, and KLX12A.*

# 6 Summary and discussions

The formation factors obtained in KLX07A, KLX08, KLX10 and KLX12A range from $7.8 \cdot 10^{-6}$ to $4.8 \cdot 10^{-3}$. The formation factors appear to be fairly well distributed according to the log-normal distribution in boreholes KLX07A, KLX08 and KLX10. The distributions for borehole KLX12A, intersecting two different rock domains, feature two peaks. The obtained in situ distributions have mean values for $\log_{10}(F_f)$ between –4.54 and –3.78 and standard deviations between 0.173 and 0.395. The arithmetic mean values range between $3.37 \cdot 10^{-5}$ and $2.37 \cdot 10^{-4}$. In essence the formation factors reported in this work do not deviate from those previously reported for the Laxemar site /e.g. 20/.

The fractured rock formation factors were on average significantly larger than the rock matrix formation factors. This indicates that the retention capacity for non-sorbing species due to open, but hydraulically non-conductive, fractures may be important in the rock surrounding these boreholes.

A significant, but still minor, fraction of the obtained in situ rock resistivities may have been affected by limitations of the in situ rock resistivity tool.

# References


/1/ **Nielsen U T, Ringgaard J, Fris Dahl J, 2005.** Geophysical borehole logging in boreholes KLX07A, KLX07B, HLX20, HLX34 and HLX35. Oskarshamn site investigation. SKB P-05-228, Svensk Kärnbränslehantering AB.

/2/ **Nielsen U T, Ringgaard J, 2005.** Geophysical borehole logging in boreholes KLX08, HLX30, HLX31 and HLX33. Oskarshamn site investigation. SKB P-05-270, Svensk Kärnbränslehantering AB.

/3/ **Nielsen U T, Ringgaard J, Fris Dahl J, 2006.** Geophysical borehole logging in borehole KLX10. Oskarshamn site investigation. SKB P-06-20, Svensk Kärnbränslehantering AB.

/4/ **Nielsen U T, Ringgaard J, 2006.** Geophysical borehole logging in boreholes KLX12A, KLX09G, KLX10B and KLX10C. Oskarshamn site investigation. SKB P-06-198, Svensk Kärnbränslehantering AB.

/5/ **Sokolnicki M, Rouhiainen P, 2005.** Difference flow logging of boreholes KLX07A and KLX07B. Subarea Laxemar. Oskarshamn site investigation. SKB P-05-225, Svensk Kärnbränslehantering AB.

/6/ **Sokolnicki M, Pöllänen J, 2005.** Difference flow logging of borehole KLX08. Subarea Laxemar. Oskarshamn site investigation. SKB P-05-267, Svensk Kärnbränslehantering AB.

/7/ **Väisäsvaara J, Heikkinen P, Kristiansson S, Pöllänen J, 2006.** Difference flow logging of borehole KLX12A. Subarea Laxemar. Oskarshamn site investigation. SKB P-06-185, Svensk Kärnbränslehantering AB.

/8/ **Löfgren M, Neretnieks I, 2005.** Formation factor logging in situ and in the laboratory by electrical methods in KSH01A and KSH02: Measurements and evaluation of methodology. Oskarshamn site investigation. SKB P-05-27, Svensk Kärnbränslehantering AB.

/9/ **Waber H N, Smellie J A T, 2006.** Borehole KLX08. Characterisation of pore water. Part 1: Methodology and analytical data. Oskarshamn site investigation. SKB P-06-163, Svensk Kärnbränslehantering AB.

/10/ **Ehrenborg J, Dahlin P, 2005.** Boremap mapping of core drilled boreholes KLX07A and KLX07B. Oskarshamn site investigation. SKB P-05-263, Svensk Kärnbränslehantering AB.

/11/ **Dahlin P, Ehrenborg J, 2006.** Boremap mapping of core drilled borehole KLX08. Oskarshamn site investigation. SKB P-06-42, Svensk Kärnbränslehantering AB.

/12/ **Ehrenborg J, Stejskal V, 2004**. Boremap mapping of core drilled boreholes KSH01A and KSH01B. Site investigation report SKB P-04-01, Svensk Kärnbränslehantering AB.

/13/ **Löfgren M, Neretnieks I, 2002.** Formation factor logging in situ by electrical methods. Background and methodology. SKB TR-02-27, Svensk Kärnbränslehantering AB.

/14/ **Löfgren M, 2001.** Formation factor logging in igneous rock by electrical methods. Licentiate thesis at the Royal Institute of Technology, Stockholm, Sweden. ISBN 91-7283-207-x.

/15/ **Ohlsson Y, 2000.** Studies of Ionic Diffusion in Crystalline Rock. Doctoral thesis at the Royal Institute of Technology, Stockholm, Sweden. ISBN 91-7283-025-5.

/16/ **Löfgren M, 2004.** Diffusive properties of granitic rock as measured by in situ electrical methods. Doctoral thesis at the Royal Institute of Technology, Stockholm, Sweden. ISBN 91-7283-935-X.

/17/ **Löfgren M, Neretnieks I, 2006.** Through-electromigration: A new method of investigating pore connectivity and obtaining formation factors. Accepted for publication in Journal of Contaminant Hydration, 2006.

/18/ **SICADA, 2006.** Site Characterisation Data Base, Svensk Kärnbränslehantering AB.

/19/ **Löfgren M, 2007.** Formation factor logging in situ by electrical methods in KFM01D and KFM08C. Forsmark site investigation. SKB P-07-XXX, Svensk Kärnbränslehantering AB.

/20/ **Löfgren M, Pettersson M, 2006.** Formation factor logging in situ by electrical methods in KLX05 and KLX06. Site Investigation Report SKB P-06-146, Svensk Kärnbränslehantering AB.

/21/ **Thunehed H, 2007.** Resistivity measurements on samples from KLX03, KLX04, KLX05, KLX10, KLX12A and KLX13A. Oskarshamn site investigation. SKB P-07-XXX, Svensk Kärnbränslehantering AB.

/22/ **Johnson R A, 1994.** Miller and Freund's probability & statistics for engineers, 5ed. Prentice-Hall Inc., ISBN 0-13-721408-1.

# Appendix A1: In situ rock resistivities and fractures KLX07A

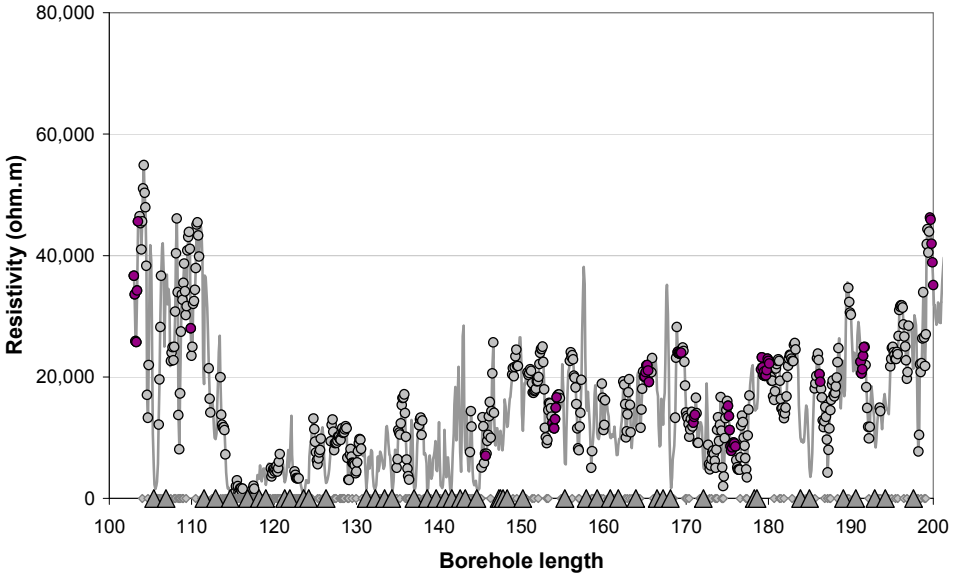


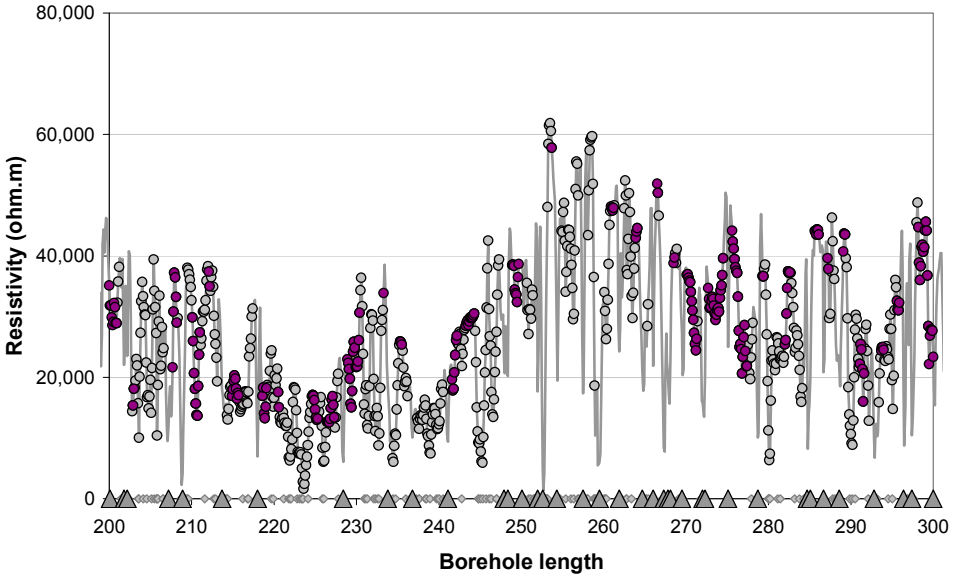


Rock resistivity
Fractured rock resistivity
Rock matrix resistivity
Location of broken fracture parting the drill core
Location of hydraulically conductive fracture detected in the difference flow logging

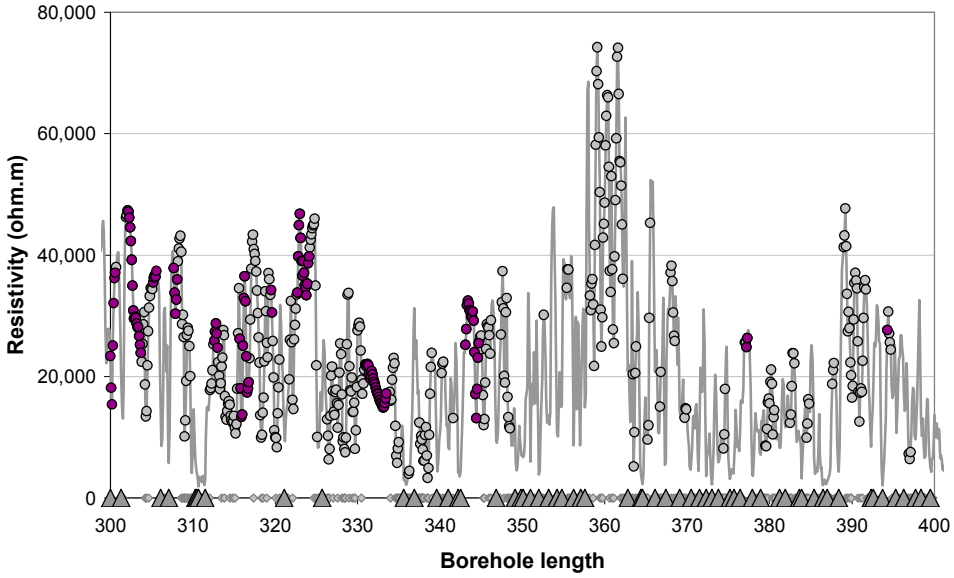


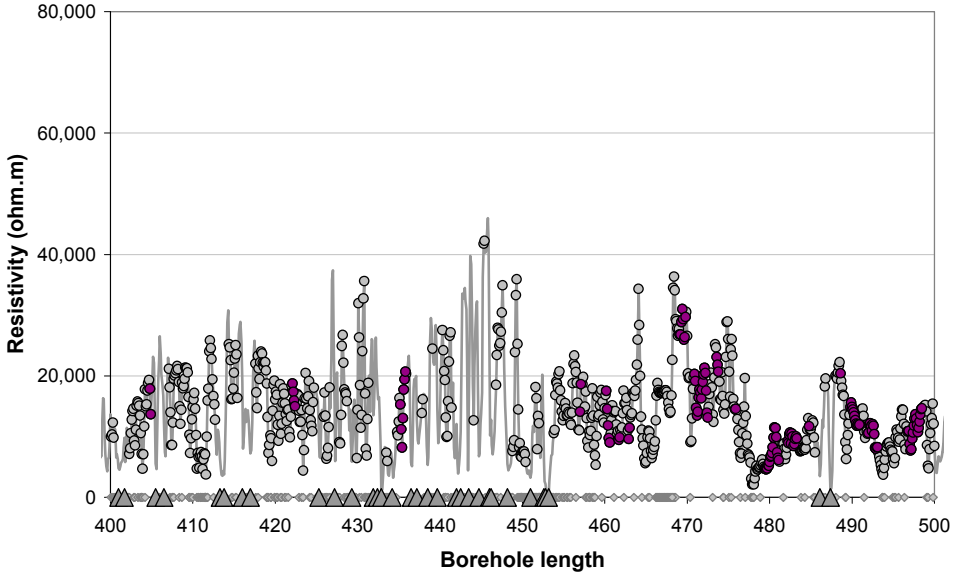


Rock resistivity
Fractured rock resistivity
Rock matrix resistivity
Location of broken fracture parting the drill core
Location of hydraulically conductive fracture detected in the difference flow logging

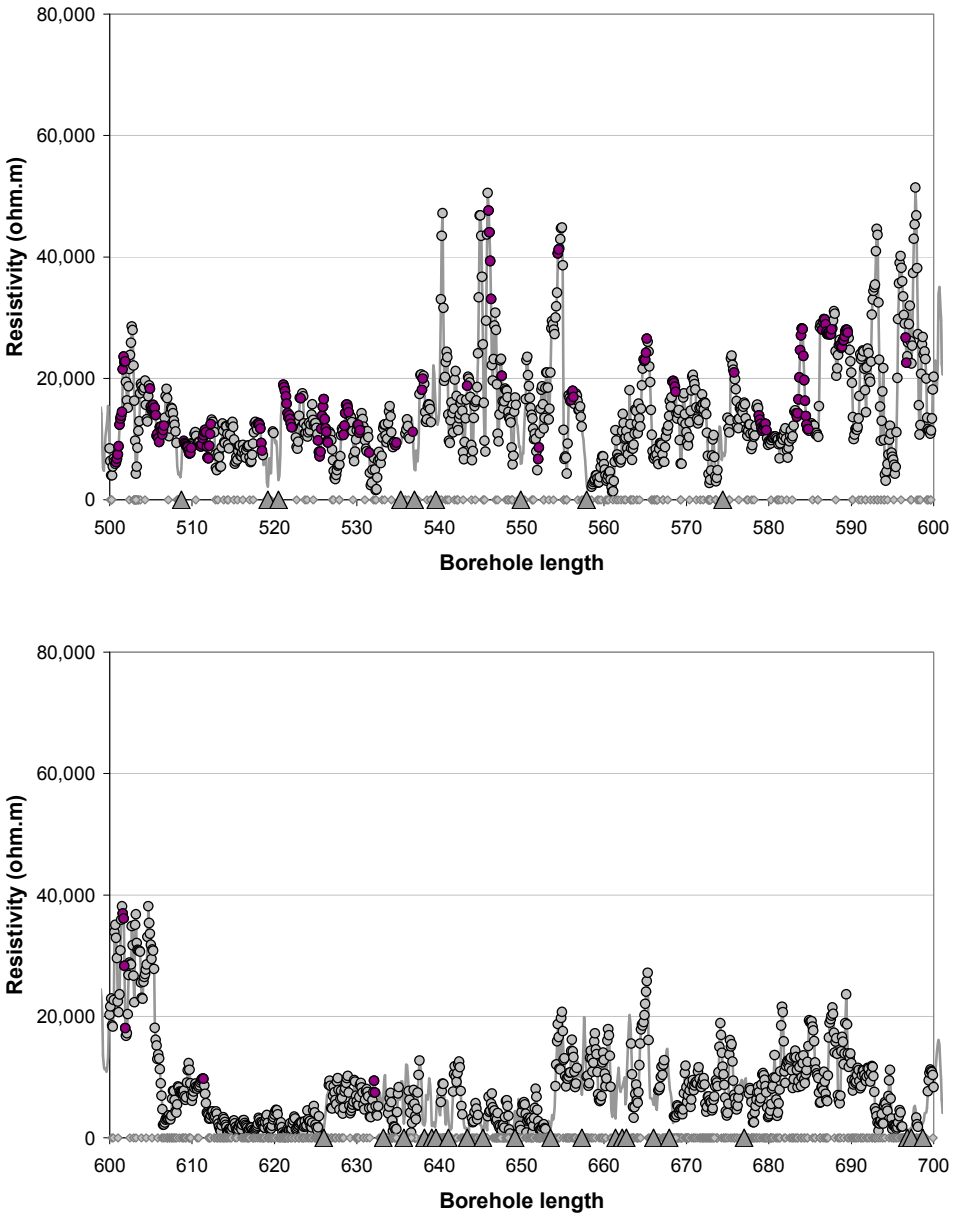
80,000
60,000
40,000
20,000
0
Resistivity (ohm.m)
500
510
520
530
540
550
560
570
580
590
600
Borehole length
80,000
60,000
40,000
20,000
0
Resistivity (ohm.m)
600
610
620
630
640
650
660
670
680
690
700
Borehole length
Rock resistivity
Fractured rock resistivity
Rock matrix resistivity
Location of broken fracture parting the drill core
Location of hydraulically conductive fracture detected in the difference flow logging

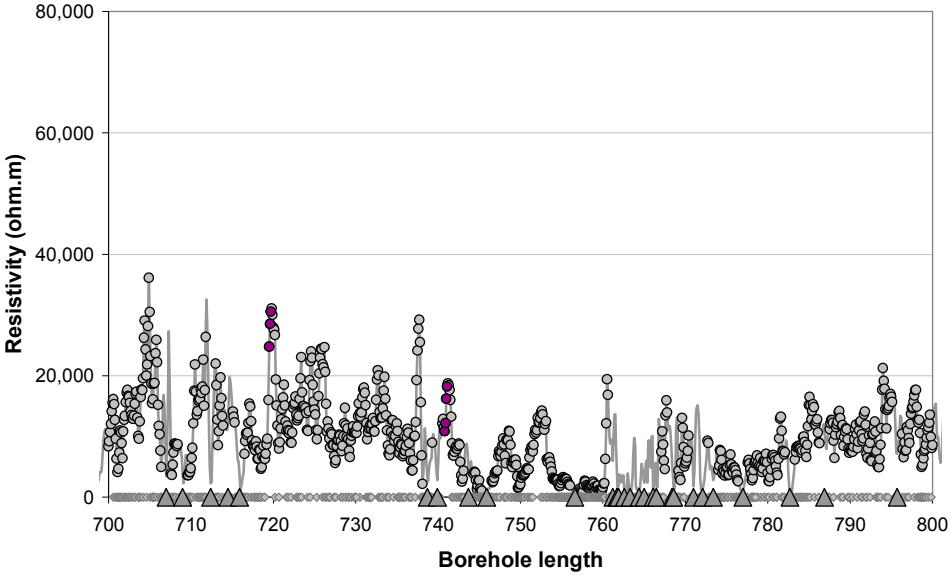


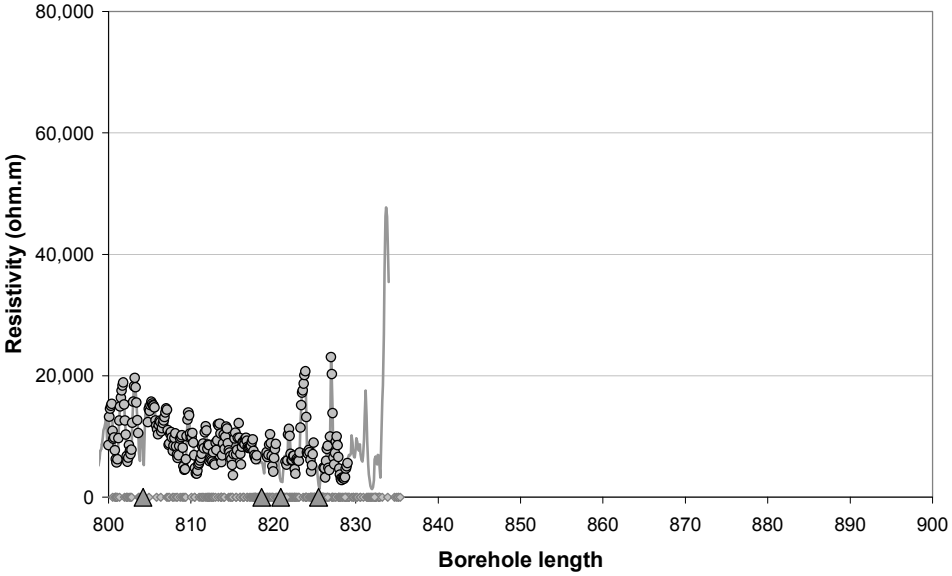


Rock resistivity
Fractured rock resistivity
Rock matrix resistivity
Location of broken fracture parting the drill core
Location of hydraulically conductive fracture detected in the difference flow logging

# Appendix A2: In situ rock resistivities and fractures KLX08

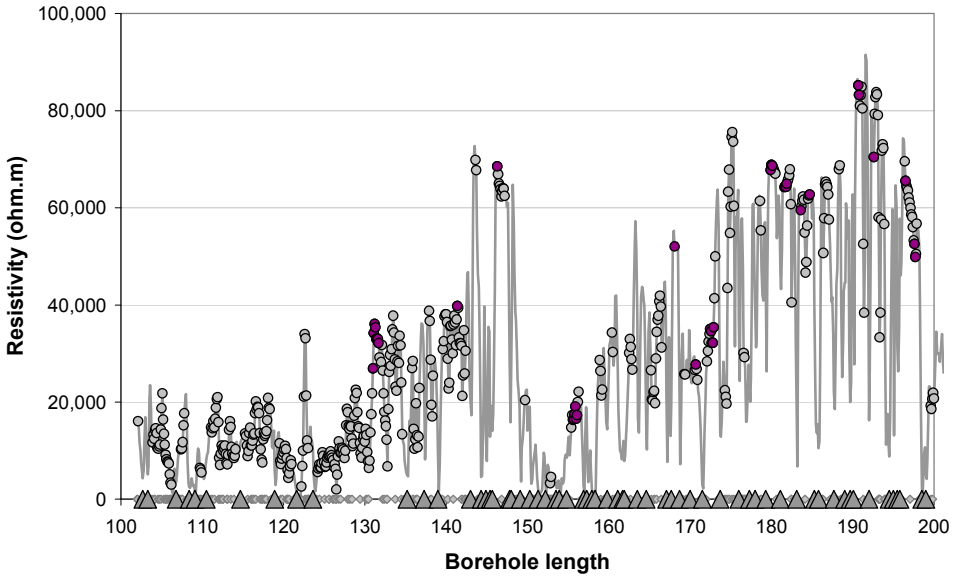


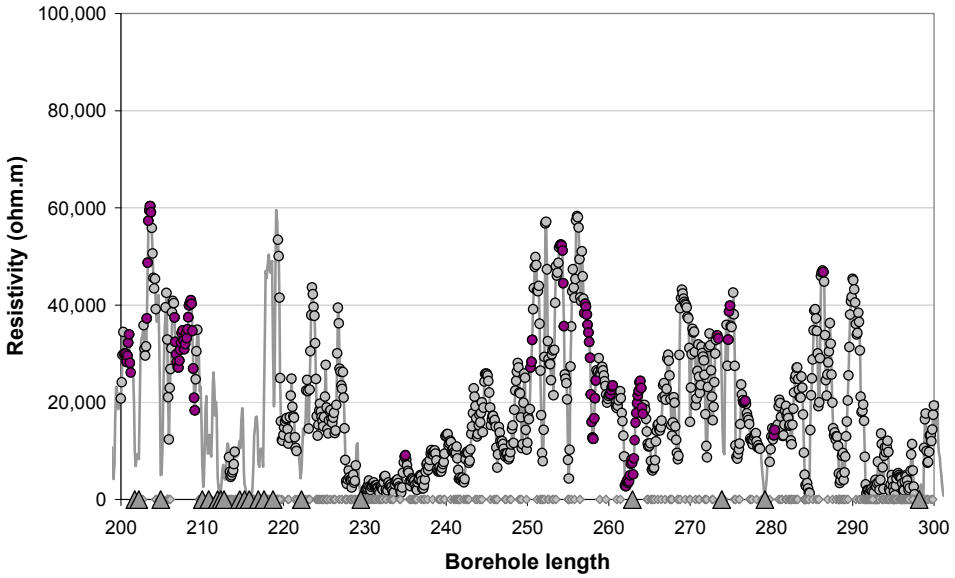


Rock resistivity
Fractured rock resistivity
Rock matrix resistivity
Location of broken fracture parting the drill core
Location of hydraulically conductive fracture detected in the difference flow logging

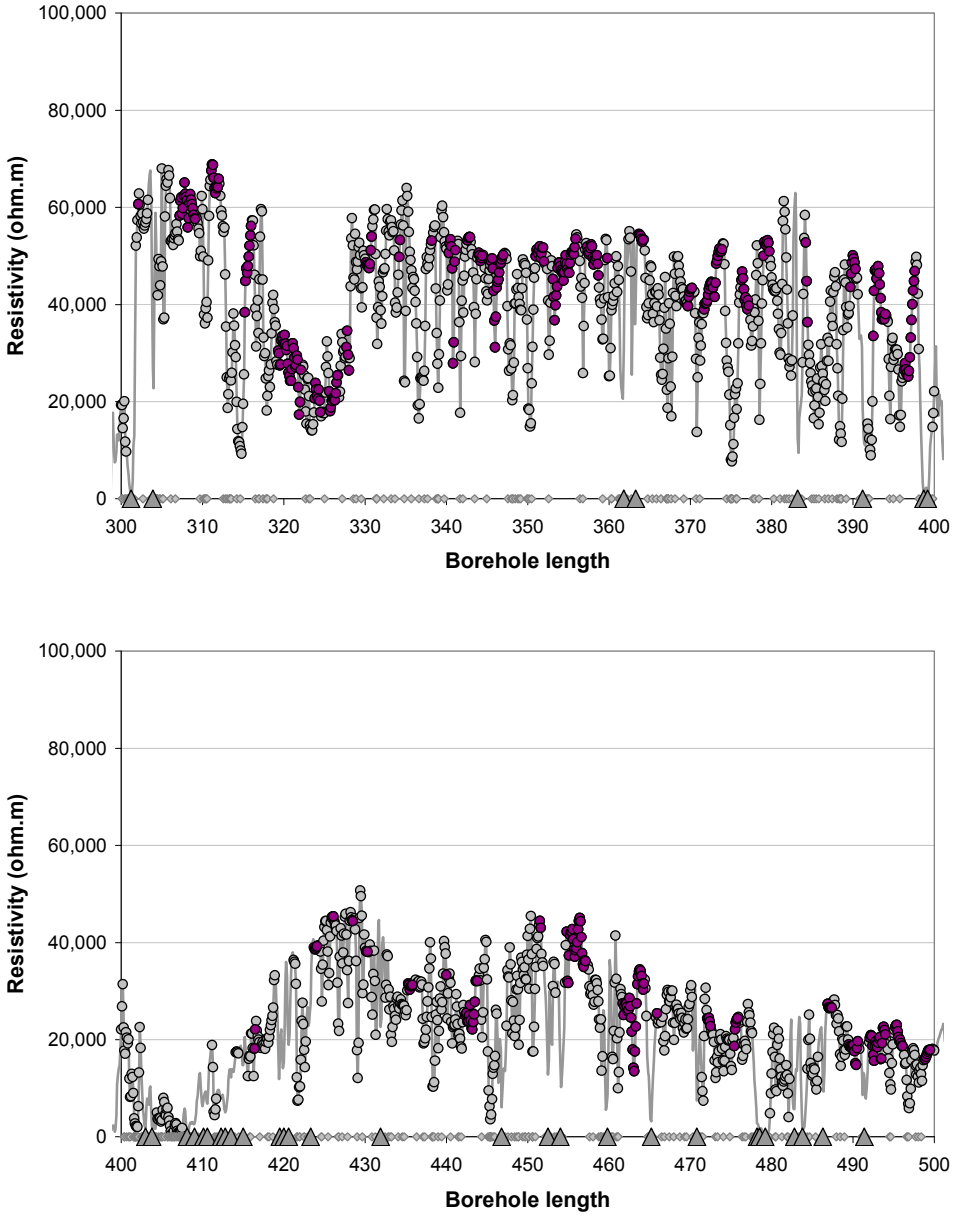
100,000
80,000
60,000
40,000
20,000
0
Resistivity (ohm.m)
300
310
320
330
340
350
360
370
380
390
400
Borehole length
100,000
80,000
60,000
40,000
20,000
0
Resistivity (ohm.m)
400
410
420
430
440
450
460
470
480
490
500
Borehole length
Rock resistivity
Fractured rock resistivity
Rock matrix resistivity
Location of broken fracture parting the drill core
Location of hydraulically conductive fracture detected in the difference flow logging

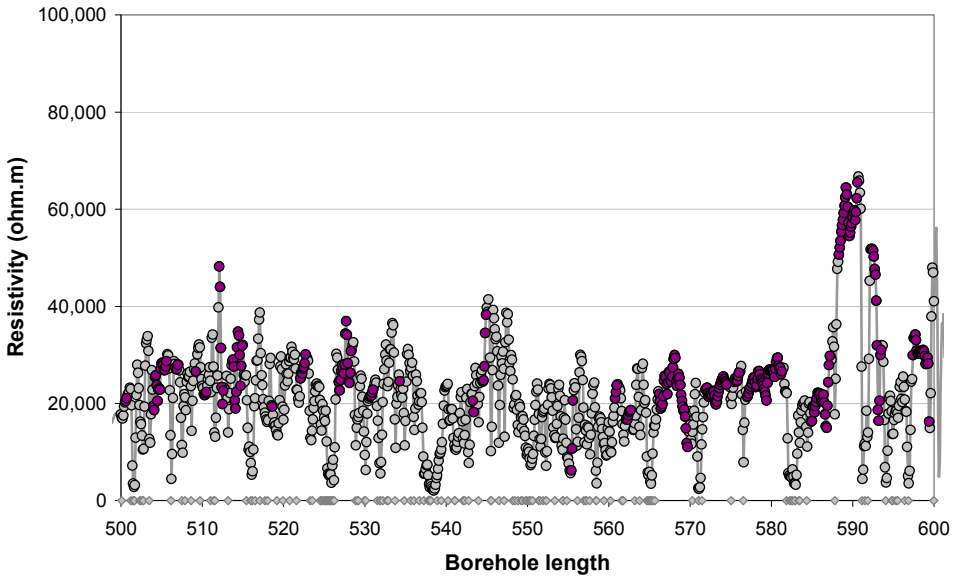


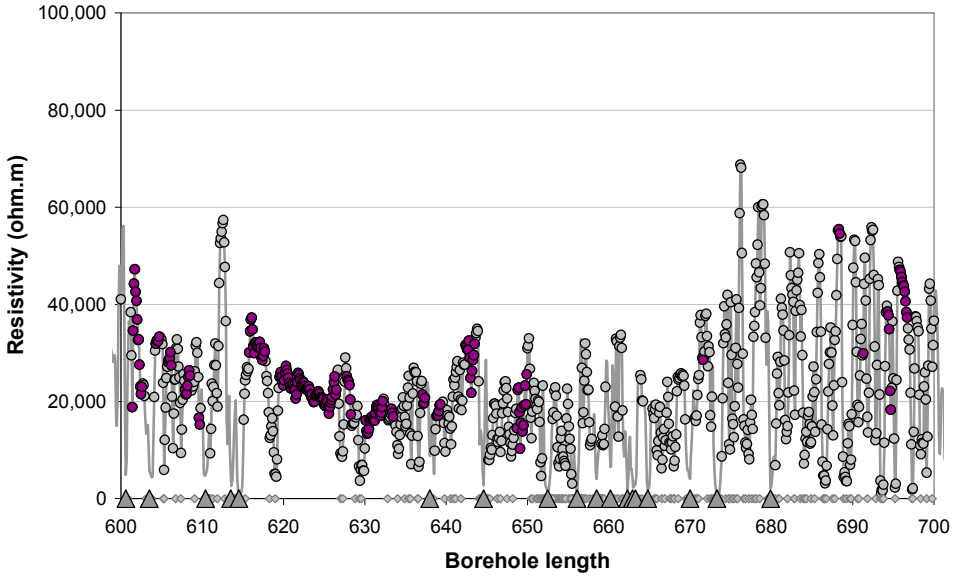


Rock resistivity
Fractured rock resistivity
Rock matrix resistivity
Location of broken fracture parting the drill core
Location of hydraulically conductive fracture detected in the difference flow logging

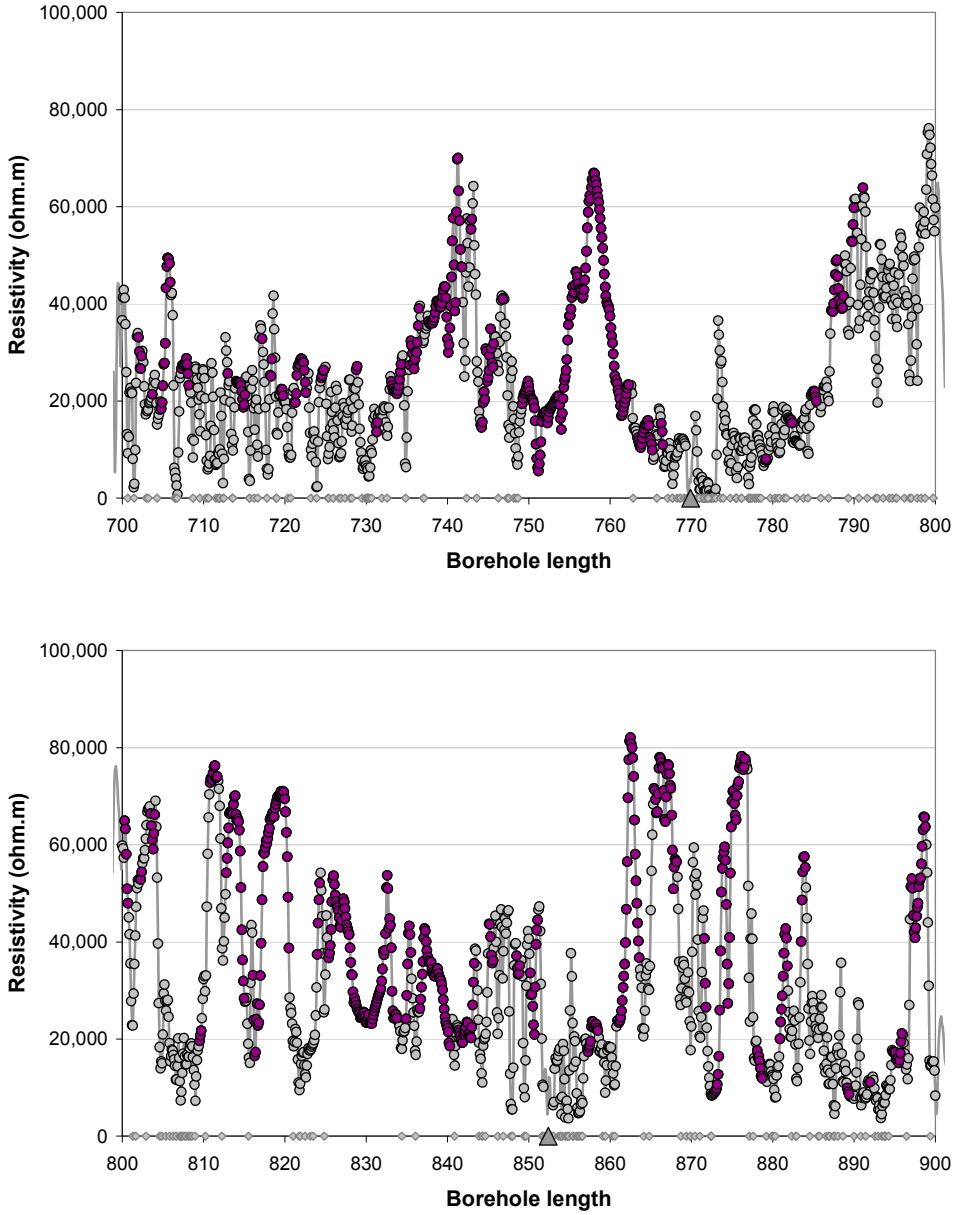
100,000
80,000
60,000
40,000
20,000
0
Resistivity (ohm.m)
700
710
720
730
740
750
760
770
780
790
800
Borehole length
100,000
80,000
60,000
40,000
20,000
0
Resistivity (ohm.m)
800
810
820
830
840
850
860
870
880
890
900
Borehole length
Rock resistivity
Fractured rock resistivity
Rock matrix resistivity
Location of broken fracture parting the drill core
Location of hydraulically conductive fracture detected in the difference flow logging

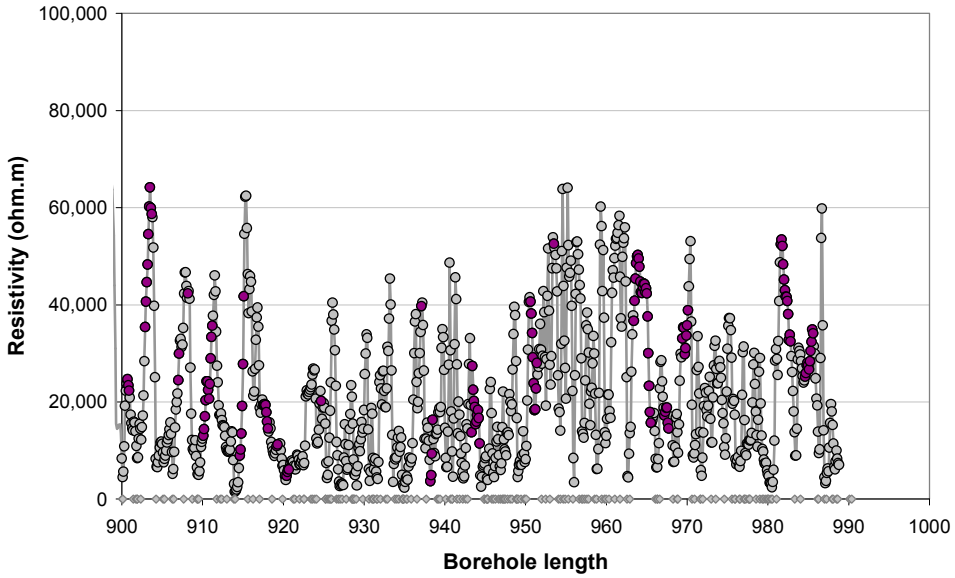


Rock resistivity
Fractured rock resistivity
Rock matrix resistivity
Location of broken fracture parting the drill core
Location of hydraulically conductive fracture detected in the difference flow logging

# Appendix A3: In situ rock resistivities and fractures KLX10

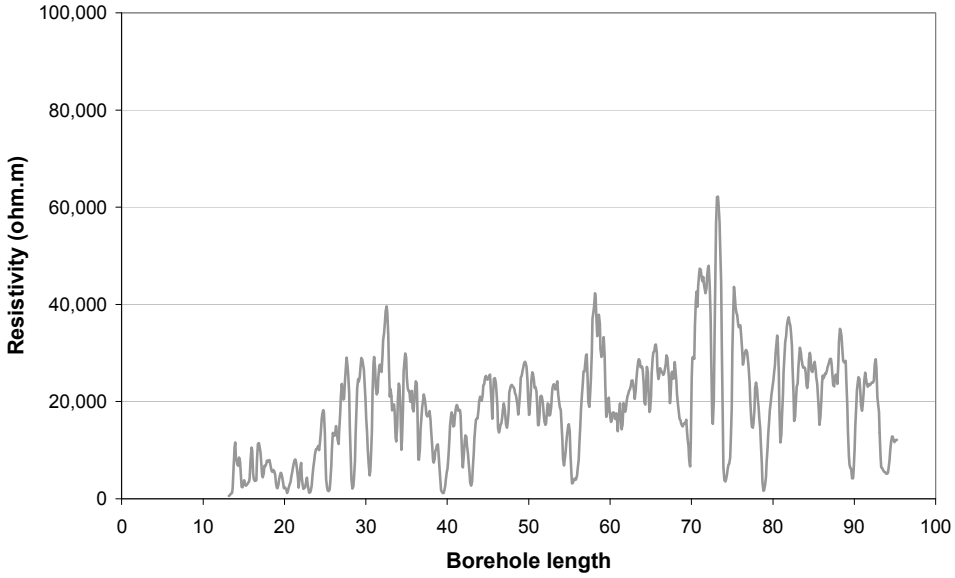


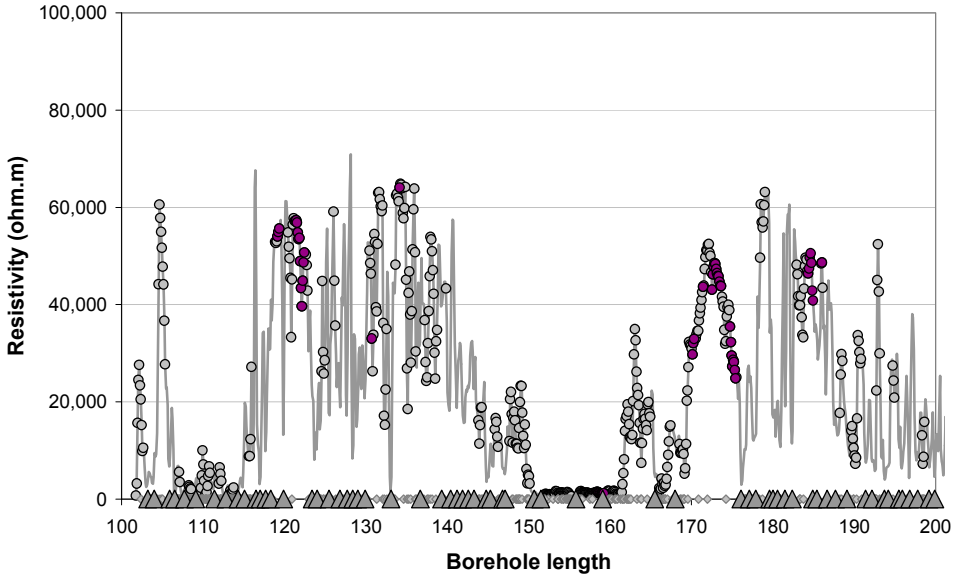


Rock resistivity
Fractured rock resistivity
Rock matrix resistivity
Location of broken fracture parting the drill core
Location of hydraulically conductive fracture detected in the difference flow logging

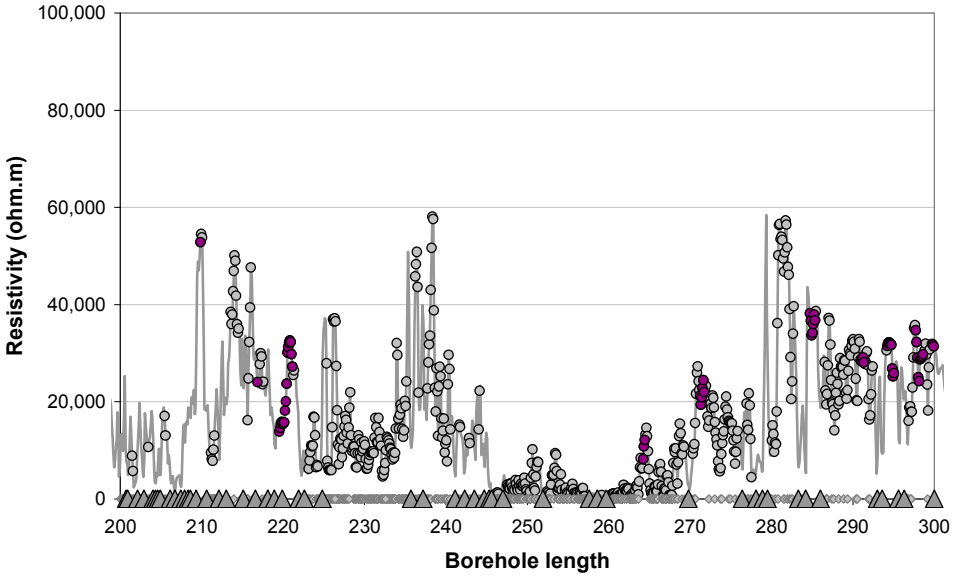


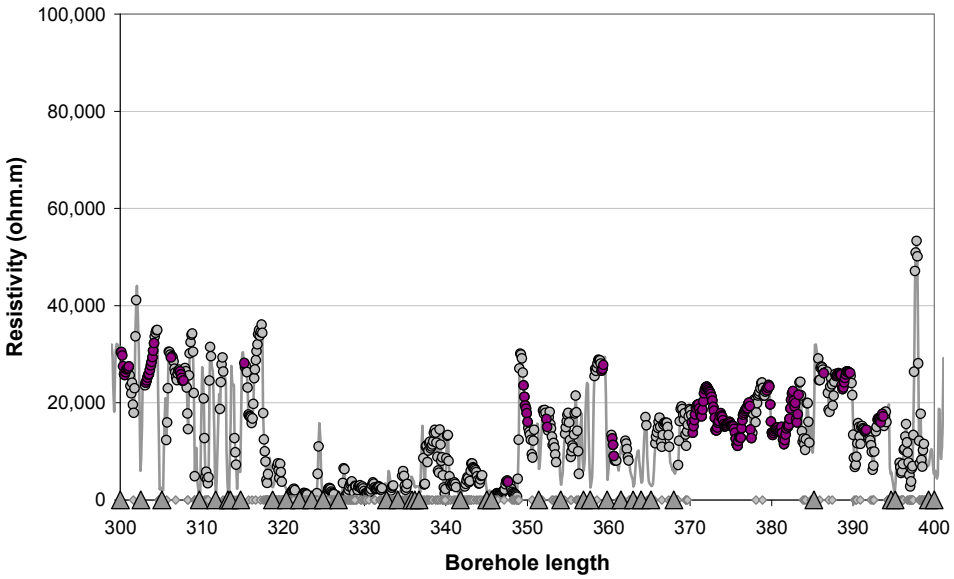


Rock resistivity
Fractured rock resistivity
Rock matrix resistivity
Location of broken fracture parting the drill core
Location of hydraulically conductive fracture detected in the difference flow logging

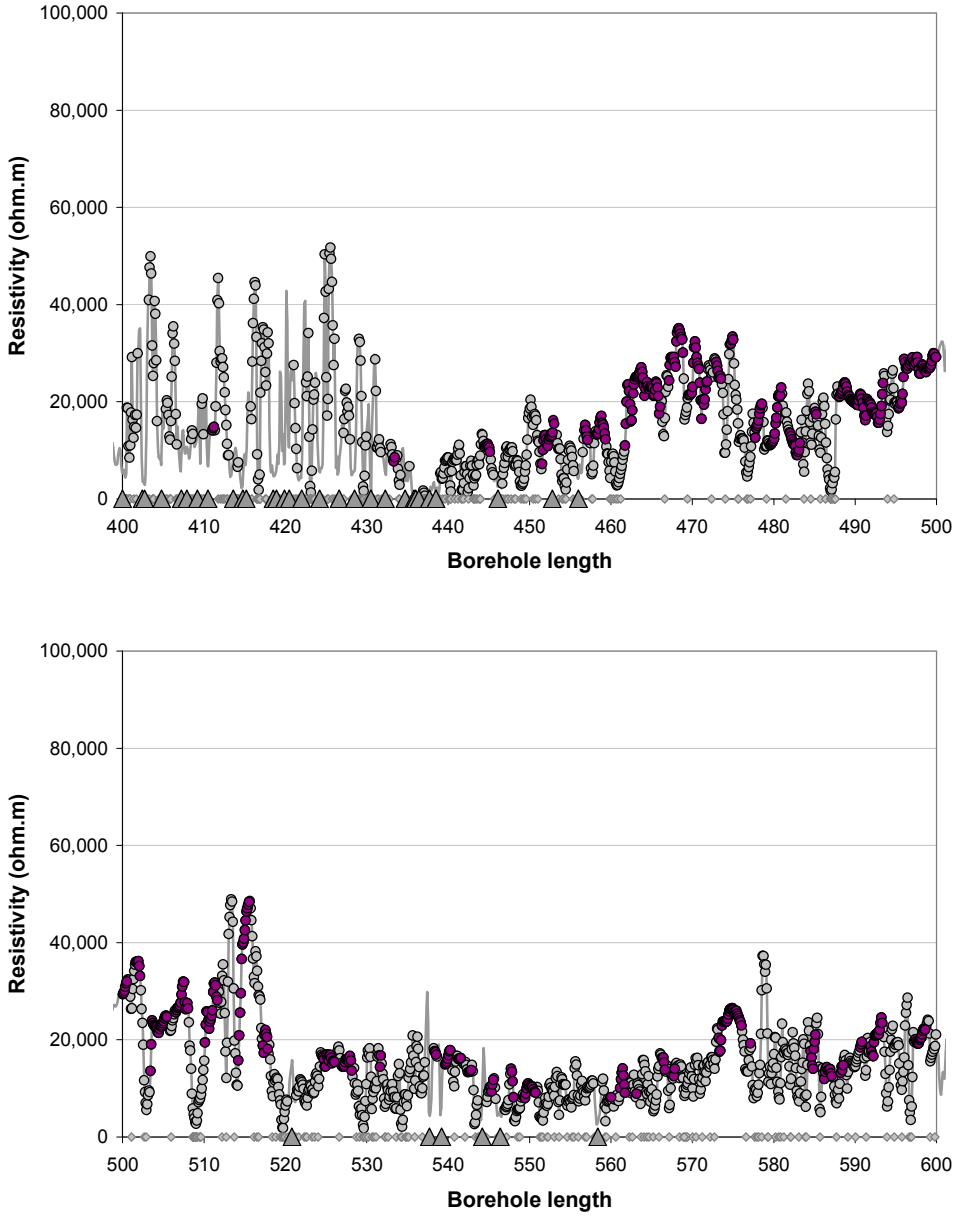
100,000
80,000
60,000
40,000
20,000
0
Resistivity (ohm.m)
400
410
420
430
440
450
460
470
480
490
500
Borehole length
100,000
80,000
60,000
40,000
20,000
0
Resistivity (ohm.m)
500
510
520
530
540
550
560
570
580
590
600
Borehole length
Rock resistivity
Fractured rock resistivity
Rock matrix resistivity
Location of broken fracture parting the drill core
Location of hydraulically conductive fracture detected in the difference flow logging

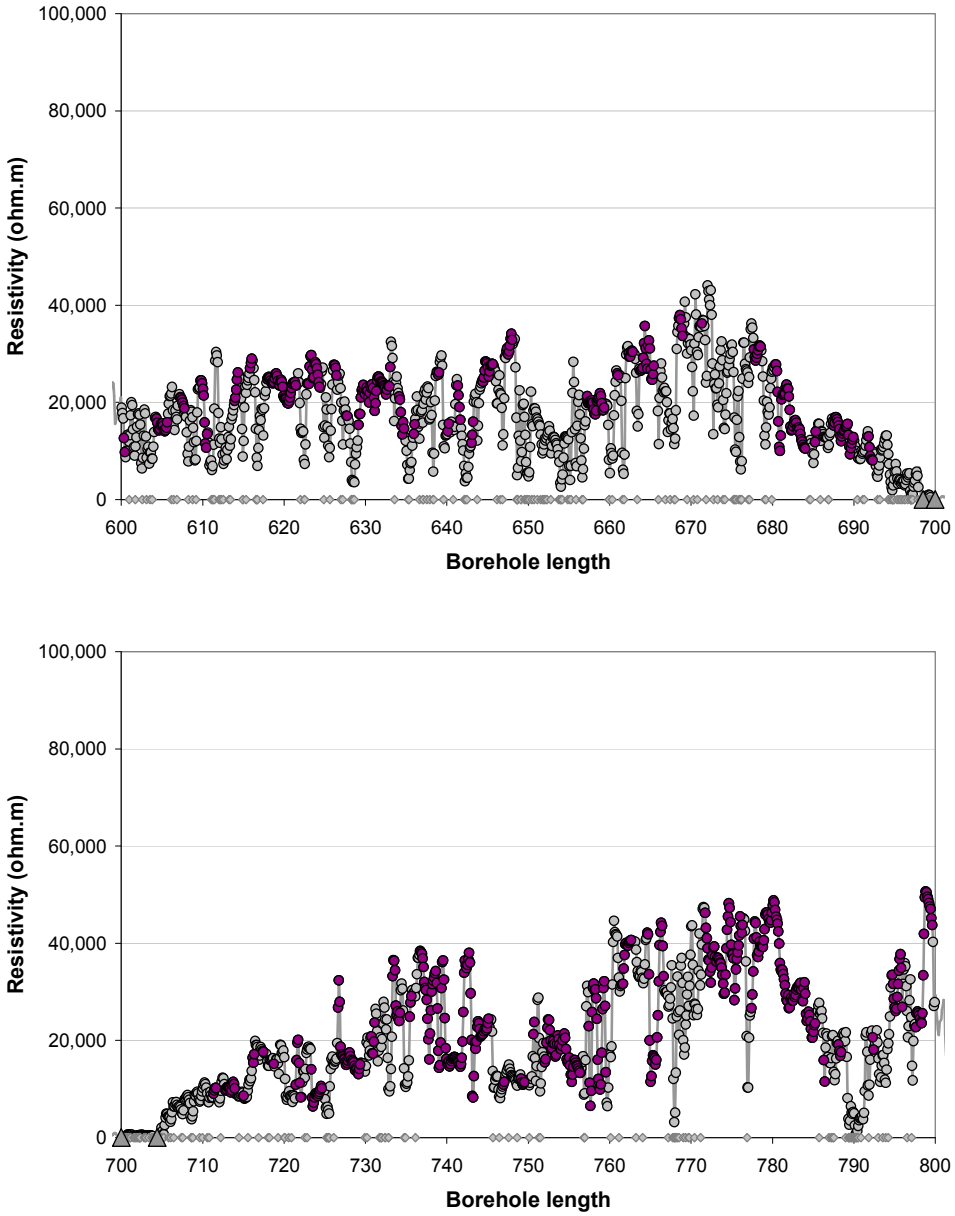
100,000
80,000
60,000
40,000
20,000
0
Resistivity (ohm.m)
600
610
620
630
640
650
660
670
680
690
700
Borehole length
100,000
80,000
60,000
40,000
20,000
0
Resistivity (ohm.m)
700
710
720
730
740
750
760
770
780
790
800
Borehole length
Rock resistivity
Fractured rock resistivity
Rock matrix resistivity
Location of broken fracture parting the drill core
Location of hydraulically conductive fracture detected in the difference flow logging

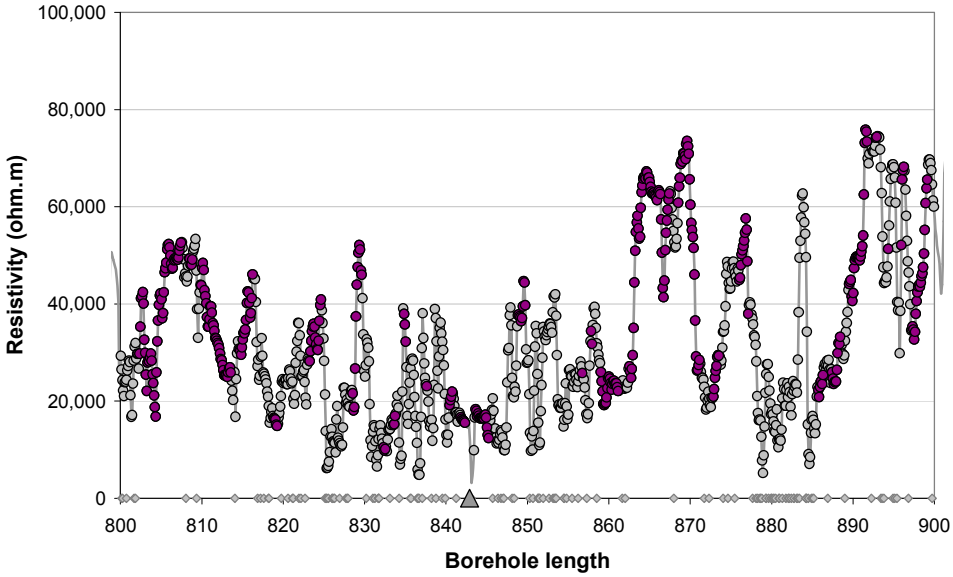


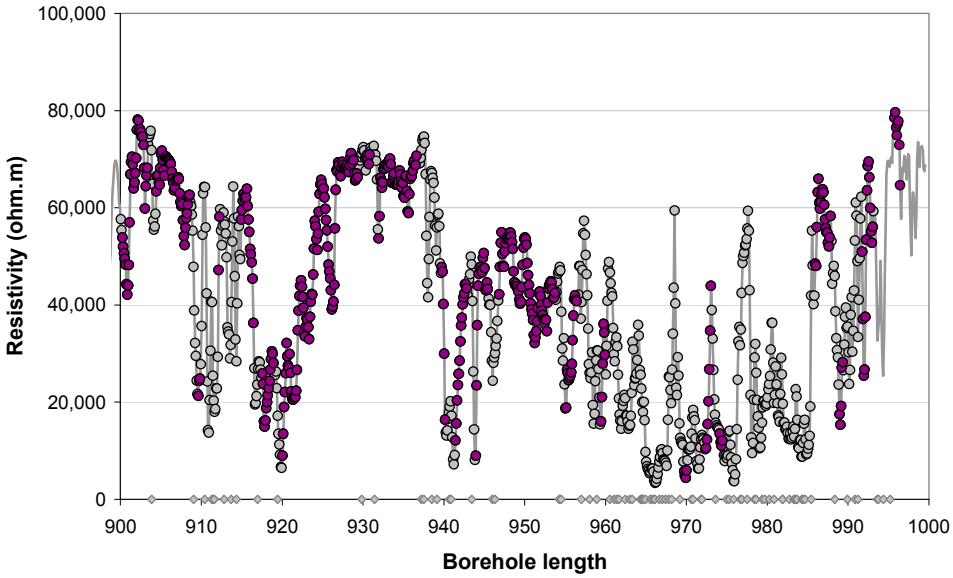


Rock resistivity
Fractured rock resistivity
Rock matrix resistivity
Location of broken fracture parting the drill core
Location of hydraulically conductive fracture detected in the difference flow logging

# Appendix A4: In situ rock resistivities and fractures KLX12A

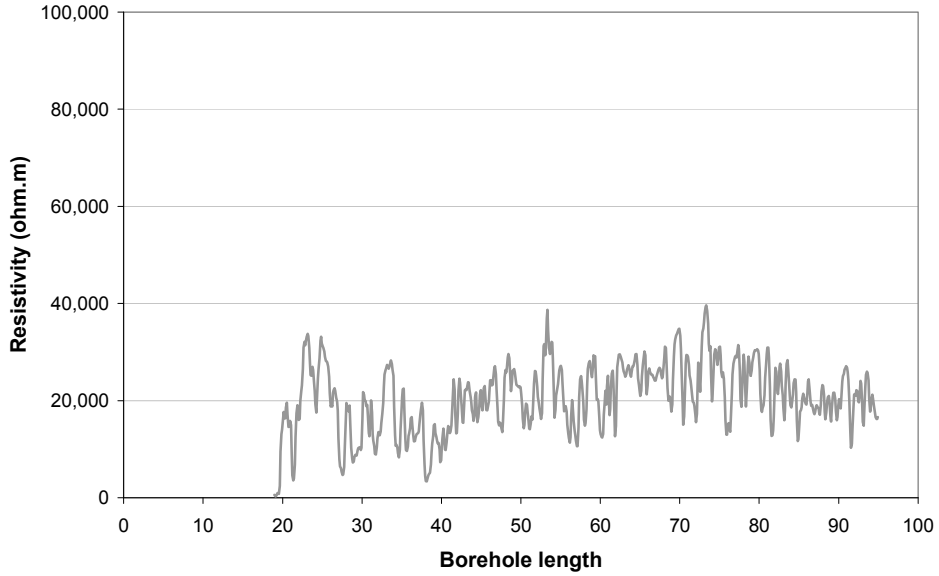


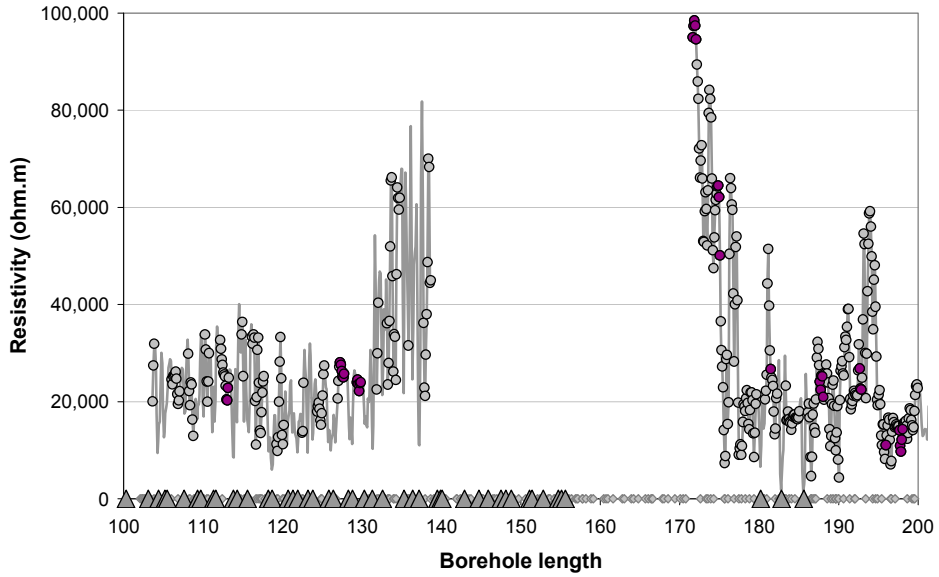


Rock resistivity
Fractured rock resistivity
Rock matrix resistivity
Location of broken fracture parting the drill core
Location of hydraulically conductive fracture detected in the difference flow logging

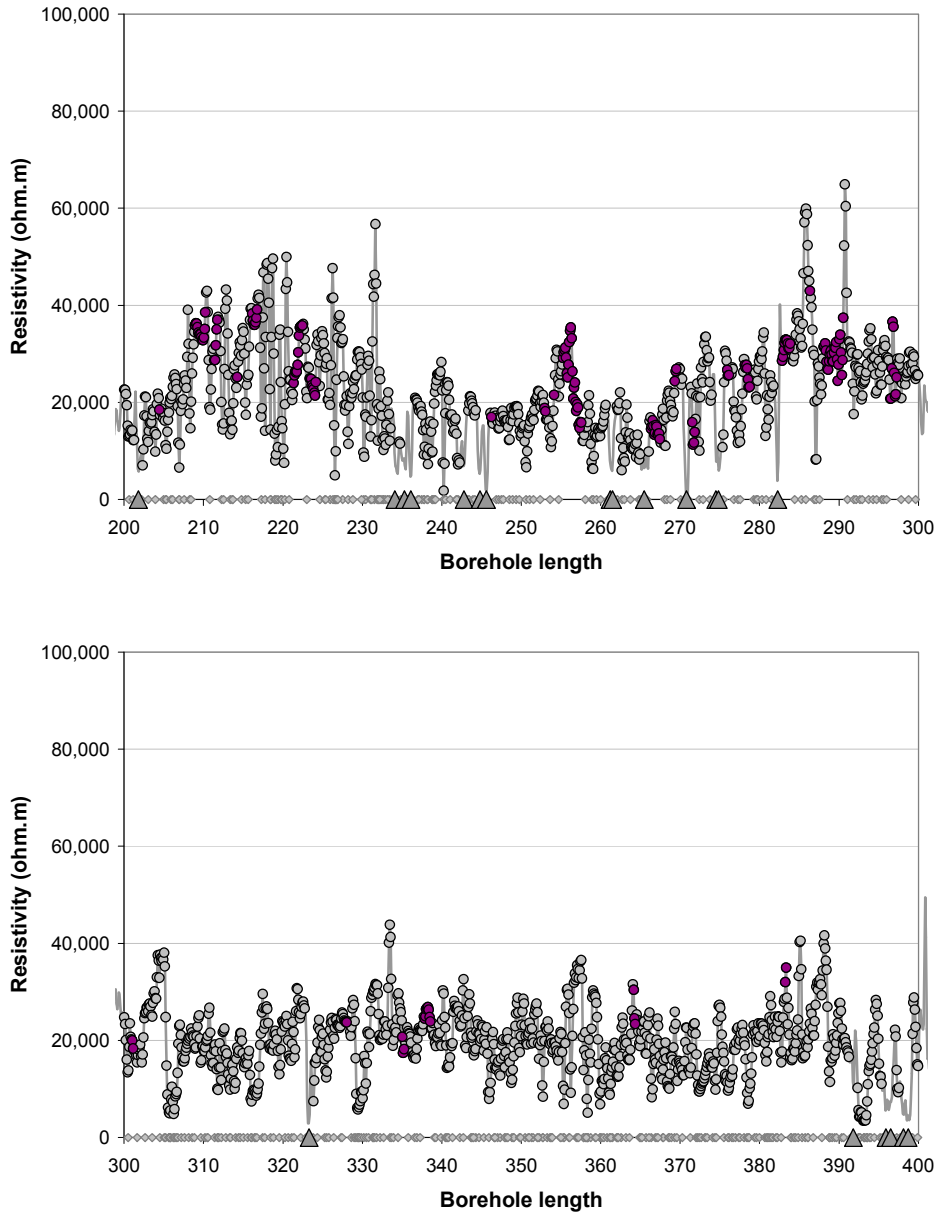
100,000
80,000
60,000
40,000
20,000
0
Resistivity (ohm.m)
200
210
220
230
240
250
260
270
280
290
300
Borehole length
100,000
80,000
60,000
40,000
20,000
0
Resistivity (ohm.m)
300
310
320
330
340
350
360
370
380
390
400
Borehole length
Rock resistivity
Fractured rock resistivity
Rock matrix resistivity
Location of broken fracture parting the drill core
Location of hydraulically conductive fracture detected in the difference flow logging

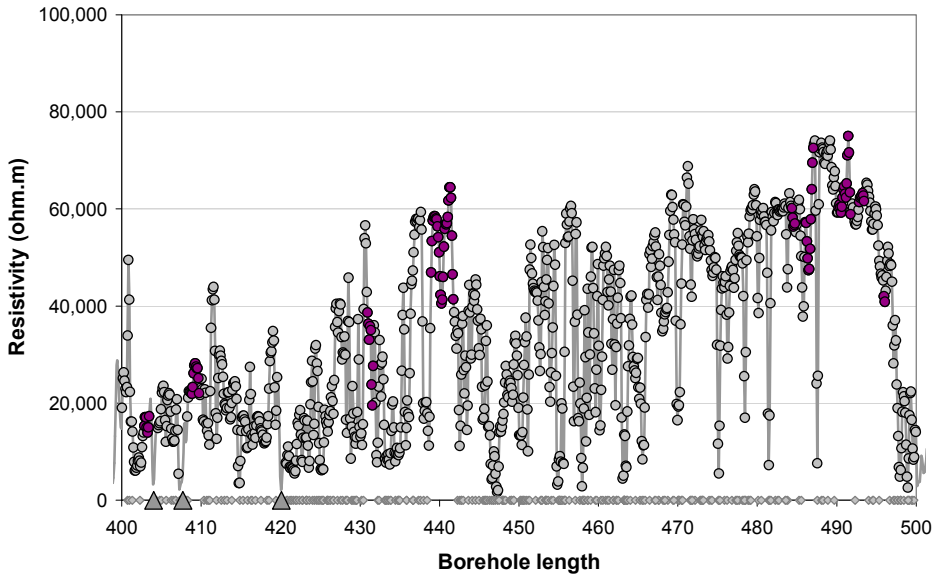


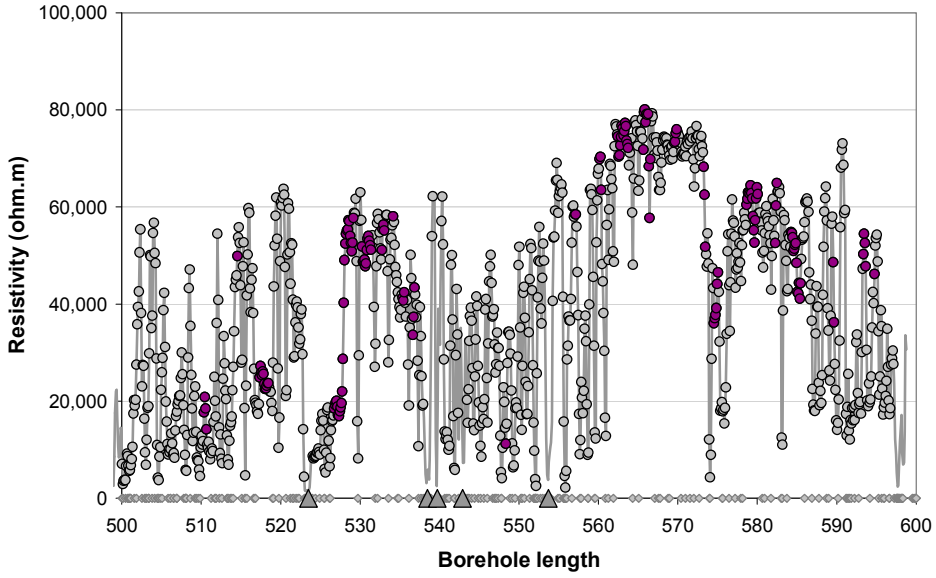


Rock resistivity
Fractured rock resistivity
Rock matrix resistivity
Location of broken fracture parting the drill core
Location of hydraulically conductive fracture detected in the difference flow logging

# Appendix B1: In situ formation factors KLX07A

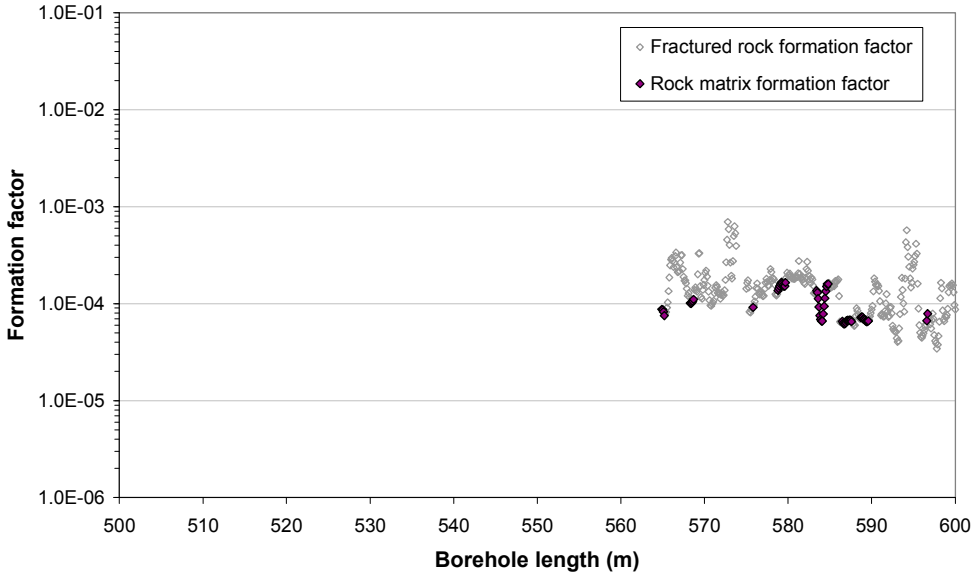


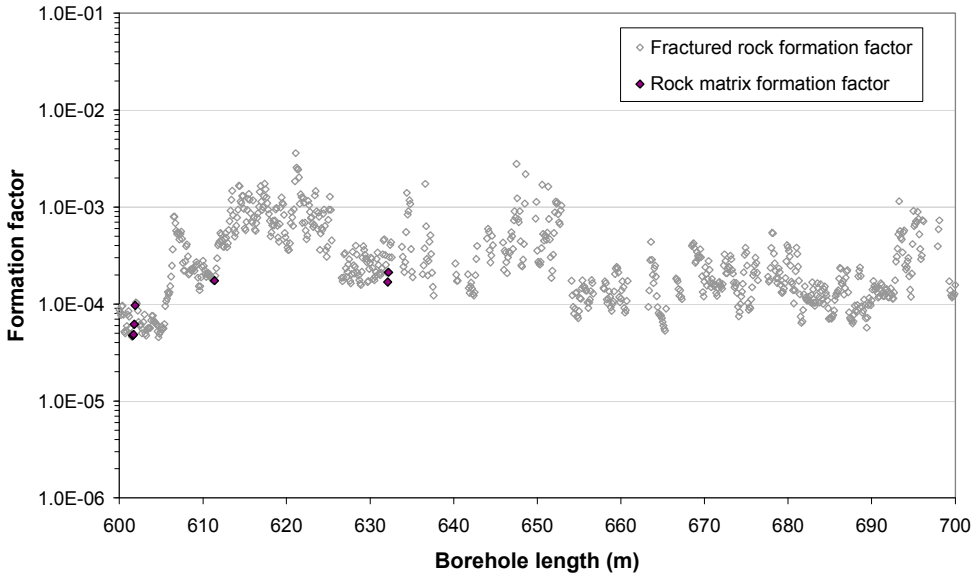

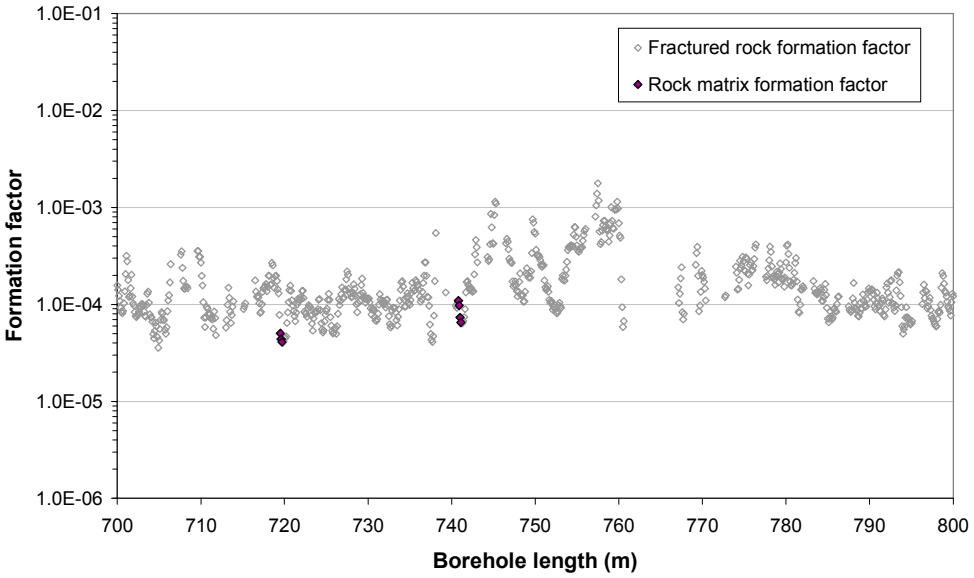
Fractured rock formation factor
Rock matrix formation factor
Formation factor
1.0E-01
1.0E-02
1.0E-03
1.0E-04
1.0E-05
1.0E-06
700
710
720
730
740
750
760
770
780
790
800
Borehole length (m)

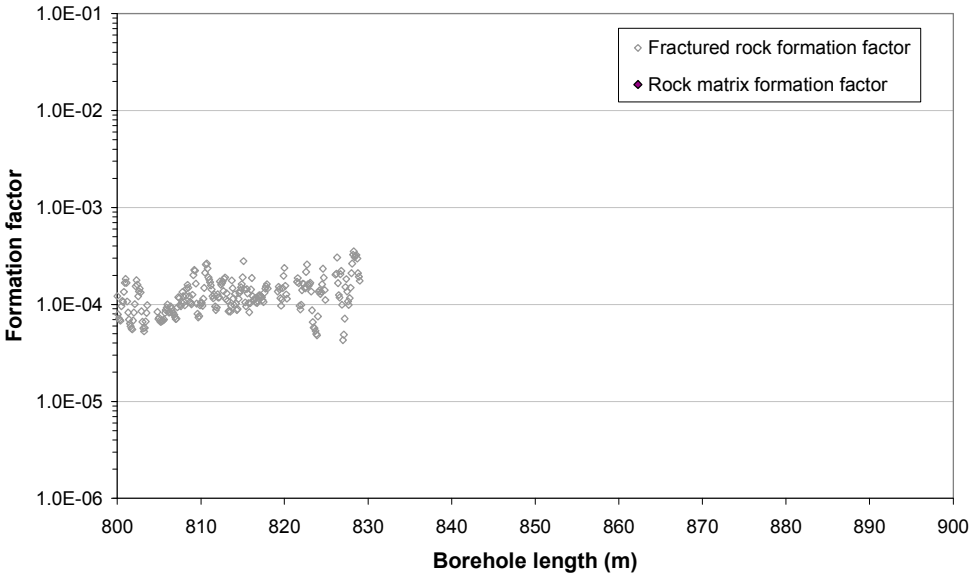
Fractured rock formation factor
Rock matrix formation factor
Formation factor
1.0E-01
1.0E-02
1.0E-03
1.0E-04
1.0E-05
1.0E-06
800
810
820
830
840
850
860
870
880
890
900
Borehole length (m)

# Appendix B2: In situ formation factors KLX08

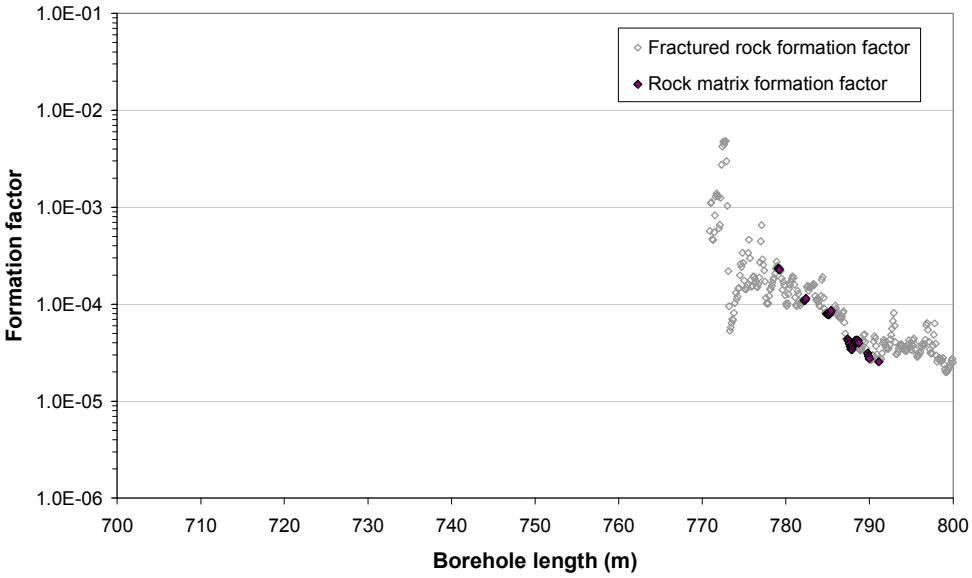


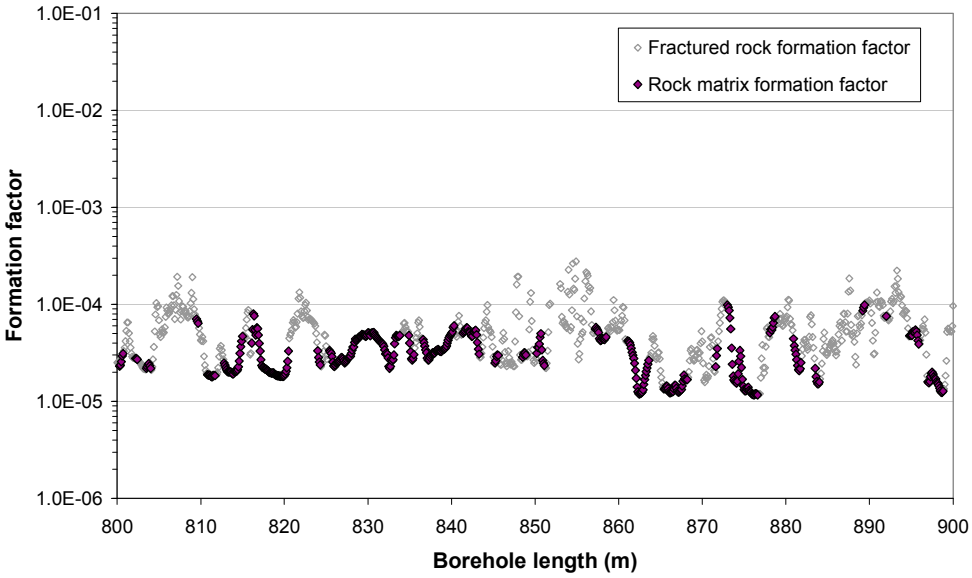

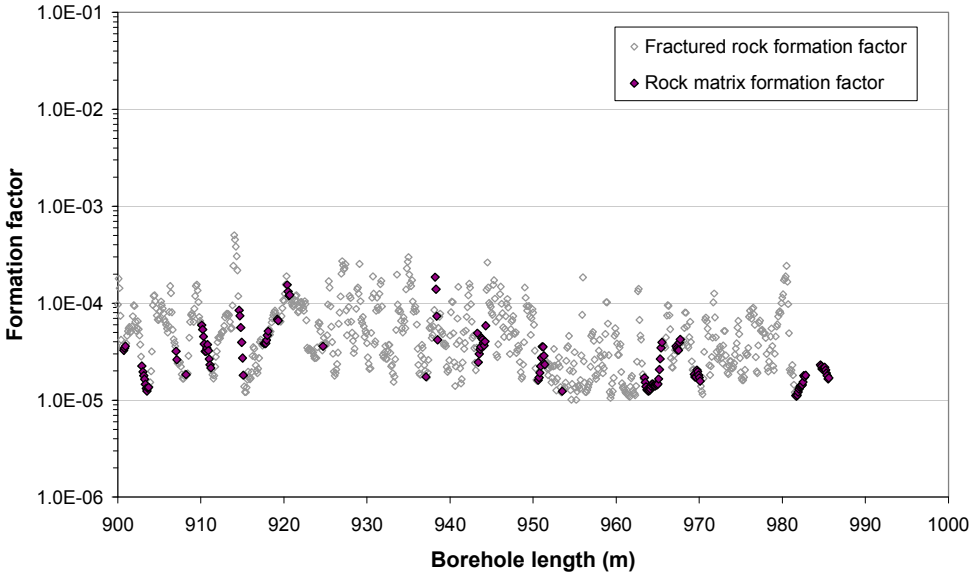
1.0E-01
1.0E-02
1.0E-03
1.0E-04
1.0E-05
1.0E-06
Formation factor
900
910
920
930
940
950
960
970
980
990
1000
Borehole length (m)
Fractured rock formation factor
Rock matrix formation factor

# Appendix B3: In situ and laboratory formation factors KLX10

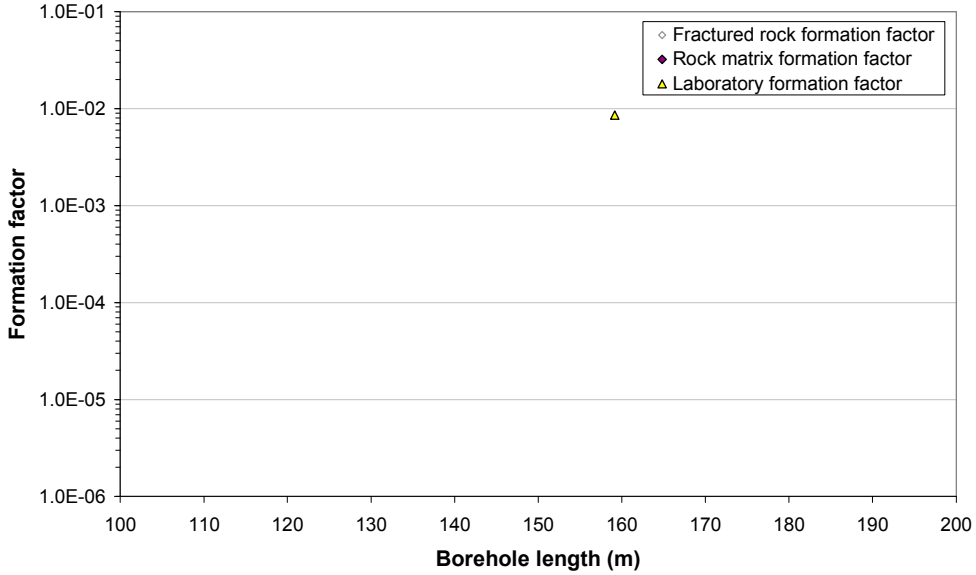


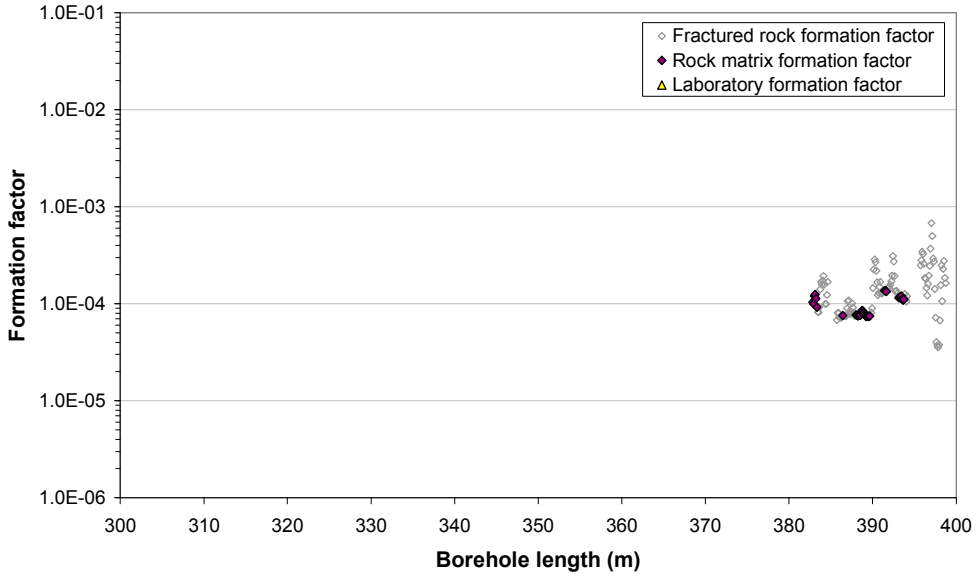

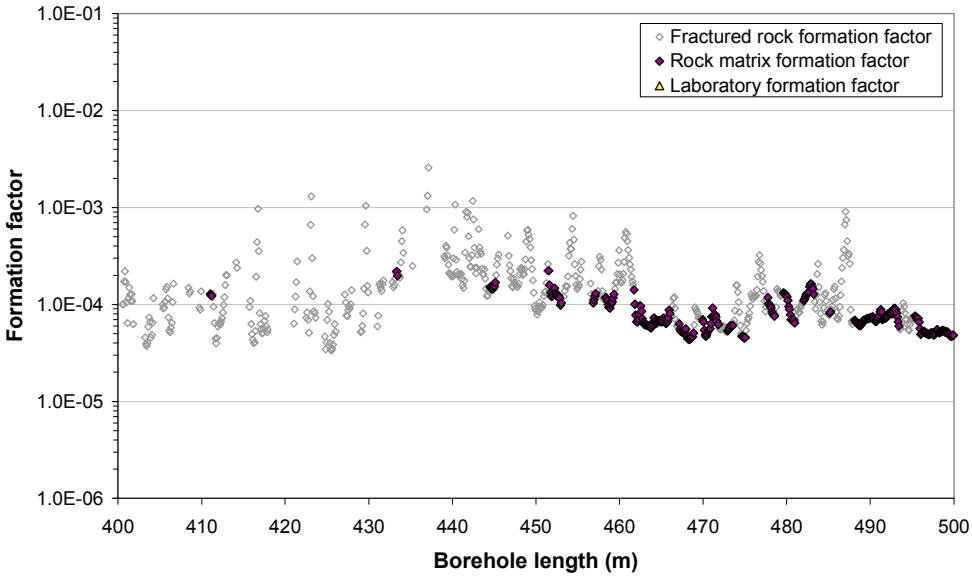
Fractured rock formation factor
Rock matrix formation factor
Laboratory formation factor
Formation factor
1.0E-01
1.0E-02
1.0E-03
1.0E-04
1.0E-05
1.0E-06
400
410
420
430
440
450
460
470
480
490
500
Borehole length (m)

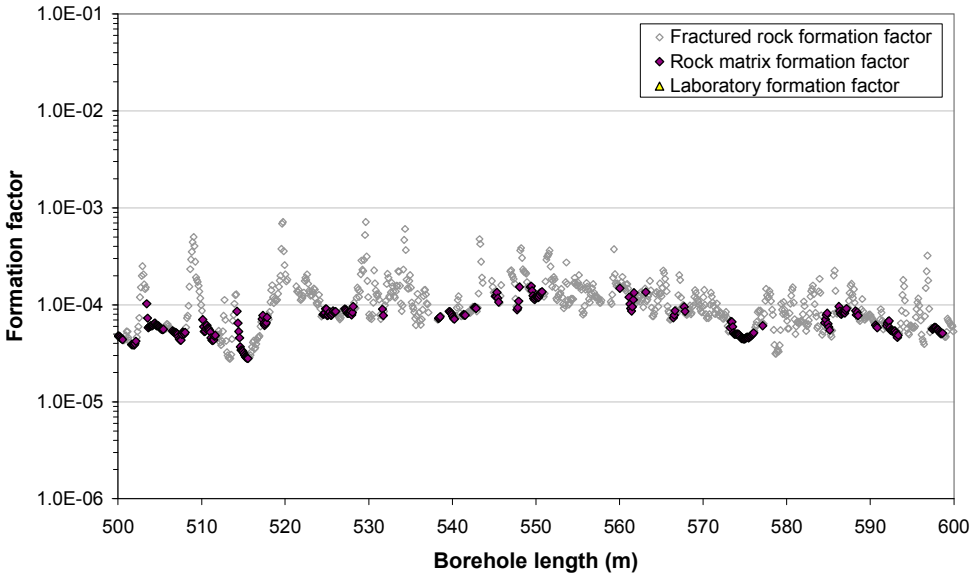
Fractured rock formation factor
Rock matrix formation factor
Laboratory formation factor
Formation factor
1.0E-01
1.0E-02
1.0E-03
1.0E-04
1.0E-05
1.0E-06
500
510
520
530
540
550
560
570
580
590
600
Borehole length (m)

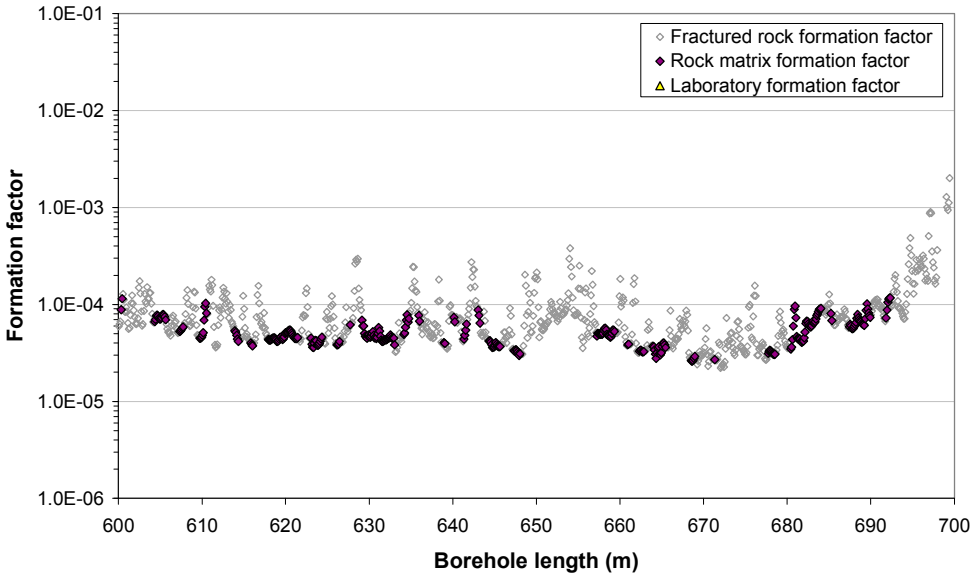
Fractured rock formation factor
Rock matrix formation factor
Laboratory formation factor
Formation factor
1.0E-01
1.0E-02
1.0E-03
1.0E-04
1.0E-05
1.0E-06
600
610
620
630
640
650
660
670
680
690
700
Borehole length (m)

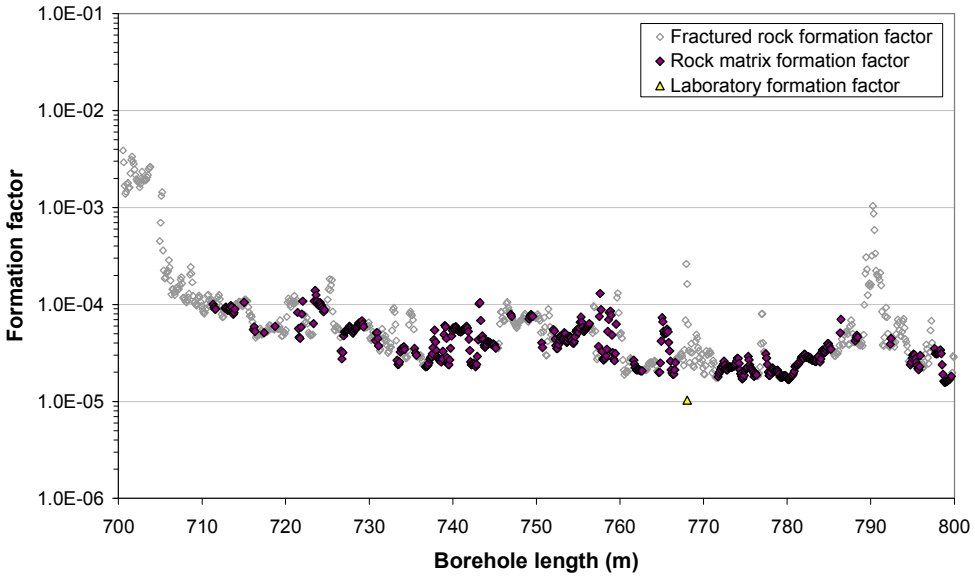
Fractured rock formation factor
Rock matrix formation factor
Laboratory formation factor
Formation factor
1.0E-01
1.0E-02
1.0E-03
1.0E-04
1.0E-05
1.0E-06
700
710
720
730
740
750
760
770
780
790
800
Borehole length (m)

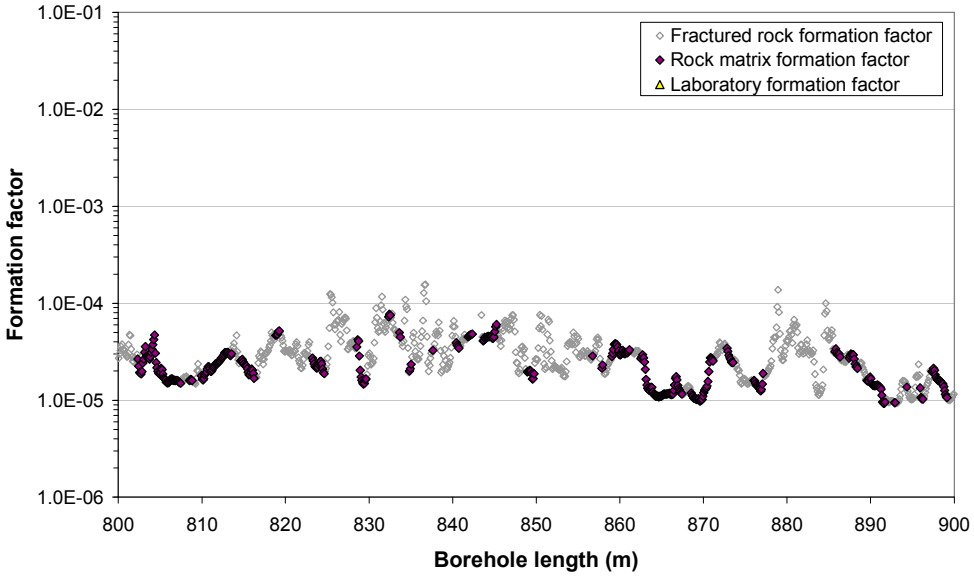
Fractured rock formation factor
Rock matrix formation factor
Laboratory formation factor
Formation factor
1.0E-01
1.0E-02
1.0E-03
1.0E-04
1.0E-05
1.0E-06
800
810
820
830
840
850
860
870
880
890
900
Borehole length (m)

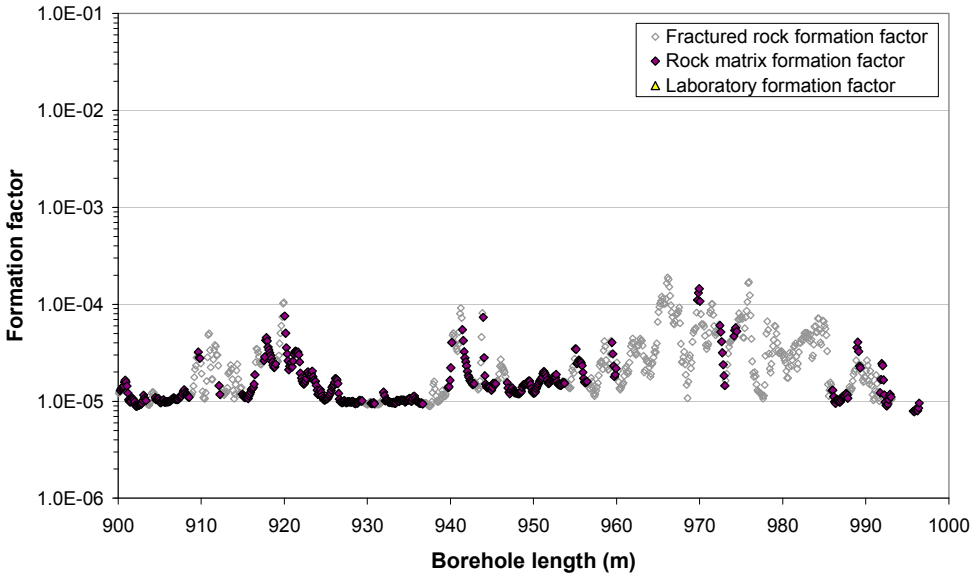
Fractured rock formation factor
Rock matrix formation factor
Laboratory formation factor
Formation factor
1.0E-01
1.0E-02
1.0E-03
1.0E-04
1.0E-05
1.0E-06
900
910
920
930
940
950
960
970
980
990
1000
Borehole length (m)

# Appendix B4: In situ and laboratory formation factors KLX12A

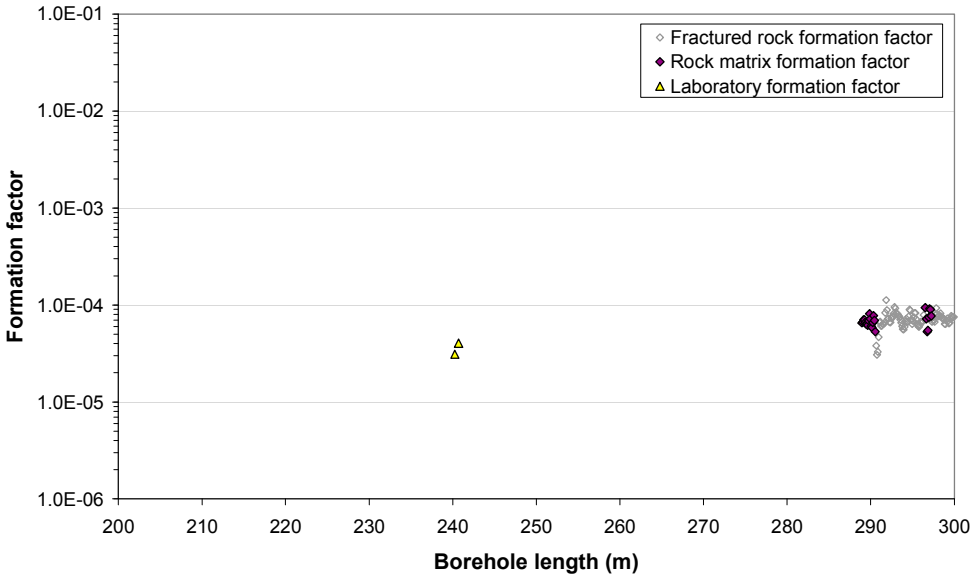


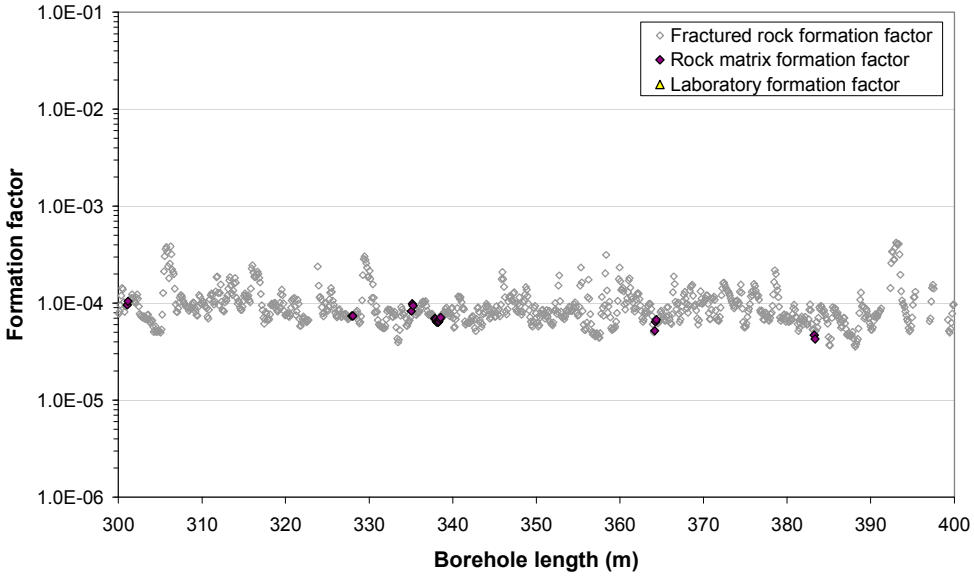

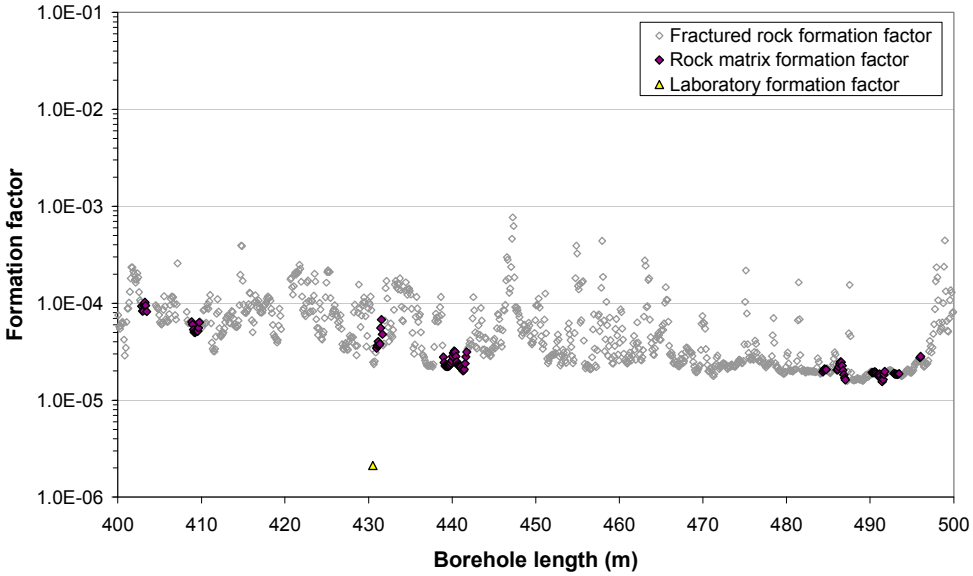
Fractured rock formation factor
Rock matrix formation factor
Laboratory formation factor
Formation factor
1.0E-01
1.0E-02
1.0E-03
1.0E-04
1.0E-05
1.0E-06
400
410
420
430
440
450
460
470
480
490
500
Borehole length (m)

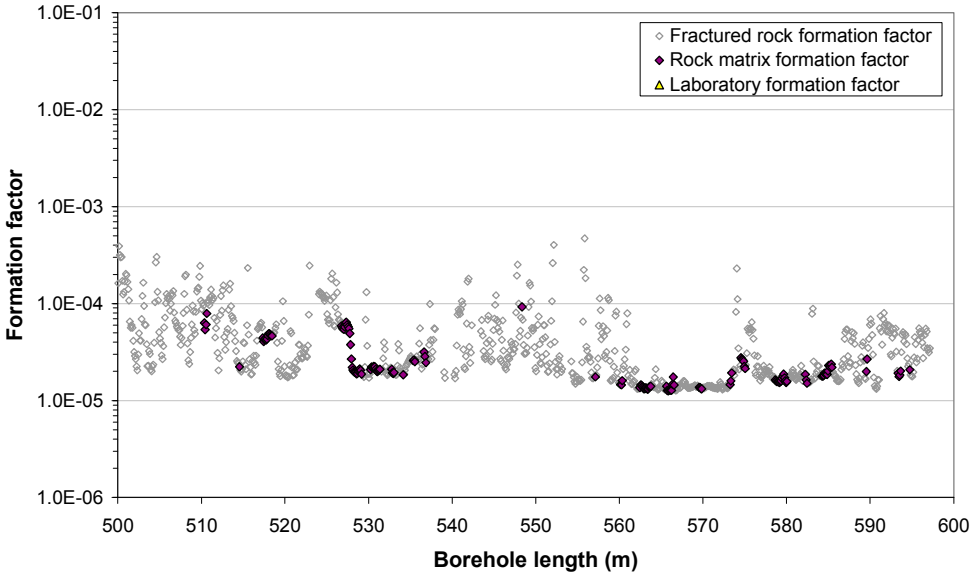
Fractured rock formation factor
Rock matrix formation factor
Laboratory formation factor
Formation factor
1.0E-01
1.0E-02
1.0E-03
1.0E-04
1.0E-05
1.0E-06
500
510
520
530
540
550
560
570
580
590
600
Borehole length (m)